UPGRADATION OF LOCALLY AVAILABLE SILICA FOR THE PRODUCTION OF SOLAR GRADE SILICON

by

Marzia Hoque Tania

A thesis submitted in partial fulfillment of
the requirements for the degree of

MASTER OF PHYLOSPHY IN MATERIAL SCIENCE

Department of Materials and Metallurgical Engineering
BANGLADESH UNIVERSITY OF ENGINEERING AND TECHNOLOGY
Dhaka-1000, Bangladesh

April, 2014

CANDIDATE'S DECLARATION

This is to certify that the work presented in this thesis is original and this thesis or any part of it has not been submitted elsewhere for the award of any degree or diploma.

Marzia Hoque Tania

CERTIFICATE OF RESEARCH

This is to certify that the work presented in this thesis is carried out by the author under the supervision of Associate Professor Dr. Fahmida Gulshan, Department of Materials and Metallurgical Engineering, Bangladesh University of Engineering & Technology, Dhaka.

Dr. Fahmida Gulshan

Marzia Hoque Tania

Acknowledgement

First of all, thanks to the almighty Allah for giving me the strength and patience, for completing this thesis work.

I want to express my utmost gratitude to my supervisor, Assoc. Prof. Dr. Fahmida Gulshan for her continuous support, valuable advice, understanding and keeping faith in me. I was never set back in this work due to my supervisor's inspiration and appreciation.

My parents continuously encouraged me for getting the higher degree. I won't be able to finish this M.Phil. degree without their contribution.

I am especially indebted to Prof. Dr. ASW Kurny, Dept. of MME, BUET. He was the prime mover and mentor of the entire thesis work. His guidance, orchestrating and advice helped me the most for finishing this thesis.

I am thankful to Prof. Dr. Zahid Hasan Mahmood, Dept. of Applied Physics, Electronics and Communication Engineering, University of Dhaka for originating the concept of the work. I am gratified to Dr. Shaestagir Chowdhury, Principal Engineer, Logic Technology Development, Intel Corporation for his advice, support and revitalization of the global aspect of the work.

I would like to thank Dr. Abdul Gafur, Project Director, "Development of Materials for Tools and Bimetallic implant", PP & PDC, BCSIR for providing me the access to his lab. I am also grateful to Rakibul Qadir, Engineer, PP &PDC, BCSIR, for his sincere cooperation. I would also like to thank Dept. of Glass and Ceramics, BUET and Geological Survey, Bangladesh.

I am also thankful to the Department of Materials and Metallurgical Engineering for providing me the facilities for this work. I would like to acknowledge the teachers of the department for encouraging me throughout this period of my post graduate studies.

I would like to thank all the staff members of MME Dept. specially Md. Ashiqur Rahman, Mr. Ahammad Ullah and Md. Wasim Uddin acquainting me with a wide range of equipments and helping me in time of need.

Dedicated to my parents…

Abstract

The purpose of the work was to initiate a systematic investigation within the country on the possibility of producing solar grade (SoG) silicon from local silica deposits and to achieve that the objective was to identify a suitable deposit of silica within the country and to develop techniques for the purification of silica of this deposit so as to make it suitable for the production of SoG-Si. The characterization and upgradation processes were employed on five sand samples, collected from Dalia (district Nilphamari), Patgram (district Lalmonirhat), Bipinganj (district Netrokona), Kuakata (district Patuakhali) and Sharighat (district Sylhet). The minimum required percentage of silica for the production of SoG-Si is >98%. The received sand samples contained SiO_2 ranging from around 65% to 97%. The characterization was performed on the basis of material composition, particle size, density, sphericity, moisture content, material composition and crystallinity on the samples. All five sand samples contain minimum amount of moisture and negligible organic matter. In case of bulk density deviation was observed from standard value of 2.65g/cc. Variation was observed in particle size distribution for Patgram, Dalia and Bipinganj sand. Most of Kuakata sand is sized ~ 75µm and for Sylhet it is 0.2mm. The sample containing minimum impurity and perfect quartz crystal form, collected from Bipinganj was found to have high potential. The sample from Sylhet containing ~ 86% SiO_2 was also considered as a strong contender for further processing. Traditional beneficiation methods like attrition, acid washing and alkali washing were performed on the samples. Based on stereomicroscopic observation and XRF result the optimum level was identified for each beneficiation step e.g. for attrition optimum stirring speed and time was found to be 800 rpm and 30 minutes respectively. Finally a methodology was developed for the purification of the samples which lead to the upgraded point of 99.45% and 95.31% SiO_2 for Bipinganj and Sylhet sand sample respectively. The result concludes Bipinganj sand can be used as raw material for the production solar grade silicon.

Table of Contents

Nomenclature

XRF	X-ray fluorescence
XRD	X-ray diffraction
TGA	Thermogravimetric analysis
DTA	Differential thermal analysis
SoG	Solar Grade
GSB	Geological Survey, Bangladesh
PPM	Parts per million
RPM	Revolution per minute

List of tables

List of figures

Chapter One

Introduction

1.1 Purpose of the work

The amount of sand reserve is abundant in nature. In nature, silica, SiO_2 occurs in different forms such as quartz (crystalline); chalcedony, agate, flint and jasper (crptocrystalline), and opal (hydrous form); sandstone (sedimentary deposit composed of small grains of quartz); quartzite (metamorphosed derivative of sandstone) and silica sand (weathered sandstone or quartzite enriched in silica) [1-2]. Quartz raw material is often thought of as an "excessive" commodity that easily may be exploited. This may be correct for low purity quartz commodities with more than 300 parts per million (0.03 wt %) impurities, but intermediary (50 to 300 ppm) to high purity qualities (<50 ppm) are much more challenging to find in nature [3]. As the prime source of silica the mineral has wide large volume application in the manufacture of glass, ceramics, refractory materials and other traditional uses. A special category of high purity sands known as high quartz sand, silica sand, industrial sand, or glass sand is essential for making glass and a large number of high value products. The silica sands command much higher prices but must meet demanding specifications. They are produced in much smaller quantities and from more limited areas around the world. Only very few deposits are suitable in volume, quality and amenability to tailored reefing methods for specialty high purity applications. As such high purity silica has become one of today's key strategic minerals with applications in high-tech industries that include semiconductors, high temperature lamp tubing, telecommunications and optics, microelectronics, and solar silicon applications [4]. For an example, the dominant material used in PV cells is silicon. About 95% of the current solar cell module market is based on silicon as raw material [5]. Silicon, the main constituent of silica does not occur in free-state, but silicon compounds are abundantly available and constitute about 28% of the earth's crust. But silica for the photovoltaic applications requires purity greater than 98%, which costs 200 to 2000 USD per ton or even more [3, 6]. For the production of solar grade (SoG) silicon, silica sand as raw material has a great influence in choosing proper beneficiation techniques and in the production cost. That's why high purity silica is preferred for such case. The more impure the raw material more infeasible the SoG-Si production is. Thus, even in economic crisis, the global outlook for high purity quartz using industries is still positive with growth rates between 3 to 5%, specifically in certain lighting, semiconductor and photovoltaic applications [4].

The beneficiation of raw silica into refined high-purity products involves several refinement steps

which need to be adapted to effectively minimize the specific impurities of the individual raw silica feed to comply with stringent end-use specifications. The cost effectiveness and technical feasibility greatly depends on the characteristics of the raw silica. That's why the deposits of high purity silica should be reserved for the high-tech applications only.

Bangladesh has over hundred million tons of reserve of glass or silica sand. Every year this reserve is being used from construction to glass and ceramic industries. Once in awhile new deposit is being explored. There are very few deposits in the world where silica sand is naturally as pure as >97% [3]. But Bangladesh is rich in this case. Geological Survey Bangladesh has identified new deposits of silica sand. However, systematic characterization of sands of these deposits is yet to be undertaken.

This study seeks the possibility of using the locally available silica sand in high-tech industries such as semiconductors, telecommunications and optics, microelectronics, solar silicon applications etc.

1.2 Outline of the work

The objectives of this work can be summarized as follows:

- Characterisation of the samples on the basis of parameters that include composition, size, density, sphericity, moisture content, material composition and crystallinity.
- Beneficiation of the sample with locally available and easily affordable techniques.
- Identification local resources (silica) that could be used as raw material for the production of solar grade silicon.

The outline of the work is mentioned bellow:

- The sand samples were collected from Nilphamari, Patuakhali, Lalmonirhat, Netrokona and Sylhet district.
- The mineralogical composition of the samples was determined by x-ray fluorescence analysis.
- The morphology of the samples was studied via optical and scanning electron microscopes.
- The physicochemical characterisation was performed to study bulk density, particle size distribution and moisture content.

- The phase was determined by X-ray diffraction analysis and differential thermal analysis.
- The differential thermal analysis and thermogavitimetric analysis were conducted to determine the thermal effects.
- To trace organic material a chemical method was employed and cross checked with thermogavitimetric analysis.
- Based on the characterisation, predominantly two sand samples with highest potential were taken into account for upgradation.
- The samples were washed with distilled water and optimum time and speed were determined.
- The samples were washed with acids and alkali. The change was observed through optical microscope.
- The final beneficiation point was quantified by x-ray fluorescence analysis.
- Based on the characterisation and plausible beneficiation, a suitable deposit of silica within the country was identified and feasible techniques were developed for the purification of silica of this deposit so as to make it suitable for using it as raw material for the production of solar grade silicon.

Chapter Two

Literature Review

Sand is a naturally occurring granular material composed of finely divided rock and mineral particles. The composition of sand is highly variable, depending on the local rock sources and conditions, but the most common constituent of sand in inland continental settings and non-tropical coastal settings is silica.

Silica is the name given to a group of minerals composed of silicon and oxygen, the two most abundant elements in the earth's crust. Silica is found commonly in the crystalline state and rarely in an amorphous state. It is composed of one atom of silicon and two atoms of oxygen resulting in the chemical formula SiO_2.

Sand consists of small grains or particles of mineral and rock fragments. Although these grains may be of any mineral composition, the dominant component of sand is the mineral quartz, which is composed of silica (silicon dioxide). Other components may include aluminium, feldspar and iron-bearing minerals.

2.1 Overview of Silica

Silica (SiO_2) in crystalline and non-crystalline (amorphous) form makes up 12.6 weight% of the Earth's crust. At least 15 modifications are known [4] i.e. mineral phases with the formula SiO_2 but a different crystal structure. All silica minerals (excluding stishovite and seifertite- which should be considered as oxides as they are not made of SiO_4 tetrahedra) are united in the silica group according to Dana's classification, and in the quartz group (including stishovite and seifertite) according to Strunz's classification (Table 2.1) [7]. The classification of certain non- and microcrystalline silica polymorphs and varieties is often more complicated (modified after Graetsch), since these minerals are mostly fine-grained and intimately inter-grown [8].

Table 2.1: The SiO_2 system (modified after Strunz and Tennyson)

Group	Varity	Remark
Quartz-tridymite-cristobalite (atmospheric and low pressure)	Low (α)-quartz	Trigonal
	High (β)-quartz	Hexagonal
	Tridymite	Monoclinic
	High-tridymite	Hexagonal
	Cristobalite	Tetragonal
	High-cristobalite	Cubic
	Melanophlogite	Cubic
	Fibrous SiO_2 (syn.)	Orthorhombic
	Moganite	Monoclinic
Keatite-coesite-stishovite (high and ultra-high pressure)	Keatite (syn.)	Tetragonal
	Coesite	Monoclinic
	Stishovite	Tetragonal
	Seifertite	Orthorhombic
Lechatelierite-opal (amorphous phases)	Lechatelierite	Natural silica glass
	Opal	H_2O-bearing, solid SiO_2 gel

Quartz (trigonal low-temperature α-quartz) is the most important silica modification in nature and also most frequently used in technical applications. Many chemical and physical properties of quartz and the other silica polymorphs such as trace element content, isotopic composition, luminescence behaviour, etc. are determined by their real structure. The close relation between specific pTx-conditions of formation and different types of defects are often reflected in varying properties (so called typomorphic properties) (e.g., Blankenburg et al. 1994; Götze and Zimmerle 2000; Götze 2009a) [9-11]. These varying properties of quartz and other silica minerals result in the existence of numerous varieties, i.e. mineral phases with the same chemical composition of SiO_2 and the same crystal structure, but different appearance in shape, colour or varying physical properties. Among these varieties are colour varieties such as in the case of amethyst, smoky quartz, rose quartz and agate or certain growth phenomena such as fibre- and sceptre quartz or chalcedony and quartzite [4]. Later, in Table 2.6, properties of few silica polymorphs are mentioned.

2.2 Applications

The commonest use of silica sand is in the manufacture of glass (>35%) [12]. Quartzite, sandstone, quartz and other siliceous rocks lime mica schists are used in the manufacture of silica bricks. Quartz and quartzite are used in making ferro-silicon for the manufacture of silicon steel. Pure quartz sands are known as industrial sand, silica sand, high quartz sand or simply silica by industries. Carefully sized quartz sand is used extensively for filtering water. Raw, angular quartz sand is mixed with clays to make heat-resistant molds or cores for casting metal parts. Fine sand is used for precision coatings such as jewelry, high precision parts, or dental devices. Ceramic items depend on quartz for toughness and resilience, and for their glazes. Quartz is used to make refractory (temperature resistant) bricks for lining furnaces, limited specialized niches, and fused quartz can be made into many complex shapes for laboratory devices. Refined quartz produces a huge range of silicon chemicals used in drugs, cleaners, and pharmaceuticals. Quartz can provide silicon metal or ferrosilicon which is an alloying agent for various metals. Silicon carbide, an important abrasive made from quartz and natural quartz, both has been used for a myriad of abrasive tasks such as sandpaper. Quartz sand is used as a filler or extender for such products as paints, plastics, gels, and other suspensions. It imparts considerable toughness to rubber or plastics, and can provide some temperature resistance. Coarse, spherical sand grains introduced into oil-bearing geologic formations increase permeability of certain rock units by propping open fractures, thus allowing for easier and more complete production of oil. Quartz has use in farming, forestry, and animal husbandry for soil conditioning, as a carrier for farm chemicals, and as additives for animal feed. Quartz sand is even used in recreation such as golf, volleyball, and other sports. In short, we depend on quartz every bit as much as our ancient ancestors and probably even more due to its importance in chemicals and computers.

This thesis work focuses on very special category of applications, i.e. in the high-tech applications, particularly in solar silicon applications. The high-tech industries include semiconductors, high temperature lamp tubing, telecommunications and optics, microelectronics, and solar silicon applications. Fig 2.1 projects such applications. Specific requirements as to tolerable limiting values differ from industry to industry.

(a)

(b)

(c)

(d)

(e)

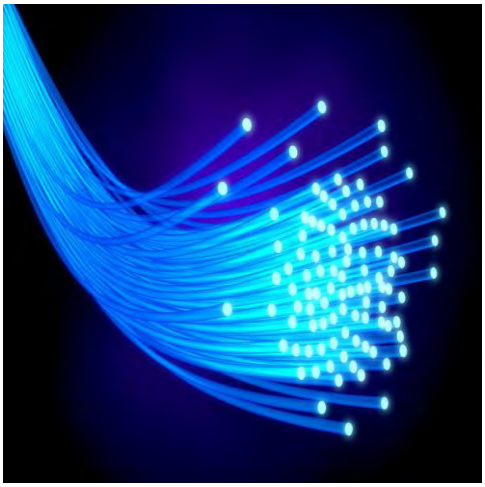

(f)

Fig 2.1: Applications of high purity silica- (a) crucible, (b) microprocessor, (c) silica rod, (d) solar PV panel, (e) silicon chips and (f) optical fibre

The semiconductor industry places the most stringent requirements on silica purity. From single crystal silicon growth in quartz crucibles via the Czochralski process to the handling and processing of wafers in clean rooms, high purity quartz ware is employed. Fused quartz is the basic material for quartz ware used in the semiconductor industry since it combines excellent high temperature properties (i.e. thermal shock resistance and thermal stability) and high purity in a unique way. It withstands the high temperature gradients and high rates of heat transfer in rapid thermal processing which are commonly applied to wafers in order to modify their properties. The high purity of the quartz prevents contamination of wafers during the different processing steps.

Silica glass is widely used as basic material for optical fibers and additional optoelectronic devices in the telecommunications industry. It is used in the optical industry in microlithographic applications, excimer laser optics, beamers and other specialised applications. In the microelectronics industry, a major application is as filler material in epoxy moulding compounds (EMC) for electronic components.

Silicon is the most common material for the production of solar cells in the photovoltaic industry either in mono- or polycrystalline form. About 95% of the current solar cell module market is based on silicon as raw material [5].

2.3 Occurrence of High Purity Silica

Silica of every silica deposit being sand, sandstone, quartzite, hydrothermal vein or pegmatite, has its own specific properties and only a few deposits have high purity quality. There are no rules or general consensuses how high purity silica is formed and how and where it preferentially occurs.

In the early 1970s, Brazil was the world's main supplier of high purity quartz based on lascas, a term used to describe manually beneficiated rock crystal. Up to 1974, when the Brazilian government imposed an embargo on exports of lump quartz, export levels rose to in excess of 10,000 tpa. There have been efforts in Brazil to move more into processed high purity quartz supply, led by Mineracao Santa Rosa (MSR), one of the leading lump quartz and lasca suppliers in the country. The other main source of lascas has been Madagascar, which is still producing from small mining operations [13].

The currently mined high purity quartz deposits are pegmatites (Drag, Norway; Spruce Pine, USA) or hydrothermal veins (Saranpaul, Russia) [3].

High purity quartz deposits are mined in open pits or in shallow underground mines if is a sufficient tonnage of quartz economically recoverable and if the quality of the raw material and its suitability for high-value applications tested.

In 2004, global production of industrial sand (and gravel) was estimated to be 115Mt (Dolley 2004). Australian production was 4.5 Mt. The USA was the leading producer, followed by Germany, Austria, France, Spain, Australia and the United Kingdom [14].

The United States used about 28 million metric tons of industrial sand in 2004, (1,736 thousand metric tons is fiberglass alone), and worldwide consumption exceeded 115 million metric tons. Enormous amounts of quartz sand are generated so the resource is renewed. Some deposits renew themselves annually or almost annually due to floods, storms, or other acts of nature that move large volumes of sand. Others may require many years. The good news is that abundant resources of industrial sand exist worldwide, enough to satisfy human needs for hundreds of years. In addition to great existing resources new or renewed deposits of sand are being produced continuously [12].

Today, US-based Unimin Corp./Sibelco dominates the global high purity quartz market from operations in North Carolina, USA. One of the few alternative suppliers, Norsk Mineral's Norwegian Crystallites has been producing high purity quartz from its Drag plant in western Norway and several underground and open pit mines since mid-1996 when the company changed ownership. In 2011 Imerys SA has combined its US-based Spruce Pine companies KT Feldspar and The Feldspar Corp. (TFC) with Norwegian Crystallites now owned and operated by The Quartz Corp, a joint venture between Imerys and Norsk Mineral. Potential new entrants into the high purity quartz world market are still under development. Moscow-based JSC Polar Quartz (Moore 2005) has raw material supplies based on quartz deposits on the eastern slopes of the sub-polar Ural Mountains and Kyshtym Mining's (KGOK) crystal quartz deposit is situated on the eastern slopes of the South Ural Mountains. In the Soviet era Kyshtym's plant supplied 60% of domestic high purity quartz demand used to make clear glass for microelectronics and optical applications. Little is known about Chinese Donghai Pacific Quartz although it is understood to serve domestic markets. In Asia, Japan's influence is large especially in Southeast India and in SriLanka. Japan once imported quartz lumps from these regions. However, government-led efforts on the part of the quartz supplier countries were launched to stop the export of unrefined quartz lumps and to support the development of quartz processing within the country. Today these countries specialise in the production of high purity filler materials for epoxy moulded compounds (EMC) low in uranium and thorium used in the manufacture of computer chips.

Globally, the export of lump quartz has been diminishing for a variety of reasons. Both suppliers and consumers increasingly require quartz granules with the highest quality specifications. This is beneficial for suppliers who add more value to the quartz product by improving refining techniques. For consumers it saves processing cost and enables them to concentrate on their core business instead of investing in purifying steps to improve the raw material.

Given its strategic relevance to the semiconductor and photovoltaic industries many more high purity quartz deposits are under development. However, the exploration and exploitation of new suitable quartz deposits is hampered by quality assurance regulations, which are globally applied. Whilst traditional sources of quartz have been questioned in quality terms, it is in their interest to demonstrate that their material is tested and meets the standards of silica glass production. Suppliers from new quartz deposits have yet to achieve this status. This is achieved normally in several consecutive cycles of tests with increasing quantities of test material. These tests must be carried out for many of the product groups in the various application areas. These pre-business services are expensive but made necessary by increasingly strict quality regulations. They require certain personnel expertise from the potential new suppliers (e.g. for the provision of relevant raw material) and highly specialised cooperation partners well recognised within the industry [4].

2.3.1 Geological Impact

Sedimentary SiO_2 rocks are the main suppliers of SiO_2 raw materials in the industry. High-purity quartz sands represent an extraordinary geological material, which is characterized by specific properties such as extreme chemical purity and grain-size distribution. Such deposits have formed under specific geological conditions, e.g., intensive weathering, beach deposits and reworked quartz rich sediments.

Although more than 90% of quartz and other SiO_2 minerals of the lithosphere are present in magmatic rocks [15], only about 1% of industrially used SiO_2 raw materials derive from this source. The majority of quartz in SiO_2-rich igneous and volcanic rocks (granite, rhyolite) is intergrown with other rock-forming silicates. Therefore, quartz from these rocks does not play an important role as raw material. The only exception is the extraction of high-purity silica material by chemical leaching from alaskites (so called Iota quartz) [16].

Knowledge of the interrelation between genesis- specific properties- parameters for technical application of the raw material is necessary for a successful use in many industrial applications. Therefore, for the evaluation of the usability of SiO_2 raw materials for a specific application, the

limiting properties, e.g. chemical purity, are essential (e.g., Blankenburg et al. 1994; Götze 1997; Müller et al. 2005) [9, 17]. The correlation between formation and industrial use of silica has been trying to be explained by Table 2.2.

Table 2.2: Interrelation between genesis and specific properties of different types of SiO_2 raw materials and their preferred application in the industry [4]

Quartz Type		Properties	Preferred Application
Magmatic/ postmagmatic	Quartz of alaskite (‘‘Iota quartz’’)	Chemical purity	High-purity SiO_2 material, optics, lamp tubing, semiconductor and solar silicon
	Pegmatite and Hydrothermal quartz	Chemical purity, perfect crystal order	Optical and piezo quartz, quartz synthesis (‘‘lascas’’), semiconductor and solar silicon, silicon alloys, glass
Metamorphic	Quartzite	SiO_2 up to >98%, lumpy	Refractory materials, silicon and Si alloys (e.g. FeSi)
	Metamorphogenic quartz mobilisates	Chemical purity	Quartz synthesis (‘‘lascas’’)
Sedimentary	Quartz sands	Chemical purity, granulometric properties	Glass and foundry industry, cristobalite, quartz powder, silica glass, SiC
	Quartz gravel	Chemical purity, grain size	Silicon and Si alloys (e.g. FeSi), building industry
	Sedimentary quartzite	Chemical purity, cryptocrystalline silica	Refractory materials (silica stones)

2.4 Demand Situation

Silica is a widespread mineral and occurs in relatively large quantities. Because of their geographic distribution, environmental restrictions, and the strict quality requirements for some applications, not all resources are commercially viable. Overall, future growth in silica use is unclear.

The global outlook for high purity quartz using industries is positive with growth rates between 3 and 5%, specifically in certain lighting, semiconductor and photovoltaic applications. In the solar industry all signs point to further growth in the coming years.

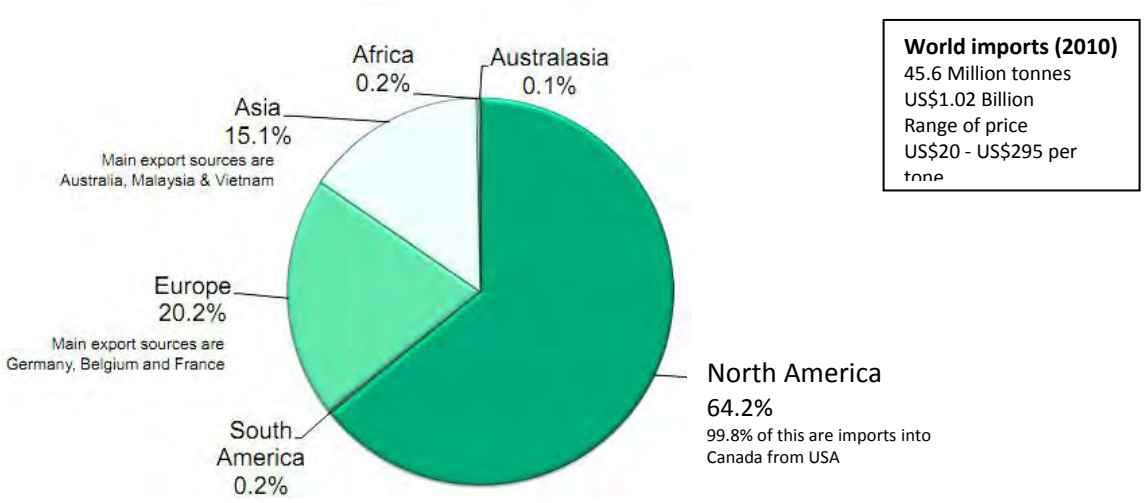

Fig 2.2 Billion US$ silica sand trade [18]

Production of c (crystalline)-Si in the 2007–2011 periods saw CAGR of 45% while Si-production for 2010–2014 is forecast to slow to CAGR in the 20–30% range reaching 300,000–400,000 tpa in 2014 (2010: 170,000 tpa). In 2010 solar cell production was up 118%, compared with 2009, when more solar cells were produced than the combined total in all prior years. Grid parity has now been achieved in a number of countries. Based on the demand in high efficiency cells, mono c-Si is expected to keep around 30% share at least for the next 3 years. However, new multi-pulling production techniques (recharging) and larger diameters of the monocrystals will demand more voluminous crucibles, i.e. less crucible silica glass per kg of monocrystal produced (volume to area ratio). Hitherto, mainly small furnaces with crucible diameters between 1600 and 2200 were used for PV applications. More recently, however, the same sizes for crucibles as are used in the semiconductor industry are being requested. Therefore, the increase in high-purity quartz granule consumption will not equal the upcoming growth in c-Si monocrystal production, but it is still estimated at above 5% p.a. Manufacturers of solar silicon are looking to remain competitive

by pushing production costs down. The result might be a process of consolidation: in 2012, the four largest producers alone—OCI, Hemlock, GCL and Wacker—could probably cover worldwide demand. Prices, which are currently still dominated by demand, should then fall and relate more to costs. This could attract new technologies which are based on high purity materials and less investment and operating costs to enter the solar silicon market. On the other hand it will raise the demand in high quality quartz, specifically low in boron and phosphorus [4].

2.5 Resource Estimation

Related to the geological conditions at the time of formation, quartz often contains fluid and/or mineral inclusions (Roedder 1984; Rykardt 1995; Hyrsl and Niedermayr 2003; Heaney et al. 1994) that need to be removed to meet stringent requirements for high purity applications. In addition detailed information about structural impurities in quartz (Flem et al. 2002; Götze et al. 2004) are of interest since they may define the economic limits in purifying the raw silica sand. In order to achieve maximum value, process technologies need to be adapted to the specific characteristics of each quartz deposit. Remnant fluids, from which quartz crystallised, occur trapped within individual crystals as do different types of mineral inclusions such as iron oxides, phosphates, silicates and heavy minerals. These inclusions need to be identified by analytical methods in order to determine what beneficiation processes will be used to remove them, as they are undesirable impurities that detract from the quality of potential quartz products. Whilst chemistry is important in determining quartz quality it is equally important to identify quantity in order to determine how long, at a given production rate, a potential mine may produce economically viable product for at least, say, 20 years as a realistic resource/venture.

Hydrothermal vein-like quartz deposits usually comprise zones reflecting different periods of mineralisation. Zones vary enormously in thickness, with individual quartz veins ranging from less than 1 up to 500 kt. Massive quartz deposits in similarly zoned pegmatites, essentially very coarsely crystalline hydrothermal host rock fissure fillings, are basically of larger volumes (up to 5 Mt) while metamorphic quartzite bodies are usually of even larger dimensions but of lower quality. In contrast, silica sand deposits are typically loosely consolidated and are of little prospect for economically viable high purity applications.

International standards, e.g. Australia's JORC or Canada's NI 43-101 codes, prescribe procedures to progressively identify, in terms of quality and quantity, the calibre of a given mineral resource from initial inferred status through increasing levels of detailed exploration and expenditure to

proven status primarily to attract and justify continuing investment in resource development before the start of extractive operations.

The main activity of geological assessment is field exploration including the mineralogical and chemical trace element analysis of samples collected from outcrops and/or drill cores showing the variation of quartz quality within the deposit. Drilling based on geological mapping and appropriate remote sensing techniques, determine the three dimensional extent of the mineralised body.

In order to reduce exploration costs information from initial drilling is combined with geophysical data derived from methods such as seismic, gravimetric, geoelectric or geomagnetic field surveys. Geophysical resistivity profiles apparent lateral variations in resistivity of rocks using a specific electrode array over constant distances in specific locations.

Vertical Electrical Sounding (VES) provides information on vertical variations in resistivity within a geological formation. Apparent resistivity values are correlated with the geological formations present to provide an interpretation of the extent of a deposit. This assists efficient drill hole siting, the results of which ideally confirm and complement, in greater detail, resistivity data.

Once a quartz deposit has been identified the precise quality of its mineral content and potential for quality improvement are key factors in determining its economic value. Representative samples are taken for detailed investigation to evaluate the potential of the raw material to be processed into a high value refined product. Determinative mineralogical techniques characterise any fluid and/or mineral inclusions that need to be removed by applying tailor-made processes. The combination of mineralogical characterisation across the whole deposit by means of representative sample analysis with the identification of appropriate specific processes to remove impurities is crucial to the thorough evaluation of any raw quartz deposit for high purity and high value applications [4].

This work doesn't intend to perform geological assessment to survey suitable deposits. Rather, focuses on material characterization based on application. The finding of application based suitable raw material is the base of deposit identification.

2.6 Silica Sand Reserve of Bangladesh

Bangladesh has rich reserve of silica sand as glass sand. According to geological survey Bangladesh (GSB), 94773 tons of glass sand has been exploited in Bangladesh during 1975-93

[19- 20] states, from the investigation performed by GSB in five districts (Balijuri, District-Sherpur, Noyapara- Shahibazar, District-Hobiganj, Noyapara- Chauddagram, District-Comilla, Lalghat-Lakma, District-Shunamganj, Madhyapara and Barapukuria, District- Dinajpur) the reserve of silica sand was recorded as 111.835 million tons.

Table 2.3: Reserve of Silica Sand in Bangladesh [20]

Area	District	Placement (from the surface, m)	Thickness (m)	Coverage (sq. km)	Reserves (million tons)
Balijuri	Sherpur	0.15- 2.4	0.15-2.6	30 lenses 0.596	0.64
Noyapara-Shahibazar	Habioanj	0.15-1.2	0.15-1.8	Length 15 km Width 0.5-1 km 36 lens ; 0.98	1.41
Noyapara-Chauddagram	Comilla	0.5-3.5	0.25-1.7	Length 16 km Width 0.5-1.5 km 34 lens; 0.234	0.285
Lalghat-Lakma	Shunamganj	23.78 & 72.95 Two Layers	1st Layer: 1.22 2nd Layer: 1.83	164 m towards concave	2.25
Madhyapara	Dinajpur	110-130	5.2- 16* (average 4)	1	17.25
Barapukuria	Dinajpur	118-180	16.48- 40.86 (average 21.90)	1	90

Table 2.3 contains the overview of glass sand deposits of Bangladesh. The 0.64 million tons of glass sand deposit of Balijuri, Sherpur has covered total area of 59610.08 square meters. GSB found the unwashed collected sand containing 83.77 to 93.79 % of SiO_2 and other noticeable components were Al_2O_3, Fe_2O_3 and TiO_2. After washing the sand with water the percentage of SiO_2 was 89.03 to 98.04 [21].

The detail study on the glass sand deposit of Chauddagram, Comilla was performed both on sand and glass sand. According to GSB, the grey to greyish yellow sand covered total area of 2, 33,741 square meters. The thickness was 0.15 m to 1.37m; unconsolidated. The sand was medium to fine grained, angular to sub angular and composed mostly of quartz. Decomposed plant materials were present in the sample. Another sample, collected by GSB was white and yellowish-white in colour. The yellow colour is due to ferruginous coating around quartz grains. The thickness was 0.15 m to 1.68 m; loose. The glass sand was medium to fine grained. Grains were angular and sub rounded and composed mostly of quartz. There were clay particles and mica particles present. Decomposed and partly decomposed plant materials were found. The collected sand sample was washed and dried in the sun and the percentage of SiO_2 was 91.48 to 97.86. The other noticeable components were Al_2O_3 and Fe_2O_3 [22].

2.7 Properties of Silica

The properties of pure silica are mentioned in Table 2.4. Though pure silica is very similar to the pure quartz but they vary in few characteristics.

Table 2.4: Properties of Pure SiO_2 [23]

Density	2.0-2.3 gm/cm3
Electrical conductivity	varies widely
Breakdown field	>1E7 V/cm in thermal oxides; can be as low as 1E6 V/cm in CVd oxides
Thermal conductivity	0.01 W/cm K (bulk)
Thermal diffusivity	0.009 cm2/sec (bulk)
Coefficient of thermal expansion	0.5 ppm/ K (Si thermal exp 2.3 ppm/K)
Refractive index	1.46 (thermal oxide)
Dielectric constant	3.9 (thermal oxide); CVD oxides vary widely depending on H

In Table 2.5 properties of quartz and fused silica are mentioned. Fused silica finds its use in semiconductor fabrication, laboratory equipment etc. because of its high working and melting temperatures. The optical and thermal properties of fused quartz are superior to those of other types of silica due to its purity.

Table 2.5: Physical, mechanical, thermal and electrical properties of quartz and fused silica [24]

Material	Quartz	Fused silica
Density (g/cm^3)	2.65	2.2
Thermal conductivity (Wm^{-1} K)	1.3	1.4
Thermal expansion coeff. (10^{-6} K^{-1})	12.3	0.4
Tensile strength (MPa)	55	110
Compressive strength (MPa)	2070	690-1380
Poisson's ratio	0.17	0.165
Fracture toughness (MPa)	-	0.79
Melting point (^oC)	1830	1830
Modulus of elasticity (GPa)	70	73
Thermal shock resistance	Excellent	Excellent
Permittivity (e') *	3.8-5.4	3.8
Tan (d x 10^4) *	3	
Loss factor (e'') *	0.0015	
Dielectric field strength (kV/mm) *	15.0-25.0	15.0-40.0
Resistivity (Wm) *	10^{12}-10^{16}	$>10^{18}$

Dielectric Properties at 1 MHz 25ºC

2. 7.1 Crystal Structure

The basic structural element of silica is the SiO_4 tetrahedron. Quartz consists of interconnected SiO_4 tetrahedra that build up a rigid three-dimensional network. There are many possible ways of connecting SiO_4 tetrahedra different from that found in quartz, realized in various other silica polymorphs. Since all of them consist of a three-dimensional SiO_4 network, all are classified as network silicates [1-2].

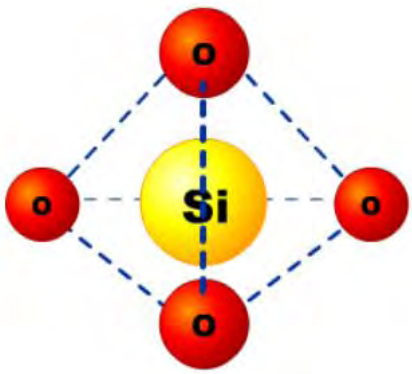

Fig 2.3: Tetrahedral coordination of silica (SiO_2)

Figure 2.4 (a) shows an idealized rendering of a quartz crystal with its most common shape. It is a six-sided prism with two six-sided pyramids at both ends. In most cases, the crystals are attached to a rock at one end, so they only show one six-sided pyramid.

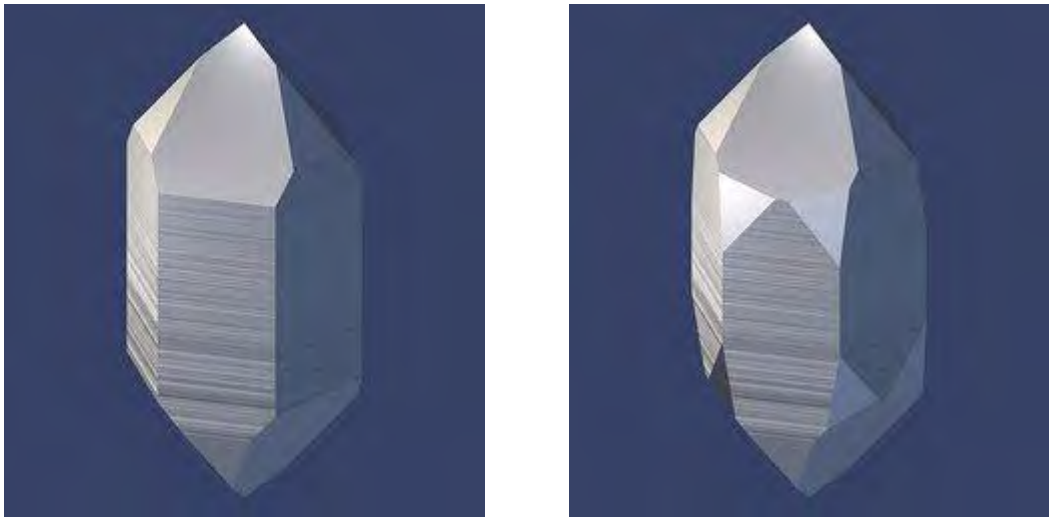

(a) Idealized Quartz Crystal (b) A Twinned Quartz Crystal

Fig 2.4: Quartz Crystal

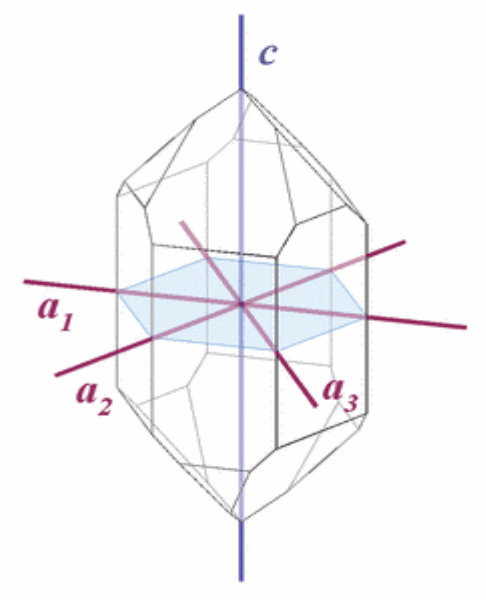

Fig 2.5: Crystallographic Axes

To describe the geometry of crystals, so-called crystallographic axes are used. These axes define a three-dimensional coordinate system within the crystals' structure, and of course - as one would expect for describing three-dimensional bodies - there are 3 axes labelled a, b, and c. For example, one can describe a crystal face as part of a plane that lies parallel to the a- and the b-axis and cuts the c-axis. This would work for quartz crystals as well, but for practical reasons and because of symmetry considerations, in quartz 4 axes defined in the hexagonal crystal system are used and labelled a_1, a_2, a_3, and c (Fig 2.5). The 3 a-axes intersect at an angle of 60° and lie on a plane (Fig 2.5, light blue), and the c-axis runs perpendicular to the plane and intersects all a-axes at an angle of 90°. Often there is no need to distinguish between a_1, a_2 and a_3 and one simply refers to the a-axis or a_0-axis.

Quartz crystals lack mirror symmetry. The mirror image of a quartz crystal is different from the original image, no matter where the mirror plane lies. Instead, quartz crystals show handedness: there are 2 types of crystals, left-handed and right-handed crystals. It is very well possible to find 3 mirror planes in Fig 4 that give perfectly identical mirror images: they run centrally through the m-faces. And this seems to be true of many real crystals, too. But this mirror symmetry is only an apparent one; the internal molecular structure of the quartz crystal cannot be mirrored: the atoms in a quartz crystal are arranged in parallel, corkscrew-like chains or helices. A helix lacks mirror symmetry and is always either left- or right-handed. The handedness of quartz is only visible on

quartz crystals that possess certain crystal faces. There is no inherent tendency in quartz to prefer one direction, and left- and right-handed quartz crystals occur at the same frequency.

2.7.2 Optical Activity

Substances that rotate the polarization plane of light waves passing through them are called optically active. This does not involve the polarization of unpolarized light, as described under "birefringence" - instead, polarization planes that are oriented differently will all be rotated by the same amount (schematically shown in Fig 2.6, identical angles of rotation are indicated by the turquoise sectors). This phenomenon has actually been discovered in quartz (by Dominique Arago), but is now better known from glucose sugar. Only enantiomorphous substances, those that lack mirror symmetry, can show optical activity. In sugar the individual molecules are enantiomorphous, so the effect can even be observed in a watery solution of sugar. In quartz the crystal structure shows enantiomorphy as a whole.

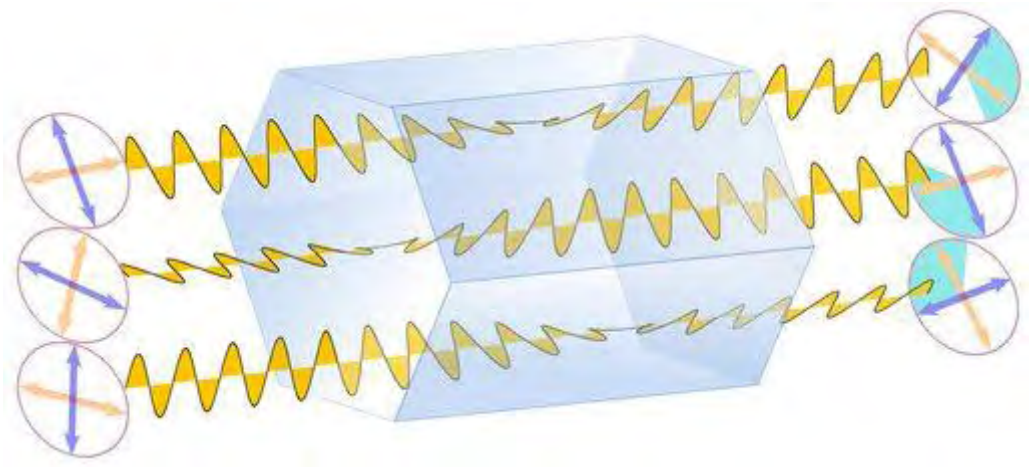

Fig 2.6: Optical Activity

If light passes a quartz crystal parallel to its c axis (from tip to tip), which corresponds to its optical axis, the orientation of the light is changed, while light that passes at an angle of 56°10' to the c axis will remain unaffected (Fig 2.7).

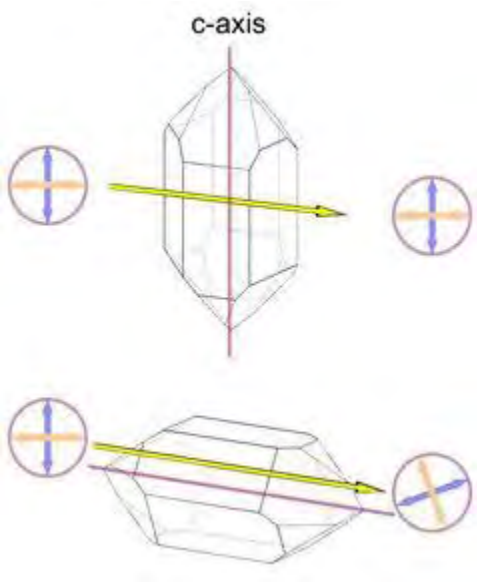

Fig 2.7: Directional Dependence of Optical Activity

The direction of the rotation depends on the symmetry of the crystal. There is right and left quartz, reflecting the orientation of helicoidal or corkscrew-like chains of SiO_4 units in the quartz crystal structure. These helicoidal SiO_4 -chains are oriented parallel to the c axis, so they run from tip to tip of the crystal. Interestingly, the polarization planes rotate in the same direction, either left or right, as the SiO_4 -chains.

So in an untwinned crystal these SiO_4-chains all turn left- or rightward. But in a Brazil law twin left and right quartz structures are intergrown and the effects of left and right quartz structures on the light ray will cancel each other out, at least partially. Brazil twins are accordingly called optical twins. In Dauphiné twins left and left or right and right structures are intergrown, and these crystals are as optically active as untwinned crystals.

2.7.3 Piezoelectricity

Many crystalline substances are made of electrically charged ions or molecules with an uneven distribution of electrical charges (inside the molecule, some atoms are more negatively and some more positively charged). In a Si-O bond the negative electrons get drawn more to the oxygen (such a bond is called polar, and oxygen is said to have a higher electronegativity than silicon), so the oxygen is more negatively and the silicon more positively charged. Of course, the crystal as a whole is electrically balanced. Figure 2.8 explains what happens if the SiO_4 tetrahedron is put

under mechanical stress (symbolized by blue arrows). The central silicon atom is surrounded by 4 oxygen atoms (one of them is omitted for readability).

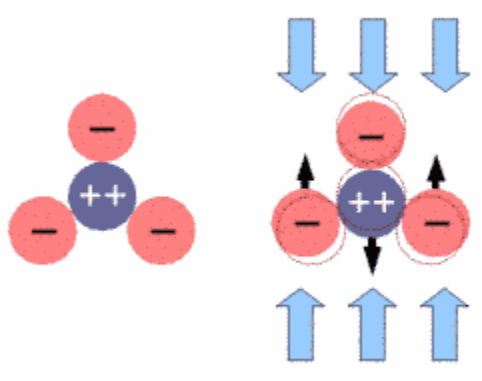

Fig 2.8: Effect of Deformation on Charge Distribution

Since every oxygen atom carries the same extra amount of negative charge taken from a silicon atom, the central silicon atoms carries 2 positive charges and the oxygen just one negative charge.

Under mechanical stress the atoms of the tetrahedron get displaced with respect to their former position (indicated by a thin red outline). The positively charged silicon is pushed away from its central position and the whole structure gets electrically polarized. If one reverses the direction of the forces, the silicon will be pulled upwards, resulting in an opposite polarization.

The direction of mechanical forces that is most effective in polarizing a quartz crystal is parallel to its a-axes, while forces parallel to the c-axis show no effect. There are 3 a-axes in quartz, however, only 2 different surface charge distribution patterns.

2.7.4 Dependence of Structure on Temperature

Silica is a polymorphic substance, capable of existing in several different forms, all having the same formula but differing in the arrangement of the structural units. Silica occurs in nature as five distinct minerals: quartz, tridymite, cristobalite, opal, and lechatelierite. Of these, quartz is very common; tridymite and cristobalite are widely distributed in volcanic rocks; lechatelierite (glass sand) is very rare. Opal and lechatelierite are amorphous. The three crystalline forms illustrate the phenomenon of enantiotropism. Each has its own stability field [25].

Conversion:

The three major crystalline forms of silica differ radically in structure, and although it is quite practicable to prepare cristobalite and (indirectly) tridymite from quartz, conversion is sluggish and involves breaking of silicon-oxygen bonds. The conversion may be summarized as follows:

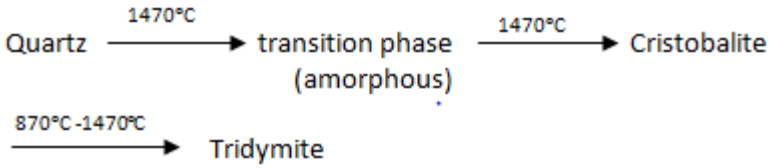

Inversion:

Although the principal three forms of silica are relatively stable within the temperature ranges, certain modifications do occur. Both quartz and cristobalite exist at room temperature in the so-called α-form, which is actually a distorted form of the structures.

In theory, at normal pressure trigonal quartz (α-quartz) transforms into hexagonal β-quartz at 573°C, upon further heating the SiO_2 is transformed into hexagonal β-tridymite at 870°C and later to cubic β-cristobalite at 1470°C. At 1705°C β-cristobalite finally melts:

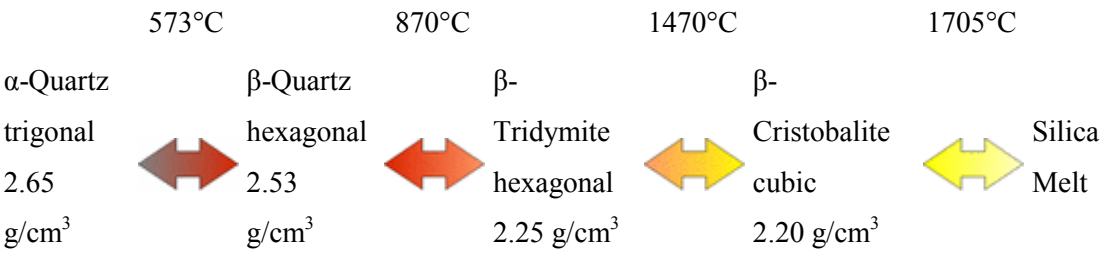

However, tridymite does usually not form from pure β-quartz, one need to add trace amounts of certain compounds to achieve this (Heaney, 1994). So the β-quartz-tridymite transition is skipped and the sequence looks like this:

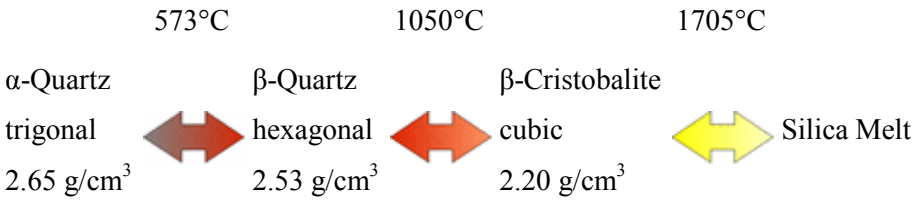

The changes in crystal structure lead to changes in the specific density: an increasing temperature corresponds to increasing vibrations of the atoms in the crystal lattice, and as these need more and

more space, more open crystal structures are favored. The atoms don't form an open structure in the first place, because the structure must also be in accordance with constraints on the geometry of the covalent bonds, in particular the angled Si-O-Si bond that connects SiO_4 tetrahedra.

As long as the temperature changes very slowly, the whole process is fully reversible.

But things get far more complex when the temperature is increased or decreased more quickly. If one heats up a quartz crystal very quickly, it will still undergo a phase transition to β-quartz, but the β-quartz will then "skip" the transition to β-cristobalite and directly melt at a much lower temperature, at 1550°C.

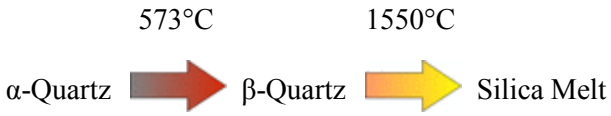

β-quartz has a lower melting point; it is less stable than β-cristobalite at that temperature and its crystal lattice is more easily broken up. So it doesn't really make sense to say that *quartz* melts at 1705°C, because low quartz never melts, and because the melting temperature depends on how quickly the temperature is raised. However, this process is not reversible. Instead, if a silica melt is cooled quickly, its liquid structure will be preserved and it will turn into amorphous silica glass, called lechatelierite when found in nature. There is no well defined melting point for silica glass which slowly turns into a very viscous liquid upon heating. It is often said that silica glass is an extremely viscous liquid, just like ordinary window glass, but both glasses are considered as regular solids.

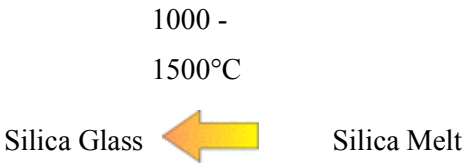

Even more strange is what happens to silica glass that is heated up: one would expect it to be converted to β-quartz, β-tridymite or β-cristobalite, depending on the temperature. But in fact it will simply turn into β-cristobalite, just as silica melt would.

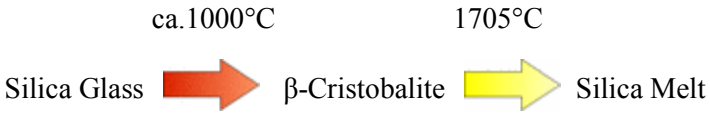

This conversion is of technical importance in the industrial production of silica glass, as great care has to be taken to avoid the formation of cristobalite crystals within the glass.

Table 2.6: Low Pressure Silica Polymorphs

high- or β-polymorph	**β-Quartz**	**β-Tridymite**	**β-Cristobalite**
stable at	573°C - 870°C	870°C - 1470°C	> 1470°C
metastable at	-	117°C - 870°C	270°C - 1470°C
crystal system	hexagonal	hexagonal	Cubic
Si-O-Si angle	153°	180°	151°
low- or α-polymorph	**α-Quartz**	**α-Tridymite**	**α-Cristobalite**
stable at	< 573°C	-	-
metastable at	-	< 117°C	< 270°C
crystal system	trigonal	triclinic	tetragonal
Si-O-Si angle	144°	140°	147°

If the polymorphs β-tridymite and β-cristobalite are cooled quickly below the respective transition temperatures, their crystal structure is first preserved until they are transformed into polymorphs with closely related structures, α-tridymite and α-cristobalite, at 114°C and 270°C, respectively:

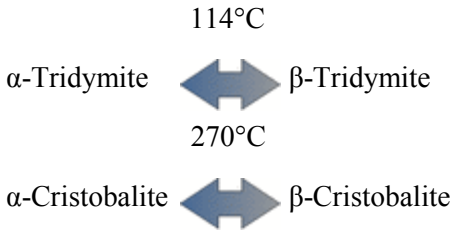

The transition is fully reversible even at relatively quick temperature changes, just like the transition of α-quartz to β-quartz.

At low pressures there are actually 3 groups of silica polymorphs each of which has 2 closely related members: one low-temperature member given an **α**-prefix, and one high-temperature member of the same name, but with a β-prefix. Some authors prefer a low-prefix and a high-prefix.

During the transition from a α- to a β-variant the atoms in the crystal lattice only get slightly displaced relative to each other, but they don't change places inside the crystal lattice (the

topology is preserved). Because these α-β-transitions are only based on alterations of the angles and the lengths of the chemical bonds, they take place instantaneously. Such a phase transition is generally called displacive, as it only requires relative displacements of the atoms without the need to break chemical bonds. Because the angular Si-O-Si bonds get straightened out, the high-temperature silica polymorphs all possess a higher symmetry than their low-temperature counterparts (hexagonal > trigonal > triclinic; cubic > tetragonal).

All the other transitions of one silica polymorph into another (like from β-quartz to β-tridymite) require the chemical bonds to be broken up and reconnected to alter the crystal structure. Accordingly, such a transition is called reconstructive. In general, complete reconstructive transitions between polymorphs need a lot of time. Quick changes in temperature do not allow for the complete rebuilding of the crystal structure, and the transition will be skipped. This is what happens when β-quartz directly melts at 1550°C without transformation into β-tridymite, and what happens if β-tridymite and β-cristobalite get cooled very quickly. β-tridymite and β-cristobalite can exist outside the temperature range at which they are stable, but as they will very slowly alter to another polymorph that is more stable at those conditions, they are called metastable polymorphs.

In Fig 2.9, phase diagram of silica is shown.

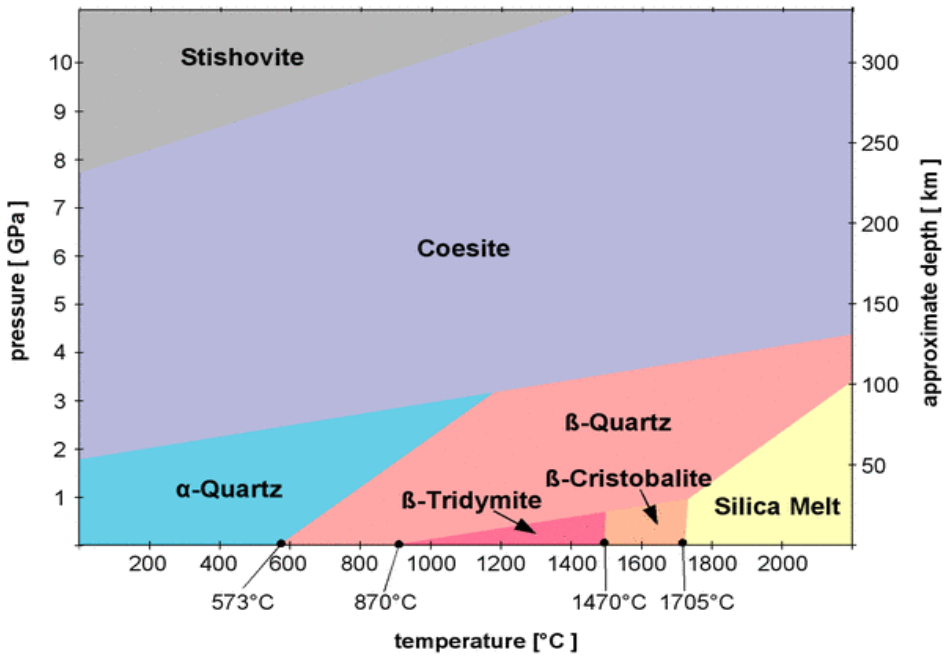

Fig 2.9: Phase diagram of silica [1, 2, 25]

2.8 Properties of High Purity Silica

For the production of glasses and ceramic materials silica with 95% purity can be used. Ceramic grade sand is less than 75 μm and has a silica content above 97.5%, impurities include <0.55% Al_2O_3 and <0.2 Fe_2O_3 [24].

The applications of high purity silica sand in the high tech industries are manifold. Specific requirements as to tolerable limiting values differ from industry to industry.

Silica is a fairly widely used ceramic material both as a precursor to the fabrication of other ceramic products and as a material on its own. For the production of silicon feedstock contains >98.5-99% SiO_2, <0.1%Fe_2O_3 and <0.15% Al_2O_3.

The main supplier of high purity quartz concentrates is the Unimin Cooperation, USA that mines pegmatite deposits at Spruce Pine, North Carolina. The quartz concentrate produced by the company is divided into several grades that have become world standards of high quality. The size of the worldwide market is estimated at about 30,000 tons per year for the 99.99% purity and above material [3]. The Unimin Cooperation sells the silica sand with the trade name as IOTA quartz, which is the ideal base material for the manufacture of fused quartz crucibles used in the Czochralski (CZ) process. Semiconductor device fabricators count on IOTA's purity and proven reliability for their diffusion and annealing process tubes, wafer etching parts and handling systems. Unimin's high purity quartz portfolio for semiconductor grade applications includes IOTA 4, IOTA 6, IOTA 6-SV, IOTA 8 and IOTA STD-SV. The impurity level of high purity silica (produced by Unimin) is shown in Fig 2.10. The low alkali content of these products results in fused quartz with high viscosity. This provides a high softening point and low crystallization rate, which extends part life and reduces the overall cost of ownership. Consistently low Boron (B) and minute levels of transition metals help maintain the purity of the silicon during crystal growth and wafer processing [26].

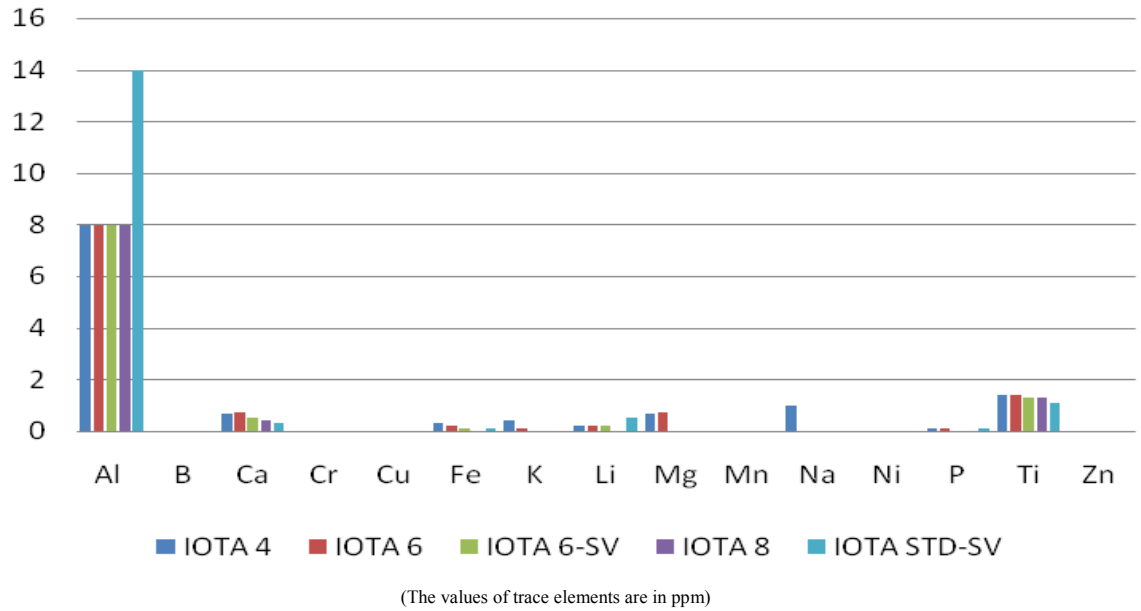

(The values of trace elements are in ppm)

Fig 2.10: Trace element concentrations of high purity quartz products sold on the world market [3, 26]

IOTA quartz is widely used in the photovoltaic industry for the manufacture of crucibles for Czochralski (CZ) single crystal silicon growth. This process is used to produce monocrystalline silicon solar cells which have the highest efficiency among commercial scale PV products.

IOTA CG (Crucible Grade) is the standard for the photovoltaic crucible industry. Crucibles made with IOTA CG are ideally suited for both long pulling times and multiple ingot pulling. In the most demanding applications, IOTA 6 can be used as a crucible liner to ensure the purity of the silicon ingot [27].

2.8.1 Important Properties of Silica for Processing Silicon in Carbothermic Process

Quartz and quartzite are the sources for silicon in the carbothermic process. Quartzite is mainly used for ferrosilicon metal production. This is because the purity of quartzites is usually lower than for other types of quartz deposits and thus is not suitable for silicon production. Nevertheless, relative pure quartzites may be used in the silicon process as well, especially if mixed with other quartzes. The industry has defined a list of absolute requirements to the quartz raw material that are necessary to achieve for the process to be optimized (Schei et al., 1998):

− Chemistry (e.g. Al, Ti, B, P, Fe and Ca)

− Lump size (typically 10 – 150 mm)

− Mechanical strength

− Thermal strength

− Softening properties

2.8.2 Established Industrial Test Methods

Today, the Si-industry uses an uncomplicated, but well approved method to test the thermo-mechanical and mechanical properties of silica. However, the test seems to be carried out after slightly different principles in the different labs - even within each company. Other methods for testing e.g. softening properties of quartz are not so frequently used.

The thermal test methods already established in the industry, and have been used during the last three to four decades, give good indications of the thermal stability of the tested quartz. However, the most of the methods are only indicative and give no final answer. Although tested quartz comes out relatively poor in the Elkem method (TSI), the quartz may operate well when used on a furnace in small or large amounts in a raw material mix. It has also been shown examples that poor quartz by the Elkem method may come out with excellent results using the Brazilian test. The differences of quality in the Elkem method and the Brazilian test may be because the Elkem method includes a mechanical test whereas the Brazilian test does not [28].

2.8.3 Properties of Solar Grade Silicon

In metallurgical grade silicon (MG-Si) the impurity level is referred as following (n ppm_w): for B 40, P 20, O 3000, C 600, Fe 2000, Al 100-200, Ca 500-600, Ti 200, Cr 50 [29]. The purity of silicon required for photovoltaic devices, which is called 'solar silicon', is 99.9999% (6N), which is less pure than that for electronics applications (11N). Table 2.7 shows the specification of solar grade silicon (SoG-Si) and it is a compromise between the necessary purity of SoG-Si and the reduction of manufacturing costs for dedicated SoG-Si [30].

The most annoying elements in the use of the quartz for the manufacturing of the photovoltaic cells are first of all the boron and the phosphor because of their difficulty of removal (by the technology of the metallurgical refinement. The maximal value is below 1 ppm for each [31]. The calcium, the aluminium and other metal oxides are also undesirable impurities in silica. To release an easy physical elimination of these impurities, it is better that these elements exists separately in minerals with a sufficient size grading, hence the importance of characterization and analysis of the undesirable elements as well as their distribution in minerals. The sand containing more than 500 ppm of iron and more than 800 ppm of aluminium is ready to be used in the industry of glass However in the photovoltaic field the required technological parameters are

stronger (Fe ≤ 100 ppm, Al≤ 400 ppm). That why the enrichment of high purity silica represents an obligatory passage, in the complete cycle of solar silicon grade production technology SoG [6].

Table 2.7: Chemical impurities in solar grade silicon [30]

Element	ppm	at/cm3
O	1	$5x10^{16}$
C	1	$5x10^{16}$
B	0.5	$2.5x10^{16}$
P	.025	$1.25x10^{16}$
As	.025	$1.25x10^{16}$
Fe, Al, Cr, Ni, Ti, Mo, V, Cu, Zn	Summed maximum 0.1	$5x10^{16}$
Concentration of each not mentioned metal		$<5x10^{16}$

It is already mentioned that the photovoltaic manufacturing of cells requires the use of a very pure silicon (purity > 99.9999 %), but the purification of the silicon begins with an enrichment of the silica, until a purity superior to 98 % to prepare it for the next stage which is the carbo-reduction to obtain a silicon solar grade at 99.95 % of purity, then a purification by chemical or pyro-metallurgical way for obtaining a silicon solar grade [6, 32].

The increasing demand of SoG-Si in 2004 and 2005 led to a shortage of SoG-Si for PV in 2005 which triggered additional discussions about the upper purity level for SoG-Si. To achieve solar cell efficiencies of 17 or 18% on multi-crystalline silicon wafers in particular it is crucial to minimize the level of transition metals in the raw Si material. To achieve low enough impurity levels, usually it is essential to use a method that involves easily cleanable silicon compounds like trichlorosilane (TCS) or monosilane. In the last five years, different activities have been started or accelerated to purify metallurgical grade silicon by means of directional solidification including additional steps to remove boron and phosphorus. It is a significant challenge to achieve the mentioned impurity levels shown in Table 2.7 with low manufacturing costs [30].

2.9 Purification Method of Silica Sand

Silica sand purification involves the removal of structural impurities, fluid inclusions, and solid inclusions [33]. While structural impurities are not easily removed [34], fluid inclusions can be removed upon heating [28].

2.9.1 Physical Separation

SiO_2 is purified up to a certain level by physical separation process. Generally, the process of purifying silica sand comprises grinding, washing and desliming the sand to remove the major part of the clay-type binder, attrition- scrubbing, drying and heating.

2.9.1.1 Size Reduction and Screening

Granulometric properties (grain size, grain shape, surface properties) of silica can be significant in many applications (Table 2.2). Since particle size is important in the glass production Caballero et al. suggested grinding and screening for uniformity of particle size and better efficiency [35]. While using reverse flotation technique D. Mowla et al. crushed the sand and sized between 150 to 840 μm to see the flotation performance. It was found that, as the particle sizes were reduced the removal efficiency was increased. This is reasonable because small size particles can be floated easier due to their lighter weights and their impure contents are more exposed to be removed [36]. Z. Zhang et al. observed that the particle sizes of the silica sand have a remarkable effect on the efficiency of iron impurity removal [37]. In case of iron removal by phosphoric acid, he suggested the optimum size of the sand to be 100 mesh. S.O. Lee et al. in his kinetics study screened the sand to fine (105–149 μm) and coarse sizes (0.5–1.4 mm) and isolated them [38]. The study showed, higher leaching rate was obtained by the fine particle size than the coarse particles because the interfaces of the liquid-solid reactants for the fine particles were much higher than for the coarse particles.

For glass production, crushing and grinding techniques need to consider both, to reduce the wear related contamination of the quartz to a minimum and to selectively liberate the mineral inclusions. Electrodynamic comminution is an enhanced technology to liberate impurities in high purity quartz crystals. It minimizes the amount of undersize particles and contamination. Since crystal boundaries host most of the mineral impurities, downstream processing is more efficient and expected yield increases significantly compared with mechanical comminution techniques. This makes electrodynamic comminution one of the favoured methods in high purity quartz processing. Classification then provides closely defined size fractions beneficial for further processing. Recent developments have proven the effectiveness of optical sorting for the production of high purity quartz. The technique separates the liberated components of raw materials on the basis of differing colour (or transparency) and shape, and may improve, or even replace, costly selective mining or hand

sorting practices. Fully automated sensor based sorting devices can be equipped with colour CCD-cameras, X-ray Transmission (XRT) and Near Infrared (NIR) technology for grain detection. After detection, non specified grains are selectively extracted from the bulk flow by a precise pulse of pressurized air from a high performance nozzle system. A specific benefit has been achieved for size fractions well below 40 mm, where manual sorting is not economical. Down to the 3–5 mm range, optical sorting is applied with high efficiency.

Optical sorting may be used to separate differently coloured quartz fractions such as patches of rose quartz, critical in solar applications owing to elevated phosphorus concentrations or smoky quartz with radiation induced discolorations. In addition clear quartz can be separated from milky quartz, being rich in fluid inclusions, and thereby often reduce the alkali content (Table 2.8) and improve the melting characteristics.

Table 2.8: Chemical characteristics of a quartz sample after optical sorting

	Al	Fe	Na	K	Li	Ti	Zr
Quartz transparent	23	0.3	6.2	0.6	2.1	1.3	<0.1
Quartz milky	25	0.8	10	1.6	2.4	1.4	<0.1

Elements are in ppm range.

Standard size reduction and liberation of differing mineral constituents use jaw and cone crushers in order to reach the product grain sizes. However, these techniques introduce high amounts of contamination, owing to wear, especially into the fine product fractions. For high purity quartz alternative comminution techniques are applied:

• Autogenous grinding
• Electrodynamic fragmentation

In autogenous grinding the high purity quartz is ground on a bed of high purity quartz. By this comminution technology contamination from the wearing internal surfaces of the autogenous mill is minimised. Electrodynamic fragmentation liberates quartz crystals in the composite rock largely without contamination and with low loss of undersize particles. A high-voltage discharge generates shock waves within the quartz lump causing it to fracture along grain boundaries [39-41]. Since most of the mineral impurities are located along crystal boundaries down-stream processing (e.g. chemical treatment) is more efficient. Yields increase significantly compared with mechanical comminution techniques. Moreover, this new technology is ideal for selective liberation of gas and liquid inclusion

trails within the quartz crystals (Table 2.9).

Table 2.9: Chemical analyses of quartz sample 0.1-0.3 mm after conventional comminution and electrodynamic fragmentation

	Al	Fe	Na	K	Li	Ti	Zr
Quartz raw material	41	4.9	12	15	0.5	1.3	<0.1
Conventional communication	23	464	10	3.5	0.6	1.9	<0.1
Electrodynamic fragmentation	28	1.3	13	4.7	0.6	0.5	<0.1

Elements are in ppm range.

The company, Nordic Mining provides raw feedstock for SoG-Si production with a purity more than 99.95% [40, 42]. E. Dal. Martello et. al. describe a study evaluating and comparing the effect of electrofragmantation to conventional mechanical crushing using hydrothermal quartz from this company. The sample is collected from Nesodden deposit of Hardanger fjord, Norway. The process is shown in Fig 2.11 and the result is shown in Fig 2.12.

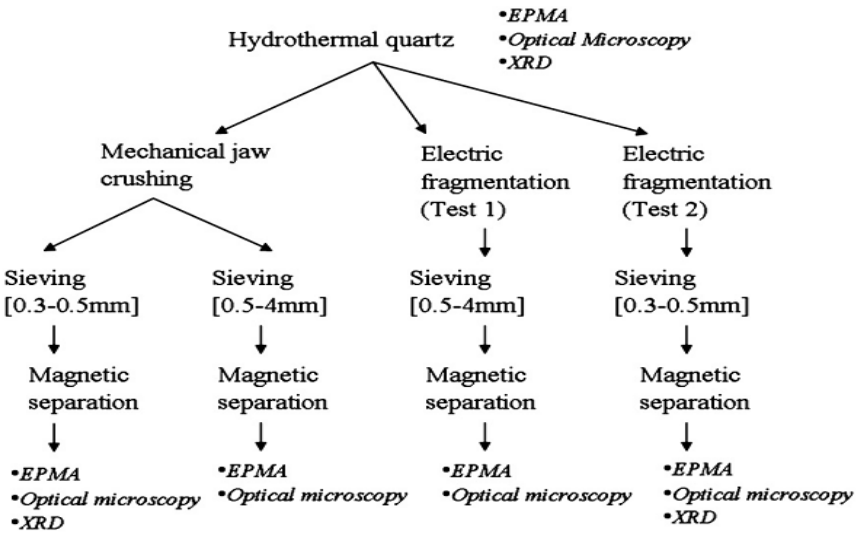

Fig 2.11: Experimental flow chart of routes for the refinement of quartz raw materials for trace mineral impurities

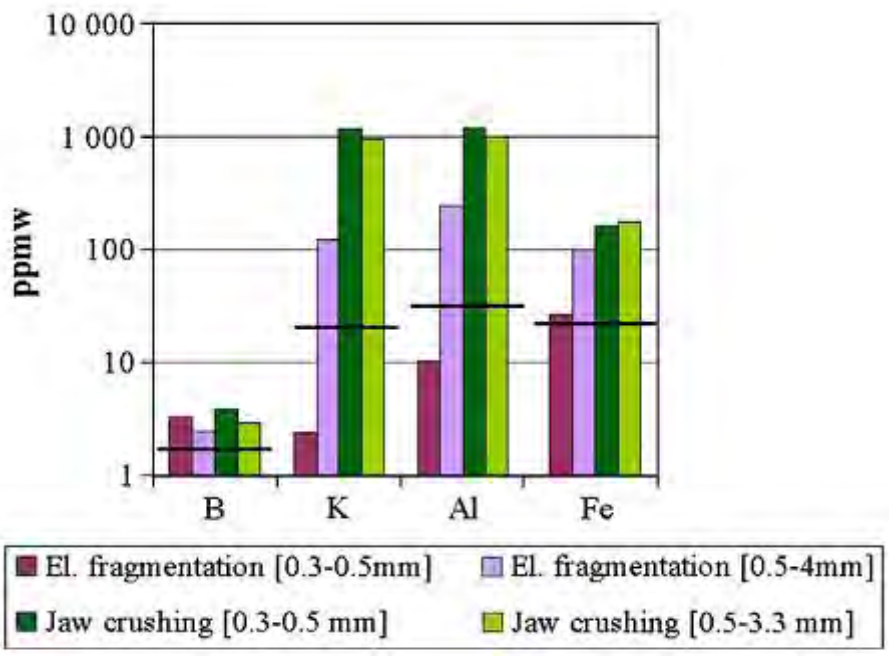

Fig 2.12: Bulk chemical analysis of the fragmented particles (in columns) and the original quartz composition (black lines)

2.9.1.2 Froth Flotation

Froth flotation selectively separates minerals according to differences in their ability to be wetted, enhanced or suppressed by conditioning reagents. Separation takes place in a water-filled medium into which the ore is fed to form a suspension which is agitated to avoid sedimentation processes. A frothing agent is added and air introduced to form rising air bubbles. Hydrophobic/Hydrophobized mineral particles (such as heavy minerals, feldspar or mica) attach to the air bubbles and rise to the surface forming froth whereas hydrophilic (wetted) particles remain below the froth layer in the suspension. The mineral-carrying froth is removed. Flotation process designs vary in complexity depending primarily on the type of mineral, degree of liberation, and the desired purity of the product. Slade et al. in US Pat No. 3914385 and Chubb, in US Pat. No. 3297402 describes processes to remove iron compound using froth flotation [43-44]. Another technique described by Caballero (Fig 2.13) refers purification process of silica sand to remove iron and aluminium impurities using frother [35]. D. Mowla et al. suggested a process to remove hematite using reverse flotation technique (Fig 2.14) [36].

2.9.1.3 High Tension Separation

High tension techniques separate minerals owing to differences in their surface conductance. For this processing step particles are uniformly passed through an electrostatic field. The electrostatic separator consists of a heated chamber where the electrodes are situated. The generated electrostatic field is up to 120 kV. Feed material is activated by heating the sample or by the addition of diluted acids to the feed material prior to heating. Typically, feldspar impurities may be separated from quartz via high tension as a dry alternative to froth flotation [4].

2.9.1.4 Magnetic Separation

Magnetic separation removes heavy minerals from silica as they are mostly paramagnetic or ferromagnetic. These minerals are attracted by a magnetic field. Silica, being diamagnetic, is repelled. Since magnetic susceptibility is strong in the case of ferromagnetic minerals only moderate magnetic field strengths are necessary for their separation, whereas higher field strengths are required to separate paramagnetic minerals. Kheloufi et al. describe a process for improvement of impurities removal from Silica sand by using leaching process, where sand sample from algerian deposit of Boussaada went through a magnetic separation on the laboratory scale [6]. Styriakova et al. describe a study on fine sand with a higher content of iron bearing minerals and clay minerals [45]. The impurities were removed by bioleaching and magnetic separation was conducted in the last step (Fig 2.15). The final product contained 800ppm of Fe_2O_3.

2.9.2 Chemical Treatment

Chemical treatment is an important addition to physical processing methods in order to achieve maximum purity silica through the removal of surface impurities. Acid washing, leaching and hot chlorination are the three chemical treatment processes. While acid washing uses less aggressive acids such as hydrochloric or sulphuric acid, leaching uses an advanced hydrofluoric acid process at elevated temperatures, to remove liberated surface impurities most effectively. In addition, those impurities enriched in micro fissures and along dislocations, will be liberated and removed owing to an enhanced dissolution rate of quartz in regions where impurities are concentrated. In the hot chlorination process, quartz is heated to temperatures of 1,000–1,200°C in a chlorine or hydrogen chloride gas atmosphere. This refining process is suitable to specifically reduce the level of alkali metal impurities (Table 2.10) which are highly restricted in lamp tubing and

semiconductor applications.

Table 2.10: Chemical analyses of quartz sample 0.1-0.3mm after chemical treatment [4]

	Al	Fe	Na	K	Li	Ti	Zr
Quartz after magnetic separation	21	0.2	3.1	1.0	2.2	1.2	<0.1
Acid Washing	21	<0.1	2.8	0.9	2.2	1.2	<0.1
Leaching	20	<0.1	0.7	0.3	2.2	1.2	<0.1
Hot chlorination	21	<0.1	0.2	<0.1	1.6	1.1	<0.1

Elements are in ppm range.

2.9.3 Elemental Separation

2.9.3.1 Removal of Iron and Iron Compound

Process for the removal of iron impurities have been known for long, and most of them rely on the basic old principle of converting the iron insoluble impurities contained by silica, into water soluble compounds, in order to render their removal from the sand easier by washing and scrubbing and the like. Thus, the iron impurities are transformed into iron salts, and this solubilization of the iron has always been effected by treatment with a chemical agent. In the glass industries, sulphuric acid is used as chemical agent in the Sulphuric Acid Treatment (SAT) [46]. For years this technique is being used. For example, Knowles et al. described a process which includes converting the iron oxide of sand into a soluble iron salt by the action of an acid solution containing sulphuric acid and sodium chloride (US Pat 230621). Adams et al. suggested purification of silica sand by reducing the surface iron oxide content [47]. The reduction is achieved only in up to about 15% of the total iron content, and comprises subjecting the sand to treatment with a hot aqueous solution containing sulphuric acid and a soluble inorganic chloride, said process being carried out in the presence of metallic copper having a large surface area so as to give an ample metallic surface contact for the sand and the solution during the purification treatment. This process is useful to remove stains due to iron content but not useful for high purity silica production. Slade et al. described a process for purifying contaminated sand, which comprises firstly removing by froth flotation a plurality of contaminants such as the kaolin clays and siderite, then treating the resulting partially purified sand with sulfuric acid for a temperature sufficient to reduce the iron oxide content thereof, and finally filtering the aqueous sulfuric acid leach liquid from the sand and

drying the sand [43]. By this process can remove impurities for certain usage but cannot remove strongly adhered iron contents. In an attempt to increase the degree of purification Sturgeon et al. suggest a process which consists in treating the minerals with an aqueous solution which is free from fluorine ions and oxalic acid but in which the dissolved constituents consist essentially of metallic salts, one of which is selected from titanous sulphate and sodium shloride, and removing the purified mineral products. Due to technical and economical feasibility this process also has been disregarded [48]. In US Pat 2952516 iron is removed by the steps of adding hydrochloric acid and fluosilic acid as such to sand to form aqueous slurry, separating the sand water until substantially free of acid. But with unwanted impurities there is a loss of silica particles itself; therefore, this process is uneconomical. Bowdish et al. proposed a special leaching method for purifying sand and other particulate materials by a series of aqueous solutions of differing compositions, differing in concentrations of leaching component in the form of an acid, and in which aqueous solutions are fed to the top of the mass of the sand and permitted to drain through gravitationally with appropriate periods of the time between solutions for reaction, said solutions of differing compositions forming series which begin with solutions low in concentration of the leaching component and continue with solutions of higher concentration thereof until the solution of highest strength has been reached by about midway, and then reversing the order by reducing the concentration of the solutions until water is reached [49]. But due to process complication and uneconomical characteristic this process also has not gained popularity.

Caballero et al. describe a process of purifying silica sand by series of steps (Fig 2.13).

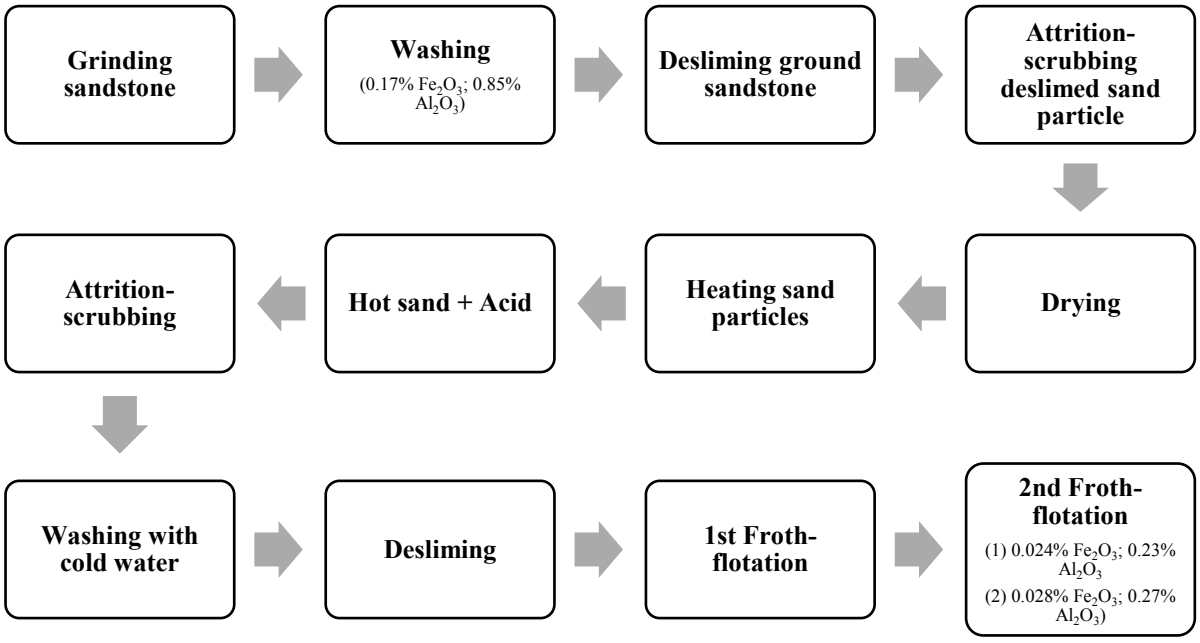

Fig 2.13: Process for purifying sand

The process comprises grinding sandstone, washing and desliming the ground sandstone to remove the major part of the clay-type binder, attrition-scrubbing the deslimed sand particles to release further amounts of binder, drying and heating the sand particles, treating hot sand with sulfuric acid to convert the iron oxides, ferrosilicates and ferro-aluminuous impurities into water soluble compounds, attrition-scrubbing the hot suspension of the chemically treated sand to release the strongly adhering stains of said impurities, washing with cold water and desliming, conditioning the sand suspension with fatty acids or petroleum sulfonate collectors, a polyalcohol frothing agent and, if necessary, a mineral acid to bring the pH to from 1.5 to 7.0 carrying out a first froth-flotation with a fatty amine collector in the presence of sulfuric acid and/or hydrofluroric acid to activate the aluminosilicate and to remove the same at a pH of a from 1.5 to 3.5.

The product obtained was highly purified silica containing 0.024% to 0.028% Fe_2O_3 and 0.23% to 0.27% Al_2O_3.

Iron content can create a great damage to the colour and properties of silica. Till date, considerable efforts have been devoted to these targets [50-60], and some agreements have been obtained [50-54]. For example, leaching percentages of impurity iron from quartz sand by oxalic acid increase with higher leaching temperature [50,52–58,60], the smaller particle sizes [51,55], and the higher acid concentrations [54–57] usually; however, some

investigations still obtained discrepant conclusions because of the differences in systems, particle sizes, leaching temperatures and concentration of oxalic acid. For example, Taxiarchou et al. thought concentration of oxalic acid had almost ‘‘no effect’’ on leaching efficiency of impurity iron removal [50]; again, Du et al.’s experiments showed that leaching percentages increased with higher stirring speeds and ultrasound power [58], but Raman and Abbas indicated that the particle size of a similar hard material was independent of the input ultrasound power [59]. There also exist different conclusions on the rate-controlling step of silica sand leaching processes. For example, Martinez-Luevanos et al. [55] and Lee et al. [57] leached impurity iron by oxalic acid at 25–60°C from low grade kaolin (60 lm on average, the same below) or silica sand (123 lm), they thought that the product layer diffusion was the rate-controlling step in the shrinking core model. Mgaidi et al. and his colleagues [60] dissolved silica by NaOH at 150–220°C, and concluded that the mechanism of the dissolving silica sand (154 lm) was a combination model, i.e. chemical reaction was the rate-controlling step at the initial stage, then transferred to the rate-controlling step of product layer diffusion.

Huang et al. describe an examination on the kinetics of iron impurity removal from extremely fine quartz of 45μm by oxalic acid was performed. The results showed that the leaching process was controlled by product layer diffusion step in the heterogeneous systems with activation energy of 45.37 KJ/mol. The leaching percentages of silica sand for coarse and fine sand, increase with increasing temperature, acid concentrations, and decreasing sample sizes. The study showed, for fine silica leaching percentages increased with decreasing speeds where as opposite phenomena occurs for coarse sand [61].

Mowla et al. describe a process that includes reverse flotation of hematite from silica sand of Iran using a batch, bench-scale mechanical flotation cell [36]. A first-order kinetics was obtained for the hematite removal from the silica sand over a wide range of particle size distributions (Fig 2.14). Z. Zhang et al. describe a study that use phosphoric acid as leaching agent in the purification of iron impurities from the quartz. H_3PO_4 has advantages of high leaching rate, low cost of production, simplified flow sheet, and of less harm to the target product. The iron removal efficiency has found to be 77.1%.

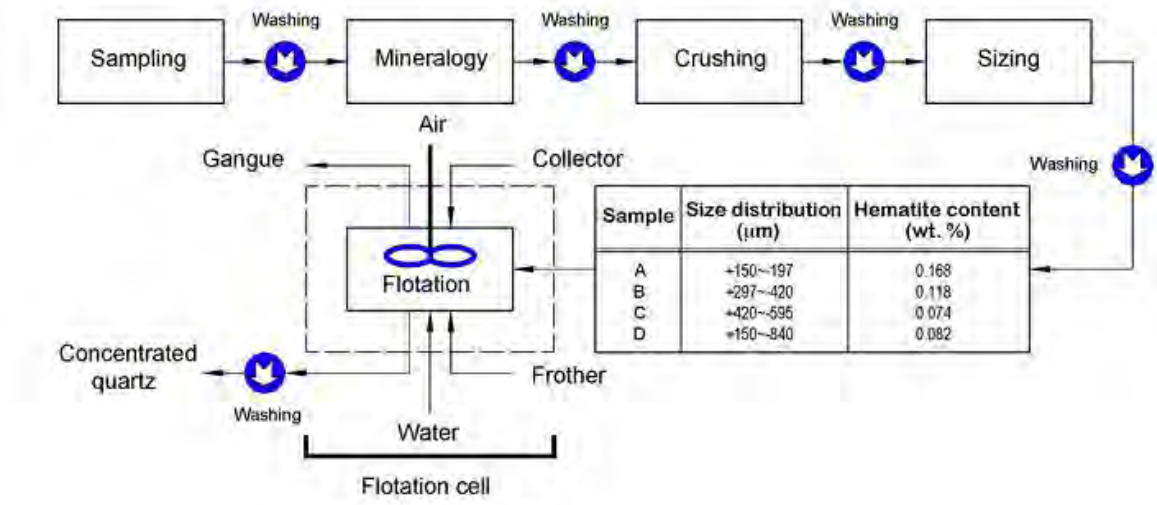

Fig 2.14: Block diagram of Hematite removal process using reverse flotation technique

Styriakova et al. describe a study that examines the in situ removal of undesirable constituents of impregnated particles from a quartz surface using indigenous heterotrophic bacteria and *Bacillus* spp. Bacteria [45]. The bioleaching of fine-grained fraction obtained from industrial washing of quartz sand (Fig 2.15). The result found could be very important for the quality improvement of silica sands.

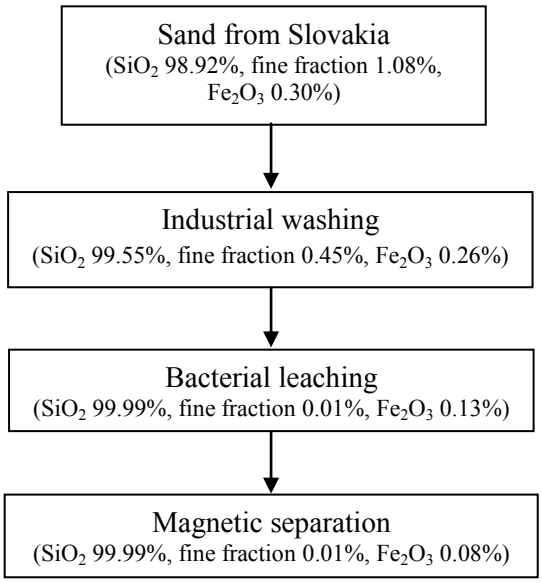

Fig 2.15: Bioleaching of clays and iron oxide coatings from quartz sands [45]

S. Ubaidini et al. describe a process to decrease iron content of ferrous quartz sands by fixed-bed column leaching with recycling of the leaching solutions in order to attain a product suitable for

industrial use [62]. Dissolution of iron was achieved by treating the sands in acid medium with oxalic acid as reducing agent to convert Fe^{III} into Fe^{II}. By the factorial experimentation, with 80°C temperature, 16 g/l OA concentration, attack solution pH as 2.5 and flow rate of 47.5ml/min (area of leach vessel: 4 cm_3) removal of 46.1% iron was obtained. The final product contained 0.0163% Fe_2O_3.

2.9.3.2 Removal of Aluminium and Aluminium Compound

Careful quartz clean-up usually results in Al concentrations of 10–100 ppm. Higher levels commonly (though not always) indicate the presence of impurities such as feldspar, muscovite or insoluble fluorides from the HF treatment. 99.5% pure quartz separate containing ~0.5% feldspar still has an Al concentration of ~1000 ppm.

Coke et al. describe a method of reducing the content of alumina in washed silica sands and in controlling the residual content of alumina to within low and narrow limits. The removals are based on froth flotation using a fatty acid amine collector. The final product contained not more than about 0.25 of refractory alumina [63]. But by this process silica particles would be carried away by the flotation froth together with silico-aluminates that the flotation process is intended to remove from the silica particles. To solve the problem Caballero et al. describe a process of purifying silica sand already mentioned in Art. 2.6.2.1. By the process mentioned in Fig 2.15 final product obtained as the amine flotation tails contain 0.23% Al_2O_3. Instead of neutral flotation if acid flotation is used the product obtained as the amine flotation tail contain 0.27% of Al_2O_3.

There is another popular method (Fig 2.16-2.17 and Table 2.11). To reduce the heavy metals like Al, silica sand is dried to reduce water content and diluted hydrochloric acid is added. Warm water bath with occasional shaking and supplementation of water is done.

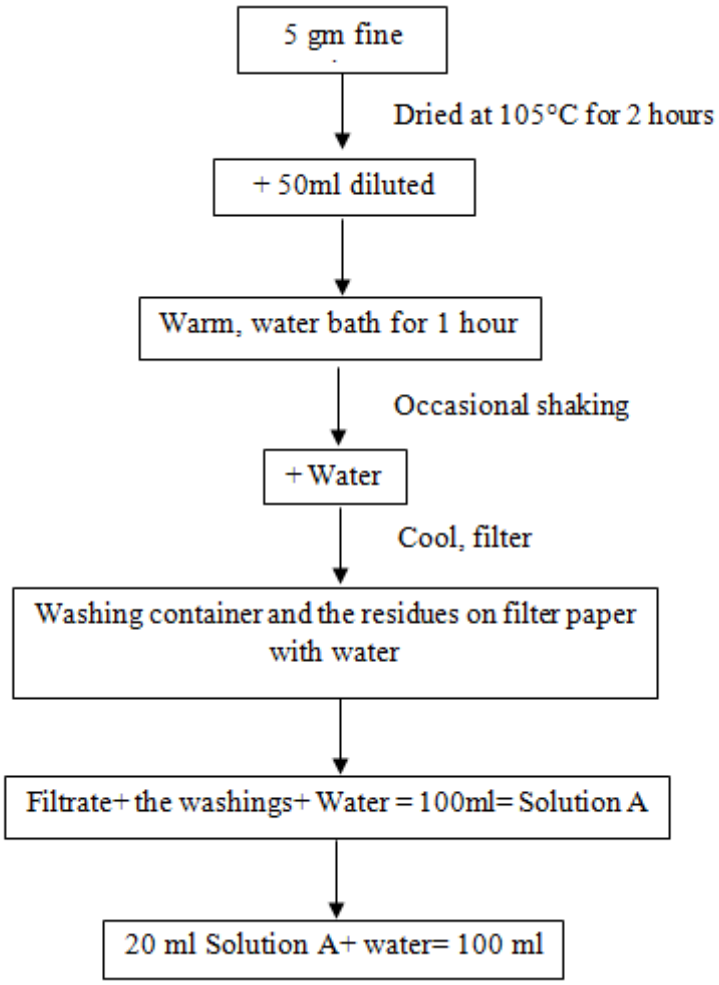

Fig 2.16: Test Solution for Aluminium removal

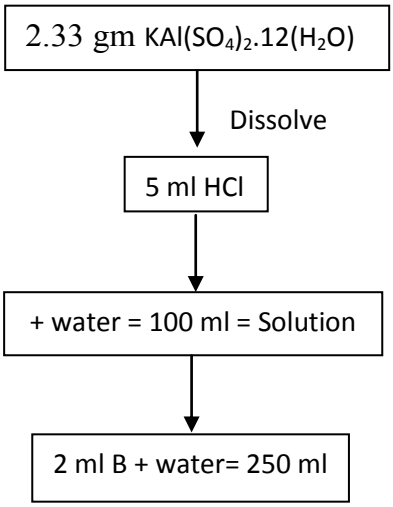

Fig 2.17: Control Solution for Aluminium elimination

The atomic absorbance needs to be determined under the operating conditions mentioned in Table 2.11.

Table 2.11: Operation Condition

Light source	Aluminium hollow cathode lamp
Wavelength of analysis line	309.3nm
Supporting gas	Dinitrogen monoxide
Combustible gas	Acetylene

The atomic absorbance of the test solution is not more than the control solution. The final product contains not more than 0.20% Al_2O_3. But even for small quantity this process is little complicated.

Stone et al. revised a method to separate Al and Be for AMS analysis from pure quartz samples. After adding Be carrier, quartz is dissolved in HF. The solution is sub-sampled for determination of total Al content, then dried to remove Si. Al and Be are separated from the remaining metals (typically Fe, Ti, alkalis, Mg and Ca) and purified in 3 stages. This method covers the first two: (i) Anion exchange in HCl (removes Fe^{III}), (ii) Cation exchange in dilute H_2SO_4 and HCl (removes Ti and alkalis, separates Be from Al). The third stage, hydroxide precipitation (eliminates residual alkalis, Mg, Ca), is carried out prior to loading cathodes for AMS. The procedure described below will cope with up to ~10 mg of Fe and 3-5 mg of Ti, assuming the total amount of Al, Be and other metals is less than 3-5 mg. It can be modified to accommodate larger samples by increasing the size of vessels, ion exchange columns, etc. Strength and quantities of reagents specified for the ion exchange procedures may vary, depending on the size of columns used, type and age of resin, etc. The ion exchange procedures should be calibrated independently before using this method on valued samples. Yields close to 100% can be obtained.

2.9.4 Routes to Process of High Quality Silica

As this thesis work put emphasis on silica as raw material for solar grade silicon, it should be mentioned that it is a long route to process the final product from the received raw silica. In Fig 2.16 a process route to produce the final product from silica sand containing > 98% SiO_2 is shown. Based on the composition of raw silica, purification method varies even for application in particular industry.

Whatever the method is used to achieve SoG-Si, the enrichment of high purity silica represents an obligatory passage, in the complete cycle of SoG-Si production technology.

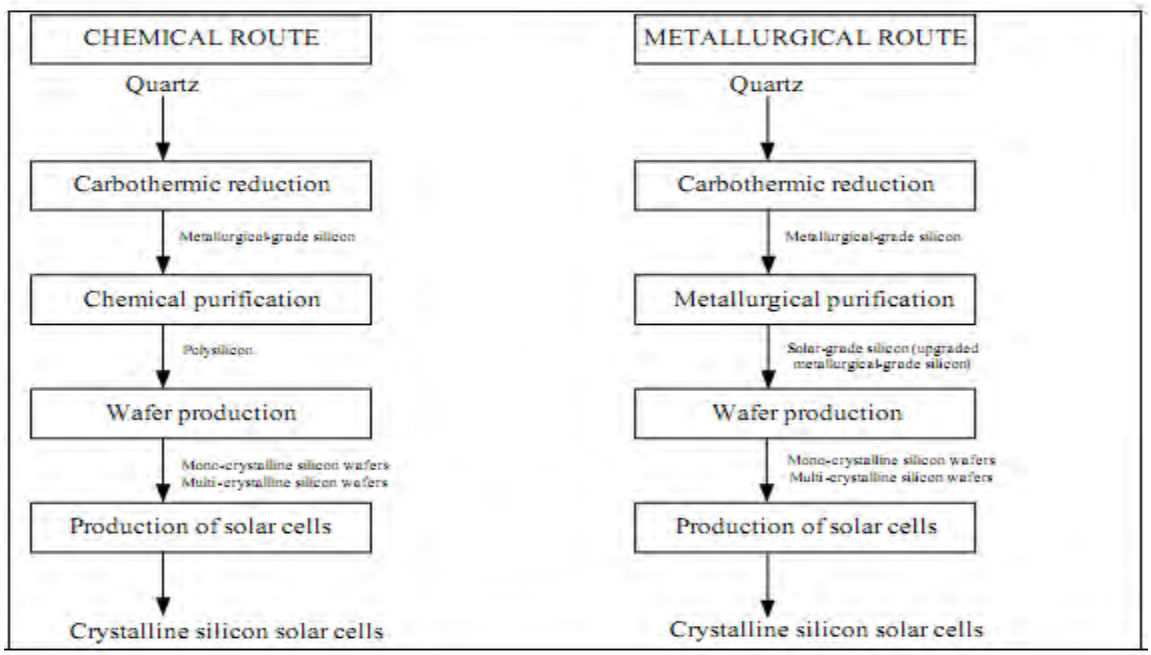

Fig 2.18: Stages for the production of crystalline silicon solar cells from silica [64]

Kheloufi et. al. describe a purification process of silica sand collected from Algerian deposit of Boussaada [6]. The method to purify silica by this process is shown in Fig 2.19.

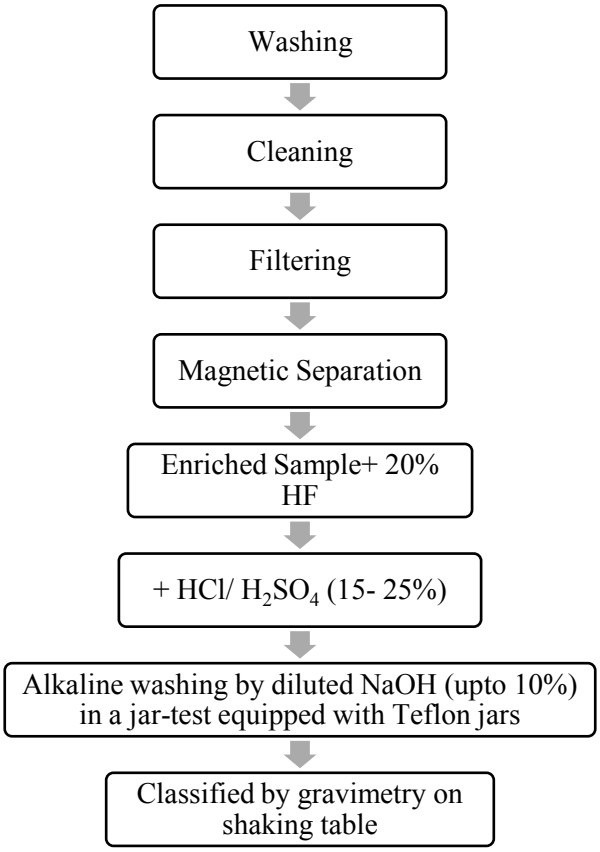

Fig 2.19: High purity silica processing method

In this process, after characterization and enrichment the sample was attacked by HF. HF is chosen for its chemical compatibility with silica (highly hydrophobic). It removes the most possible impurities, while leaving the molecular structure of silica intact. The second acid attack by hydrochloric acid (HCl) or sulfuric acid (H_2SO_4) is intended to remove the residual impurities (Fe, Al, and Ti) in solution. Finally, this acid attack is followed by an alkaline attrition using a solution at 10% of sodium hydroxide (NaOH) in order to eliminate the residual metal from the sand quartz surface. The result shows heavy metals; especially iron and aluminium are significantly eliminated.

2.9.5 Process Routes of Silica Upgradation Used in Bangladesh

Geological Survey, Bangladesh (GSB) uses the route describe in Fig 2.20 to separate pure silica from the sand.

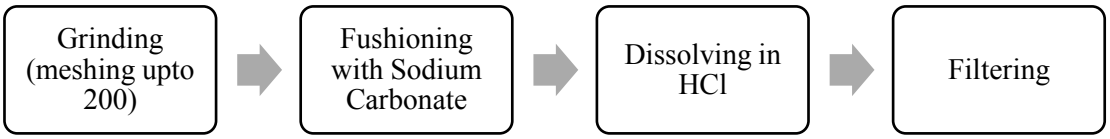

Fig 2.20: Separation of SiO_2

Sand sample is fused with Sodium Carbonate and the temperature is gradually increased to 1000~1200°C. The fusion is performed in a platinum crucible to make sure the least contamination. The ratio of $NaCO_3$ is kept at least three times higher than silica sand. Finally dissipated silica is found which contains 98- 100% SiO_2. Though this method is applied by GSB in regular basis but it is not feasible to be used industrially for two reasons- use of platinum crucible and inconsistency in reproducibility.

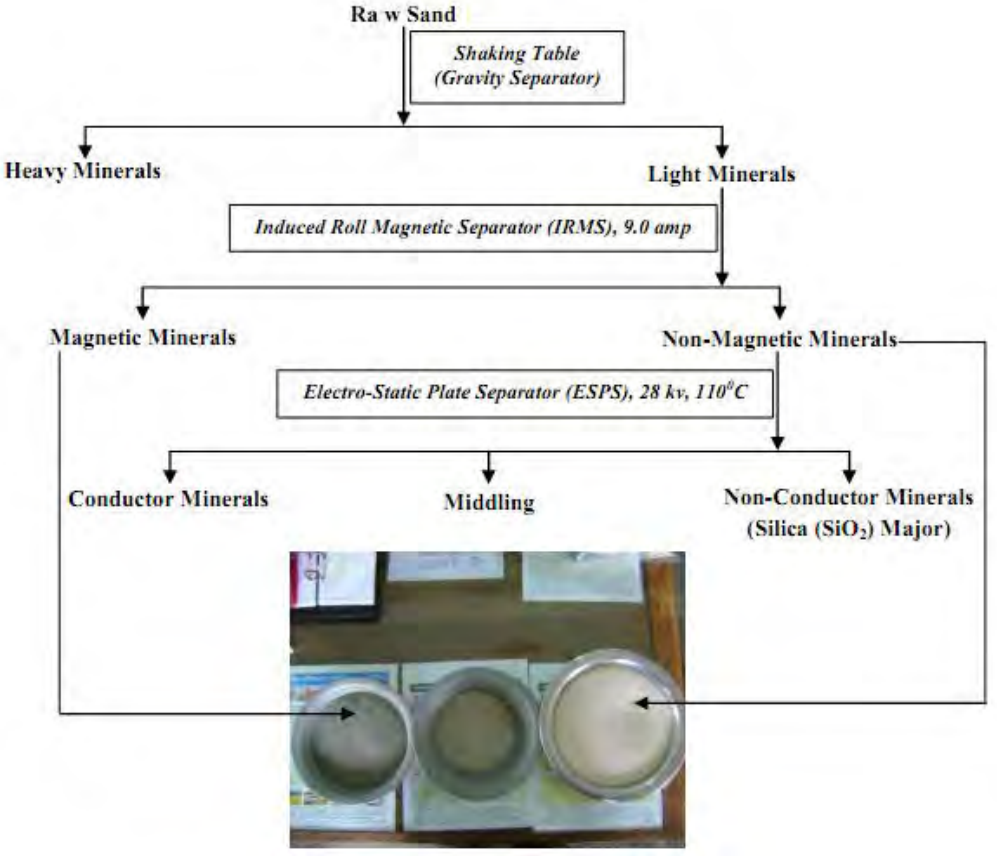

Fig 2.21: Generalized flow sheet for upgradation of silica in bulk sample of river sand

Rajib et. al. a process of physical upgradation of river silica of Bangladesh (Fig 2.21) [65]. This particular study is conducted to find use in the glass industry. But the process route is applied in the pilot project of Beach Sand Minerals Exploitation Center (BSMEC), Cox's Bazar using the

beach sand containing heavy minerals. Using very some physical separation procedures like density, magnetic and electric separation techniques different elements specially heavy minerals are separated at BSMEC. After separation the silica content can potentially be enriched upto 90-95%.

Chapter Three

Experimental

3.1 Sample Collection

For the thesis work 6 samples were collected from various sites of Bangladesh (Table 3.1). All of the samples are collected from little beneath of the surface. A white sand sample was collected from the site near shameshwari river- a locality called Bipinganj, sub-district Durgapur, district Netrokona. Currently this white sand is used in ceramic industries of Bangladesh.

Two samples were collected from different sites near Tista River- one from sub-district Patgram of Lalmonirhat district and another from a locality called Dalia, sub-district Jaldhaka of Nilphamari district.

Two silica sand samples were collected from two different locations in Sylhet District. Sylhet sand is known for its use in export quality glass making. Geological Survey, Bangladesh (GSB) has identified several deposits in/near Sylhet District [19-20]. In this work, a fine sand was collected from a locality called Sharighat near Shari River, sub-district Jaintiapur and a coarse sand was collected near from the bank of Dawki, Jaflong, sub-district Gowainghat of Sylhet District.

A study on a beach sand of Bangladesh has already been performed i.e. Cox's Bazar beach [65]. It's processed by Beach Sand Minerals Exploitation Centre (BSMEC), Bangladesh Atomic Energy Commission. BSMEC is studying the sample for about four decades. The processing method is similar to Art. 2.6.5. In this work, a beach sand sample was taken into account. It was collected from Kuakata beach (Sub-district Kalapara, District Patuakhali).

Table 3.1: Sand Samples

District	Locality
Netrokona	Bipinganj, Durgapur
Nilphamari	Dalia, Jaldhaka
Lalmonirhat	Patgram
Patuakhali	Kuakata
Sylhet	Jaflong, Gowainghat
	Sharighat, Jaintiapur

3.2 Characterization

The uses of silica sand depend on its mineralogy, chemistry and physical properties. Characterization of silica plays a vital role in choosing further beneficiary techniques. In this work, characterization is performed based on various parameters including composition, size, density, transportation, moisture content, material composition, crystallinity etc. The experiments conducted are totally influenced by the locally available facilities.

3.2.1 Material Composition

The characterization begins with bulk chemical analysis of representative samples of raw/ received silica. The results serve as a reference point for all processing tests in the later stages of the sample assessment procedure. The technique most appropriate for detection of major chemical impurities is X-ray fluorescence (XRF). Because it is non-destructive, multi-elemental, fast and economical if compare to other competitive techniques.

In the present study, XRF was used to determine the chemical composition of the material (Model: Lab Center XRF- 1800). The sample for X-ray fluorescence analysis was prepared in the following way:

1) About 2 gm of samples was finely ground in an agate mortar. The prepared powder was made moisture free.
2) The powder was placed in a die and then pressed in a hand press machine to prepare disk shaped sample for analysis.
3) The disk shaped samples were placed in the machine for analysis.
4) During analysis the following operating conditions were maintained:

   Atmosphere: Vacuum; Spin: On

   Channel: Radiation- 40 kV; 95 mA; For oxide- 20 deg/min; Step: 0.10

   P10 gas (90% argon and 10% methane gas mixture) flow rate: 5.0 ml/min

   Water flow rate: 4.1 L/min.

3.2.2 Morphology

The colour, size and shape of the samples were studied under stereo microscope first (Model: KYOWA Tokyo 802855). To understand the morphology samples were observed via polarizing microscope (Model: Nikon Eclipse LV100 POL) with the help of Michel-Levy interference colour chart.

Michel-Levy chart:

Quantitative analysis of the interference colours observed in birefringent samples is usually accomplished by consulting a Michel-Levy chart.

From the traditional Michel-Levy chart [66], it is evident that, the polarization colours visualized in the microscope and recorded onto film or captured digitally can be correlated with the actual retardation value, thickness, and birefringence of the specimen. In short, it is a key to identify minerals.

Most optical microscopes are equipped with ¼-lambda and 1-lambda plates and hence one can rely on different versions of the Michel-Le´vy interference colour charts. This is commonly a big challenge not helped by the mismatch between observed interference colours and those displayed in the charts. That is why further studies are done to revise the chart.

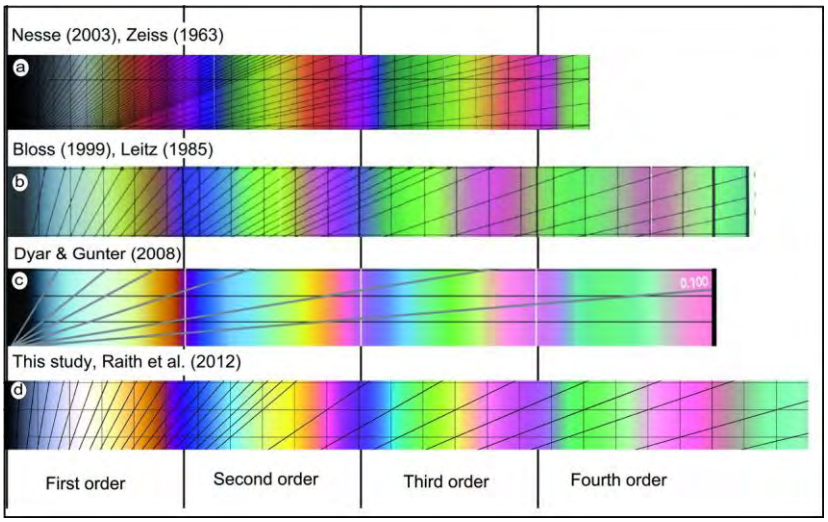

Fig 3.1: Comparison of the new chart with other available and commonly used charts. (a) The Zeiss chart, also used in Nesse (2003). (b) The Leitz chart, also used by Bloss (1999). (c) The quartz-wedge chart by Dyar & Gunter (2007). (d) This study, the calculated chart, now used by Raith *et al.* (2012) [67]

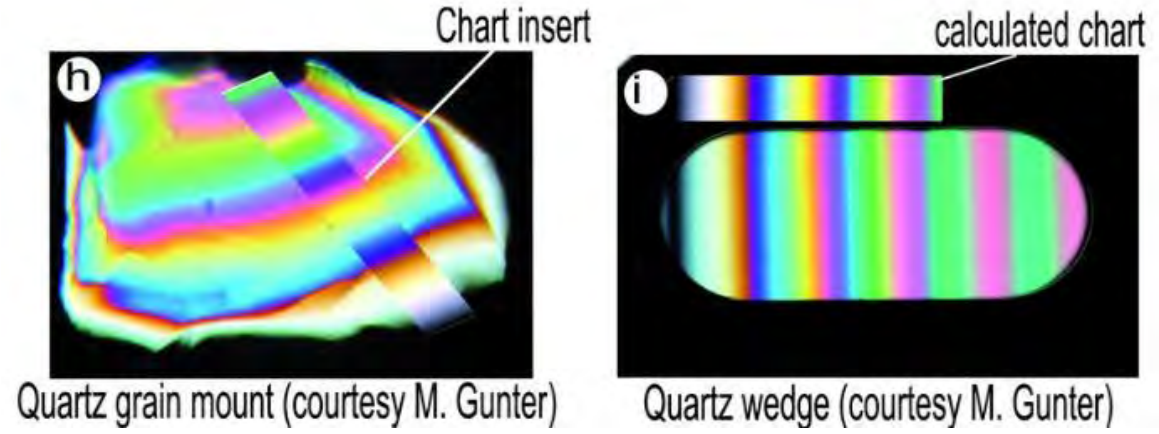

(a) (b)

Fig 3.2: Verification of the calculated Michel-Le´vy chart by optical microscope observations; comparisons for quartz in (a) immersion oil and (b) quartz wedge [67].

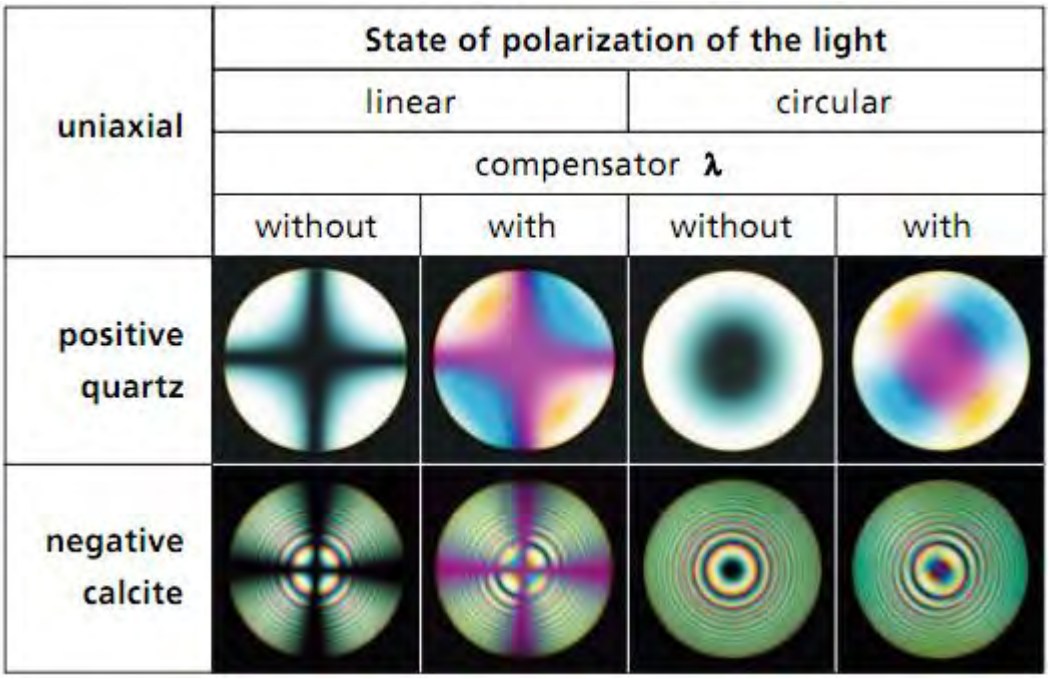

Fig 3.3: Determination of the optical character of uniaxial minerals in linearly and circularly polarized light. The reference direction ny of the λ-compensator is aligned in NE-SW.

To observe the morphology via polarizing microscope the analysis was performed in the following way:

1) About 2 gm of samples was taken and grain slides were made. It was made sure that

bubble formation is at minimum level and no moisture attacks the slide.

2) All sand samples were observed via polarizing microscope with magnification of 10X .25 Pol. (∞/- WD 7.0) to evaluate the silica percentage.
3) Later the result was compared to the silica percentage found by XRF.

3.2.3 Moisture Content

The Moisture content of sand is the ratio of the weight of water present to the weight of dry sand in a given sand mass. Moisture content plays an important role in understanding the behaviour of sand and clay. The property is used in a wide range of scientific and technical areas, and is expressed as a ratio, which can range from 0 (completely dry) to the value of the materials' porosity at saturation. Compaction of sand in the field is also controlled by the quantity of water present.

Moisture may be present as adsorbed moisture at internal surfaces and as capillary condensed water in small pores. At low relative humidity's, moisture consists mainly of adsorbed water. At higher relative humidity's, liquid water becomes more and more important, depending on the pore size.

The sample was placed in digital moisture detector (Model No: KERN RH 120-3) and the percentage of moisture was recorded.

3.2.4 Particle Size Distribution

For many applications size of silica is point of interest. In this work, particle size distribution was analyzed by Taylor sieve analysis (Model: Retsch, Type: AS000 digit)

A set of standard testing sieve was used to screen the sand (ASTME11). These sieves are stacked in sequence with the coarsed sieve at the top and placed in a sieve shaker.

About 100 g sand was placed at the top sieve and after 10 minutes of vibration at 60rpm, the weight of the sand retained in each sieve was obtained. The AFS grain fineness number of the sand was determined by taking the percentage of sand retained on each screen, multiplying each by a multiplier, adding the total, and then dividing by the total percentage of sand retained on the sieves.

AFS GNF= Total Product/ Total percentage of sand retained

The list of stainless steel-testing sieve with its size is given in Table 3.2.

Table 3.2: Testing Sieve

Sl.	Sieve series No.	Size (µm)
1.	6	3.35E03
2.	12	1.70E03
3.	30	600
4.	40	425
5.	70	212
6.	140	106
7.	200	75
8.	270	53
9.	Pan	

3.2.5 Roundness and Sphericty

Sphericity and roundness are two useful properties of particles (greater than sand size) in investigating the transport and deposition of sedimentary material. Sphericity measures the degree to which a particle approaches a spherical (round) shape. Roundness is the degree of smoothing due to abrasion of sedimentary particles.

The sphericity of a particle is determined by measuring the three linear dimensions of the particle; the longest diameter (a), diameter perpendicular to the longest diameter (b and a $\perp$ b) and diameter intersecting the other two at 45° (c).

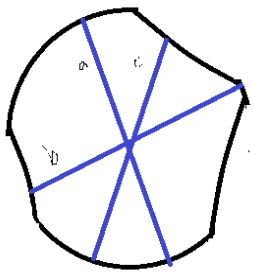

Fig 3.4: Sphericity Measurement

Sphericity= (a+ b+ c)/ 3: a

The resultant closer to 1 is more sphere in shape.

From the sphericity it is going to be identified if significant erosion has taken place in its location or not. The more the sand resembles a sphere, the more erosion it has probably witnessed.

To measure the sphericity, the samples were studied under optical and scanning electron microscope (SEM). SEM provides information about the sample's surface topography and composition. It was performed for all the samples to observe the size and shape of the samples (Model No: Philps XL30).

The sample for SEM analysis was prepared in the following way:

1) Samples were adhered to the holder.
2) Samples were gone through Agar auto sputter coater.
3) They were dried and then observed via SEM.

The sphericity measurement like Fig 3.4 was intended to be performed. But the current facility doesn't provide any means to measure in z- axis. With available facility, height and width of sample can be measured in the manner of Fig 3.5.

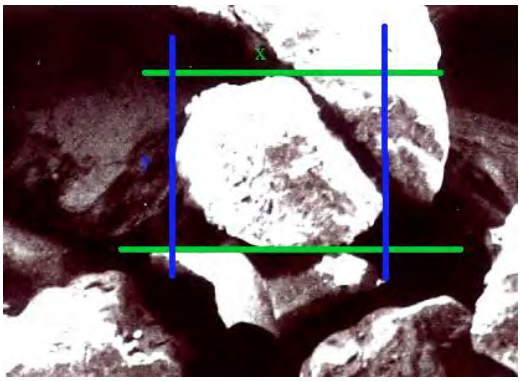

Fig 3.5: Measurement of Sand sample via SEM

Thus, to complement the task of sphericity measurement, the images found by stereo microscopic analysis were gone the previously mentioned procedure (Fig 3.4).

3.2.6 Density Measurement

The density of silica sand is defined as the quotient mass M and volume V:

$$\rho = M/V \ g/cm^3$$

The density of sand can be measured by various methods. The pycnometer method was used to determine the density of the sand.

In order to determine the density three parameters required-

i) The mass of the material
ii) The volume of the material
iii) The temperature at which determination was carried out

Using the pycnometer method, the density of the test specimen is measured by determining the weight of a volume-calibrated pycnometer filled with a certain quantity the sample is immersed. The sample volume equals the pycnometer volume minus the displaced volume of liquid of known density. The method however requires that the liquid is used to immerse the sample be less dense and must be totally inert to the sample, i.e. the liquid must not cause any swelling or salvation of the test sample. The liquid must also be non-volatile during the course of the experiment.

In this method an empty pycnometer of 50 ml capacity (V_p) was weighed (W_p). It was half filled with silica sand sample and was weighted ($W_p + W_s$). Then the density bottle was filled with distilled water and weighed ($W_{P+}W_s+W_{rl1}$). The sample of sand and water were removed and the pycnometer was again filled with water and weighed ($W_{P+}W_{rl2}$). The bulk density of the sand sample was determined as follows:

Calculation:

Weight of the solid sample, $W_s= (W_p + W_s) - W_p$

Weight of the liquid, $W_l= (W_p + W_{rl2}) - W_p$

Density of the liquid, $\rho_l= W_l/V_p$

Weight of the liquid used to immerse the solid sample, $W_{il}= (W_p+ W_s+ W_{rl1}) - (W_p + W_s)$

Volume of the liquid used to immerse the solid sample, $V_{il}= W_{il}/ \rho_l$

Volume of the solid sample, $V_s= V_p- V_{il}$

Density of the solid sample, $\rho s= W_s/ V_s$

The room temperature during the test was 20°C.

3.2.7 Phase Identification

To study the crystallinity X-ray diffraction (XRD) (Model No: Bruker D8 Advance) was performed.

X-ray diffraction is a rapid analytical technique primarily used for phase identification of a crystalline material. X-ray diffraction analysis is widely used in the study of sands primarily to identify the phases present in a particular sand sample. At ordinary temperatures quartz is always present as low quartz. But it is possible to determine the original crystal form [68].

XRD was performed for all five sand samples.

1) The diffraction patterns were recorded in the 2θ range of 5° to 85° with a Cu K_α radiation (λ=1.5406 A^o) with an accelerating voltage of 40 KV. The step was 0.02°, step time 0.6s. The study was conducted at room temperature (25 °C). 2θ= 5.000° and θ= 2.500°.

2) The diffraction lines in the recorded patterns were matched with data in the Powder Diffraction Files of ICDD (International Center for Diffraction Data). Major peaks in the diffraction pattern were marked.

The operating conditions that were maintained during the recording of the patterns were:

Voltage and current: 40 KV and 30 mA
Water flow rate: 4.7 L/min
X-ray generator source: Cu anode [Wavelength of CuKα: 1.54016 A^o]
Window for X-ray filter: Be window

3.2.8 Dependence of Structure on Temperature

Thermo gravimetric analysis (TGA)/ Differential thermal analysis (DTA) was performed to the samples to characterize the thermal effects- to trace the loss of combined water and/or, change of polymorphic form (Model No. Seiko Instrument's EXTER TG/DTA A6300).

The experimental setup for TGA is mentioned below:

Reference: Alumina
Reference Weight: 2.83 mg
Temperature: 30°C to 1000°C at the rate of 20°C/ min

3.2.9 Organic Matter Content

Organic matter influences many of the physical, chemical and biological properties of clay, sand, soil. It affects the water holding capacity and the ceramic properties of the sand too. The presence of organic matter in sand may cause the development of a ‘black core’ (a central area of different

colour, varying from black to yellow in the ceramic parts). These black cores are not expected in the finished products. The organic matter in the sand sample was determined according to the ASTM D 2974 [69]. Firstly an empty, clean and dry porcelain dish was weighed (M_P). Then a part of entire oven dried test specimen was placed in the dish and the weight of the dish and clay specimen was determined (M_{PDS}). The dish was then placed in a muffle furnace and the temperature of the furnace was gradually increased to 440^OC and the specimen was left there overnight. Then the dish was removed carefully using tongs and it was allowed to cool to room temperature and the mass of the dish containing burned clay was determined (M_{PA}).

Calculation:

i) Mass of the dry sand; $M_D = M_{PDS}-M_{P.}$

ii) Mass of the burned sand; $M_A = M_{PA}-M_{P.}$

iii) Mass of the organic matter; $M_O = M_D - M_{A.}$

iv) Organic matter content; $OM = (M_O/M_D) \times 100.$

Temperature: 440°C (gradually)

Heating Rate: 10°C/ min

Time: 1306mins

The result was cross checked with the result found via DTA.

3.3 Beneficiation

Based on the result of characterization, the beneficiation steps were developed. The basic beneficiation steps were attrition, acid and alkali washing. Different variables were taken throughout the process and by trial and error method is applied to find the optimized point.

3.3.1 Attrition

At first the samples were washed without any stirring. Next, the sample was washed with distilled water for around 20 minutes at 600 rpm and 800 rpm. And the changes were observed. Based on the result, one sample was chosen (discussed later in Chapter 4) to proceed with and the optimized speed and time was determined in the following method:

a) To find out the optimum speed, the selected sand sample was washed with distilled water.

1) A mechanical agitation was used to wash the sample. The varying stirring speeds were: 400, 600, 800 and 1000 rpm.

2) The time of agitation was kept constant, i.e. 20 minutes.

3) Then the sample was dried at 100ºC.

4) The changes were observed with stereo microscope. To quantify the result, XRF was performed on the sample.

b) Next, keeping the stirring speed constant (at optimum speed found in the previous step) attrition was performed varying the time.

1) The varying times were: 10 minutes, 20 minutes, 30 minutes, 40 minutes and 1 hour.

2) Then the sample was dried at 100ºC.

3) The changes were observed with stereo microscope. To quantify the result, XRF was performed on the sample.

3.3.2 Acid Washing

Chemical treatment such as acid washing, leaching and hot chlorination is an important addition to physical processing methods in order to achieve maximum purity quartz through the removal of surface impurities. Less aggressive acids such as hydrochloric or sulphuric acid are used acid washing. Leaching uses an advanced hydrofluoric acid process at elevated temperatures, to remove liberated surface impurities most effectively. In addition, those impurities enriched in micro fissures and along dislocations, will be liberated and removed owing to an enhanced dissolution rate of quartz in regions where impurities are concentrated.

a) Without Mechanical Stirring

In the work, 5g of each sample were taken to be acid washed and no agitation was employed. The following procedure was followed:

i) Acetic acid, Hydrochloric acid, Sulfuric Acid was primarily selected. The experiment started with 1% concentration of acid, keeping the acid to sand ration 1:1.

ii) Next with 5% concentration of acids, again without mechanical stirrer, samples were washed. Then, the ratio was increased to 1:2.

iii) With 10% concentration and 1:1 ratio acid washing is performed again with mentioned acids.

iv) All the samples were dried and the change is observed under optical microscope.

b) With Mechanical Stirring

A. Performance of Organic and Inorganic Acids

At this stage, four acids were taken in account- two organic (Acetic acid and Oxalic acid), two inorganic (Hydrochloric acid and Sulfuric Acid). Keeping the following parameter 5g of each sand sample was separately washed with each of the mentioned acids:

Acid(s): Inorganic: HCl; H_2SO_4
Organic: $C_2H_4O_2$; $H_2C_2O_4$
Concentration: 10%
Solid-liquid ratio: 1:12
Stirring speed: 700 rpm
Stirring time: 15-20 minutes

Then washed with distilled water and then dried. The change was observed in optical microscope.

B. Performance variation with Acid Concentration

Taking acid concentration as a variable, experiment was conducted with inorganic acids.

i) With HCl, varying the concentration the experiment was performed again. This time acid concentrations were 10, 15 and 20%. Other parameters were:

Solid-liquid ratio: 1:12
Stirring speed: 700 rpm
Stirring time: 20 minutes

Then washed with distilled water and then dried. The change was observed in optical microscope.

ii) With H_2SO_4, Step 'i' was repeated.

iii) Based on the results found using different acids, varying the concentration, one acid was selected to proceed with. An XRF was performed on each sample after washing the sand with the selected acid at optimum condition.

3.3.3 Alkali Washing

Alkali wash of sand sample is a very traditional method. This helps to eliminate certain metals from the sand surface [6, 60]. That's why the samples were gone through with alkali washing.

1) Two sand samples with highest percentage of silica were selected. 5gm of each sample were taken.

2) Each of the sand samples was washed with 20% NaOH in a stainless container. The agitation speed was 700rpm and the stirring time was 20mins.

3) The change was studied by performing an XRF on each sample.

3.4 Development of Methodology

After each step in Art 3.3, the optimum condition was determined. For an example, after washing the sand sample with distilled water, optimum time and speed was determined; based on the result obtained using different acids, one acid with optimum concentration was selected etc. Then, a complete methodology was developed to upgrade the sand sample with purity level of >98%.

Of course, not all five sand samples were upgraded to >98%. Based on the characterization, only two sand sample containing maximum percentages of SiO_2 were chosen to be gone through with the upgradation process. Then, XRF was performed on the selected samples succeeding the complete beneficiation route.

Chapter Four

Results and Discussion

4.1 Sample Selection

Based on the characterization sand samples were ranked according to the prospect of use in high tech applications (discussed in Chapter 5). Based on material composition one (out of two) sand sample from Sylhet district was excluded for further studies. This leaves only five sand samples for further characterization and beneficiation process. The locations of all five samples are indicated in Fig 4.1. Table 4.1 contains the location with co-ordinates from where the samples were collected.

Fig 4.1: Location of Collected Samples

(The coordinates mentioned are the zero points of the locality found by google map)

Table 4.1: Location of the Study Area

Sample	Location		Latitude (°N)	Longitude (°E)
	Sub-district	District		
Dalia	Jaldhaka	Nilphamari	26.15	89.03
Kuakata	Kalapara	Patuakhali	21.82	90.12
Patgram	Patgram	Lalmonirhat	26.35	89.02
Bipinganj	Durgapur	Netrokona	25.11	90.67
Sylhet	Jaintiapur	Sylhet	25.13	92.12

4.2 Characterization

All the experimental results about mineralogy, chemistry and physical properties are discussed in the proceeding sector. The result on characterization parameters like composition, size, density, transportation, moisture content, material composition, crystallinity etc. are shown below.

4.2.1 Material Composition

The mineralogy of the material was examined by XRF. The chemistry and the composition of the samples can be understood from Table 4.2.

Table 4.2: Sand Sample Composition (XRF Analysis)

Content (Weight %)	Dalia	Kuakata	Patgram	Bipinganj	Sylhet (Jaflong)	Sylhet (Sharighat)
SiO_2	75.06	65.22	75.52	97.05	78.61	86.85
Na_2O	1.74	1.56	1.81	0.05	1.16	0.41
MgO	1.16	2.42	1.21	0.05	0.33	0.31
Al_2O_3	11.94	11.55	12.05	0.90	8.90	5.62
P_2O_5	0.08	0.57	0.06	0.01	0.08	0.05
SO_3	0.01	0.01	0.01	0.01	0.18	0.02
Cl	0.02	0.04	0.05	0.04	0.03	0.03
K_2O	3.15	1.95	3.26	0.04	4.17	2.07
CaO	1.13	6.20	0.99	0.06	0.77	0.38
TiO_2	0.29	1.13	0.27	0.20	0.23	0.26
V_2O_5	0.013	-	-	-	-	-
Cr_2O_3	0.58	0.43	0.50	0.43	0.70	0.69
MnO	0.08	0.20	0.07	0.01	0.04	0.03
Fe_2O_3	4.62	8.52	4.12	1.12	4.66	3.17
Co_2O_3	-	0.004	-	-	-	-
NiO	0.04	0.03	0.008	0.01	0.04	0.08
CuO	0.005	-	-	-	-	0.005
ZnO	0.005	0.009	0.005	-	0.005	0.006
Rb_2O	0.012	0.007	0.013	-	0.015	0.007
SrO	0.01	0.03	0.01	-	0.02	-
Y_2O_3	-	0.02	-	-	0.009	0.01
ZrO_2	0.01	0.03	0.01	0.02	0.01	
BaO	0.05	0.07	0.04	-	0.06	-
ThO_2	0.003	-	-	-	-	0.004

The XRF result shows, all six of the samples contain mainly SiO_2 ranging from 65% to 97%. Bipinganj sand has the highest amount of $Si0_2$ content of 97.05%, whereas Kuakata sand has the lowest (65.22% $Si0_2$). Kuakata sand contains around 35% of oxides other than silica, including oxides of iron, aluminium, titanium etc. All samples, except the Bipinganj sand, contained Al_2O_3 in good quantity. Aluminium, calcium, and other metal oxides are undesirable in the silica for high

tech applications [6]. Complete removal of aluminium oxide can be difficult, which is very necessary for the production of high quality silica. Another troublesome material to be removed is iron. Kuakata sand shows more than 8.5% of iron oxide. The most troublesome elements in the use of the silica for the manufacturing of the photovoltaic cells are boron and the phosphorus [31]. From Table 4.2 small percentages phosphorus can be seen. But phosphorus in ppm range is unfavourable to high tech application. Boron is a very difficult element to be traced with XRF and no trace of boron is found in the samples.

The result of x-ray fluorescence analysis (Table 4.2) shows that the coarse sand from Jaflong contains 78.61% of silica while the fine sand sample from near Shari River contained 86.85% SiO_2. Most of the other materials are alkalis. Both the samples contain alumina and iron oxide in good percentages. There is trace of heavy minerals like titanium, zirconium, etc in each of the samples. The fine sample contains 40ppm thorium, whereas the coarse sand contains 80ppm yttrium. The coarse sand contains 800ppm and the fine sand sample contains 500ppm of P_2O_5. Based on the results of XRF analysis, only the fine sand sample from Sharighat was subjected to further investigation.

Out of five selected sand samples Kuakata sand seems least favourable to work with for further beneficiation steps due to the SiO_2%.

4.2.2 Morphology

The mineralogy of the collected samples was observed with optical microscopes. The colour, size and shape of the minerals were studied with stereo microscope (Fig 4.2)

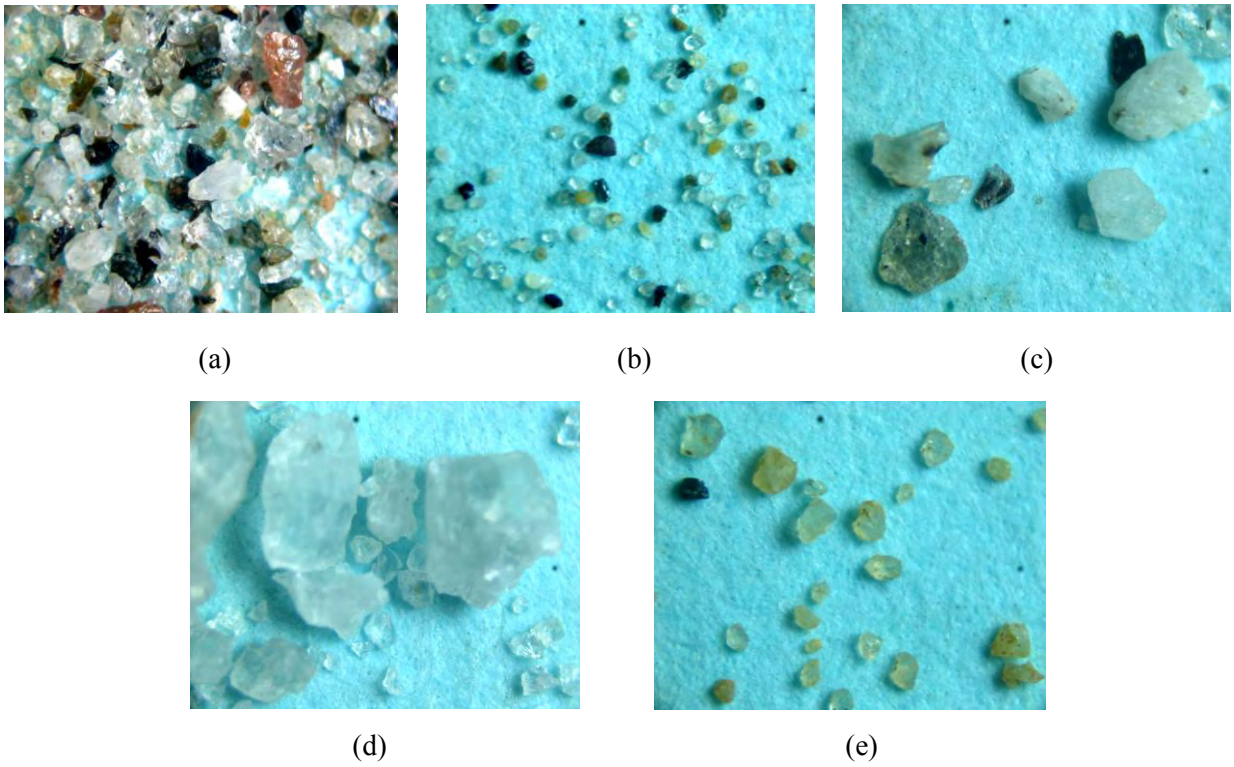

(a) (b) (c)

(d) (e)

Fig 4.2: With spot magnification of 100x stereo microscopic view of (a) Dalia, (b) Kuakata, (c) Patgram, (d) Bipinganj and (e) Sylhet sand. (Percentage of original width x height: 18%)

From Fig 4.2, presence of SiO_2 along with other minerals can be observed. From the stereo microscopic view trace of subrounded quartz is found. Presence of clay binder, iron coated silica, oxides of iron and aluminium is also seen. To understand the minerals better grain slide analysis is performed via polarizing microscope with the help of Michel-Levy interference colour chart (Fig 4.3).

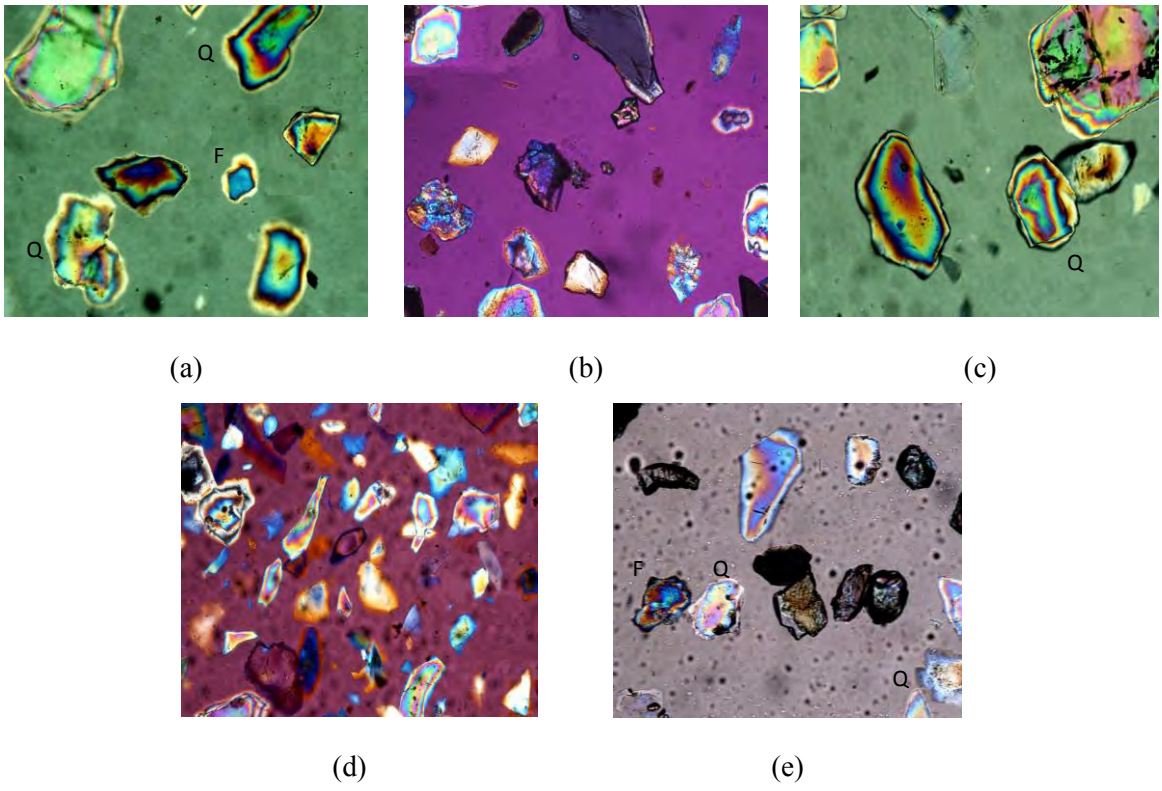

Fig 4.3: Polarizing microscopic view of (a) Dalia, (b) Kuakata (crossed polarisers), (c) Patgram, (d) Bipinganj (crossed polarisers) and (e) Sylhet (plane-polarized light). In these pictures Q= Quartz and F= Feldspar

Polarizing microscopic images indicate rich quantity of silica in Bipinganj. Analysing the images with the help of Michel-Levy interference colour chart trace of quartz, feldspar, iron oxide etc. was found in the sand samples.

Table 4.3: Polarizing Microscope data

Sample	Slide no.	Total No Particle	No of Quartz	Percentages of Quartz	Average %
1. Dalia	1.1	139	104	74.82	74.82
2. Kuakata	2.1	166	91	54.81	60.50
	2.2	145	96	66.20	
3. Patgram	3.1	119	98	82.35	81.16
	3.2	130	104	80.00	
4. Bipinganj	4.1	125	116	92.8	94.10
	4.3	217	207	95.39	
5. Sylhet	5.1	88	76	86.36	85.45
	5.2	117	99	84.62	

The quantity found by this method is the apparent quartz percentage.

The percentage of SiO_2 found in Table 4.2 and Table 4.3 is compared in Table 4.4. It can be seen that results obtained through Michel-Levy interference colour chart (Table 4.2) are in good agreement with the results of x-ray fluorescence analysis (Table 4.3).

Table 4.4: Comparison of XRF data and Polarizing Microscope Data

Sample	Percentage of quartz by Polarizing Microscope (apparent)	Wt % of $Si0_2$ by XRF
1. Dalia	74.82	75.06
2. Kuakata	60.5	65.22
3. Patgram	81.18	75.52
4. Bipinganj	94.10	97.04
5. Sylhet	85.49	86.85

The standard error limit is ±5%

4.2.3 Moisture Content

For the beneficiation process in further stages (e.g. high tech applications), one must ensure 'no' presence of water because small amount of water have an enormous fluxing effect- it lowers the melting point of silica [2].

Table 4.5: Moisture Content of the Sand Sample

Sample	Moisture %
Dalia	0.49
Kuakata	0.98
Patgram	0.59
Bipinganj	0.58
Sylhet	0.78

From Table 4.5, it can be seen that all five of the sand samples contain negligible amount of moisture. This reduces the requirement of drying while extracting silicon or any other beneficiation step. The result shows Dalia sand sample contains least amount of moisture whereas Kuakata sand contains the highest. But another interesting phenomenon is observed that Patgram sand holds moisture little bit more in winter, which may lead to drying requirement in the beneficiation step.

4.2.4 Particle Size Distribution

In this work, particle size distribution is analyzed by Taylor sieve analysis.

Detail Calculation:

1. Dalia

Table 4.6: Sieve Analysis of Dalia Sand Sample

Mesh Size	Weight	% of Sand retained (A)	Multiplier (B)	Product (A*B)
6	0.828	0.830	3	2.49
12	3.868	3.878	5	19.39
30	29.805	29.883	20	597.66
40	26.369	26.438	30	793.14
70	29.248	29.325	50	1466.26
140	7.28	7.299	100	729.91
200	0.857	0.859	140	120.3
270	0.97	0.973	200	194.51
Pan	0.514	0.515	300	154.61
Total	99.739	100		4078.22

AFS Grain Fineness No= 40.78

2. Kuakata

Table 4.7: Sieve Analysis of Kuakata Sand Sample

Mesh Size	Weight	% of Sand retained (A)	Multiplier (B)	Product (A*B)
6	0	0	3	0
12	0.029	0.029	5	0.15
30	0.015	0.015	20	0.3
40	0.01	0.01	30	0.3
70	0.663	0.66	50	33.15
140	84.471	84.46	100	8446.34
200	12.338	12.34	140	1727.165
270	2.467	2.467	200	493.36
Pan	0.016	0.016	300	4.8
Total	100.009	100		10705.55

AFS Grain Fineness No= 107.06

3. Patgram

Table 4.8: Sieve Analysis of Patgram Sand Sample

Mesh Size	Weight	% of Sand retained (A)	Multiplier (B)	Product (A*B)
6	1.476	1.55	3	4.65
12	4.308	4.53	5	22.64
30	31.156	32.75	20	654.96
40	24.23	25.47	30	764.04
70	26.525	27.88	50	1394.013
140	5.33	5.602	100	560.23
200	0.81	0.851	140	119.19
270	0.662	0.696	200	139.16
Pan	0.642	0.675	300	202.44
Total	95.139	100		3861.338

AFS Grain Fineness No= 38.61

During the experiment, mesh 6 didn't contained silica. They were mainly other silicates.

Patgram sand contained moisture. That's why it was dried before mesh analysis. The drier has a small metal ladle. Due to friction with that, very small amount of sand might have broken. So, there is a possibility of fraction of error.

4. Bipinganj

Table 4.9: Sieve Analysis of Bipinganj Sand Sample

Mesh Size	Weight	% of Sand retained (A)	Multiplier (B)	Product (A*B)
6	0.931	0.88	3	2.64
12	3.493	3.30	5	16.51
30	24.422	23.08	20	461.67
40	16.207	15.319	30	459.56
70	31.661	29.925	50	1496.27
140	21.19	20.028	100	2002.84
200	3.437	3.249	140	454.80
270	2.25	2.13	200	425.33
Pan	2.209	2.09	300	626.37
Total	105.8	100		5945.97

AFS Grain Fineness No = 59.46

5. Sylhet

Though it is mentioned in Art. 3.2.4 that vibration of sieve shaker was continued 10 minutes, for Sylhet sand vibration was continued for additional 15 minutes. This is due to the reason that sample was very fragile. 10 minutes of shaking was not enough to pass the sand through the sieve. Even the largest sieve (mesh 6) contained fragile sand sample.

Table 4.10: Sieve Analysis of Sylhet Sand Sample

Mesh Size	Weight	% of Sand retained (A)	Multiplier (B)	Product (A*B)
6	0.412	0.42	3	1.25
12	0.639	0.65	5	3.23
30	3.403	3.44	20	68.83
40	11.398	11.53	30	345.79
70	59.289	59.96	50	2997.76
140	21.262	21.50	100	2150.11
200	1.25	1.26	140	176.98
270	0.644	0.65	200	130.25
Pan	0.591	0.597	300	179.29
Total	98.888	100		6053.5

AFS Grain Fineness No = 60.53

The particle size distribution (PSD) is an important consideration that affects how the sand packs [70]. There are few companies who prefer the PSD of all grains of high purity sand to be between 100μm and 300μm in size. In addition, sometimes it is required that the majority of the particles must be around 230um in size. However, this case occurs when the sand needs to be pack correctly. Pack is the term used to describe how the sand settles together, ideally a tight pack is desired with minimal air bubble between the grains of sand. The smaller grains fill the gaps between the big ones.

If we analyze from Table 4.6 to Table 4.10, it can be observed that most of the Dalia sand is found in between 30, 40 and 70 no. sieve; more than 85% of Dalia sands are sized within 212 μm to 600 μm. The result shows, Kuakata sand size is quite uniform. Around 84% sand is 106 μm (>75 μm), around 12% is 75 μm (>53 μm). Around 82% of Patgram sand is within 212 μm to 600 μm. Bipinganj sand is sized within 106 μm to 600 μm. Around 93% of sylhet sand is sized within 425 μm to 106 μm, where 60% of Sylhet sand is sized around 212 μm (>106 μm).
The particle size distribution is plotted in Fig 4.4.

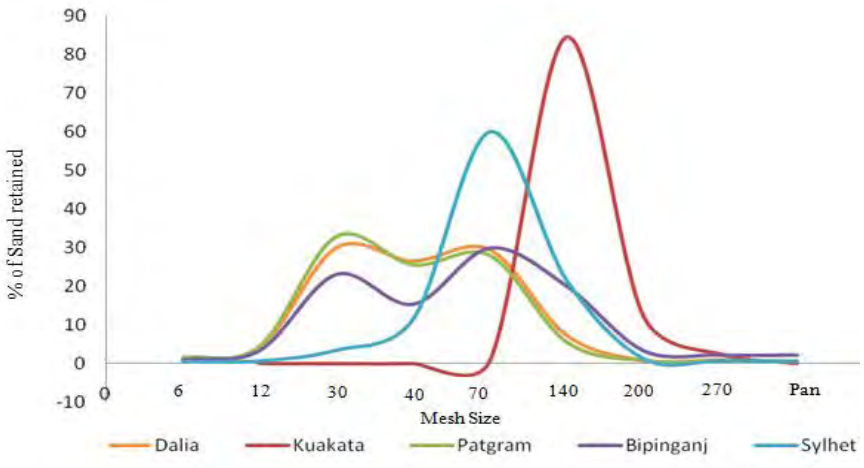

Fig 4.4: Particle size distribution of the samples. Kuakata sand is most tightly distributed. Non-uniformity in particle size was found for Dalia, Patgram and Bipinganj sand

From Fig 4.4, we can see non- uniformity in Dalia, Patgram and Bipinganj sand. If equal size distribution becomes necessary for subsequent processing, these three sand samples will require grinding and/or screening.

4.2.5 Roundness and Sphericity

The shape of the quartz particles is important as it impacts the packing density of the product, the melting characteristics and how the sand flows. If the particles are too needle-like they will not melt uniformly (the ends of the needles melt first) [70]. However, in this case, it is required that the silica does not melt.

To observe size and shape, samples were observed with SEM. Fig 4.5 shows scanning electronic microscopic view of all five samples. Table 4.11 contains length and width of the samples.

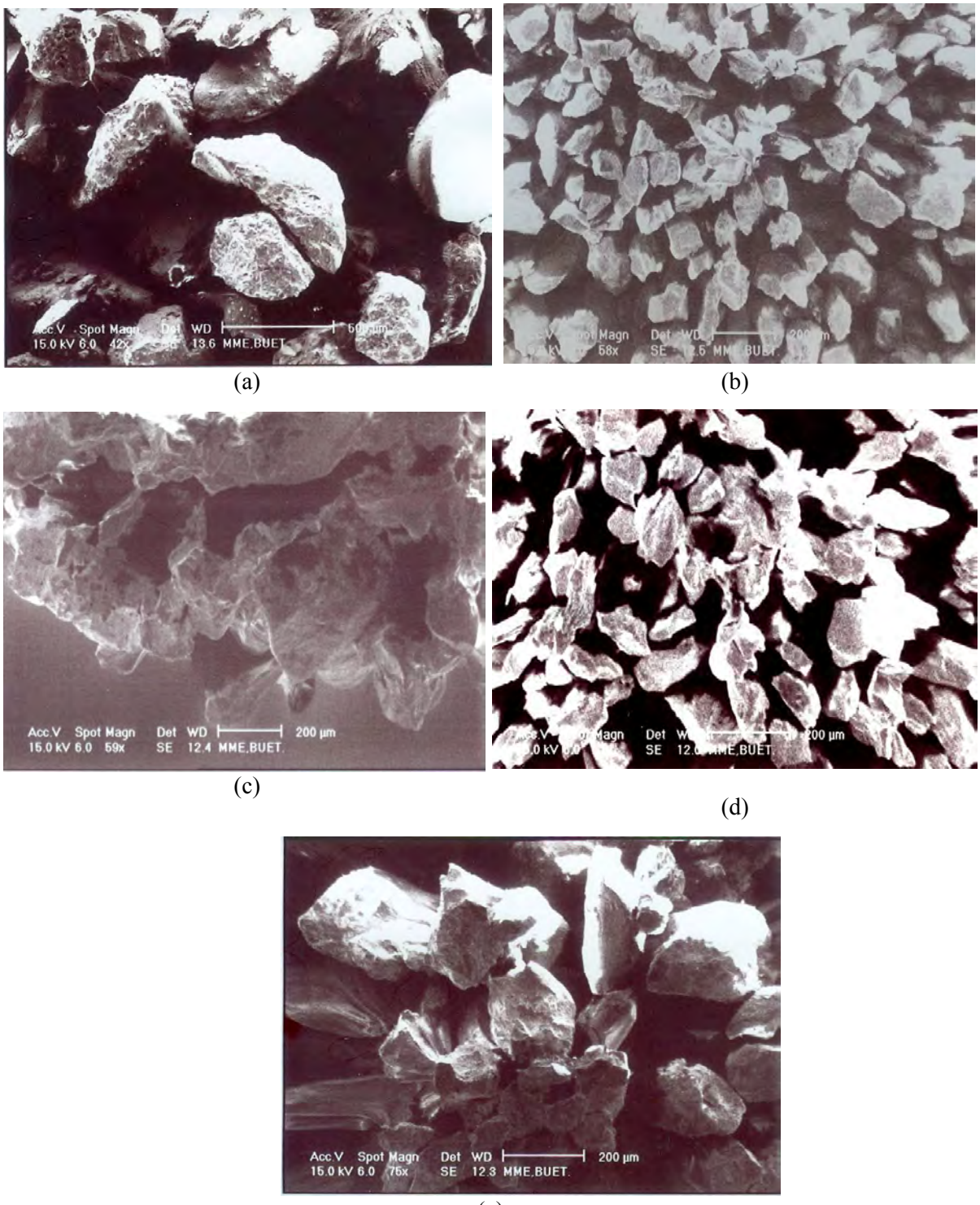

(a) (b)

(c) (d)

(e)

Fig 4.5: Scanning electron microscopic image of (a) Dalia, (b) Kuakata, (c) Patgram, (d) Bipinganj and (e) Sylhet sand. Height and width of the samples were measured by SEM.

Table 4.11: Size of sand sample via SEM

Sample	x (μm)	y (μm)
Dalia	429	353
	281	359
	552	534
Kuakata	140	121
	207	205
	143	129
Patgram	506	459
	144	178
	201	237
Bipinganj	169	114
	64.4	56
	101	133
Sylhet	302	260
	164	182
	325	357

The size and shape of the silica particles is an important consideration when producing high purity quartz sand. From Table 4.11, the size of sample can be observed. But to understand the shape better it is necessary to have three dimensional measurements. Three dimensional measurements are also required to study sphericity and roundness of the sample. The process described in Art. 3.2.5 sphericity of the samples were measured.

Table 4.12: Sphericity of Sand Samples

Sample	Sphericity
Dalia	0.83
Kuakata	0.838
Patgram	0.84
Bipinganj	0.859
Sylhet	0.86

Though five samples are collected from different sediments (Table 4.1) the sphericity measurement

shows (Table 4.12) similar values which indicate that they have gone through similar amount of erosion.

Flow is how the sand pours, like in an hourglass. The flow of the sand is important, as it must be fed into the machinery used in making quartz parts. If the sand particles are too needle-like they will bind together and not flow. Both SEM and stereo microscopic images confirms that none of the sand sample is too angular.

4.2.6 Density Measurement

Table 4.13: Bulk Density Measurement

Sample	W_p	W_p+W_s	$W_p+W_s+W_{rl}$	W_p+W_{rl2}	W_s	W_l	ρ_l	W_{il}	V_{il}	V_s	ρ_s
Bipinganj	32.32	37.324	85.157	82.071	5	49.75	0.994	47.83	48.08	1.92	2.60
Sylhet	29.68	34.682	83.089	79.96	5	50.28	1.006	48.41	48.14	1.86	2.69
Dalia	21.33	26.331	73.069	69.95	5	48.62	0.972	46.74	48.07	1.93	2.58
Kuakata	20.02	25.025	74.191	70.946	5	50.92	1.018	49.17	48.28	1.72	2.90
Patgram	29.68	34.681	83.033	79.994	5	50.31	1.006	48.35	48.05	1.95	2.57

In Table 4.13, the result shows Kuakata sand sample has the highest density (2.9 g/cc). The density of the pure SiO_2 is within 2-2.3 g/cc and 2.65 g/cc in case of pure quartz; cristobalite and tridymite have much lower densities because these two have comparatively open structures, whereas the atoms in quartz are more loosely packed [2]. The collected samples show slight deviation from the ideal value.

4.2.7 Phase Identification

At ordinary temperatures quartz is always present as low quartz. But it is possible to determine the original crystal form [68]. To study the crystallinity X-ray diffraction (XRD) and Thermo gravimetric analysis (TGA) was performed.

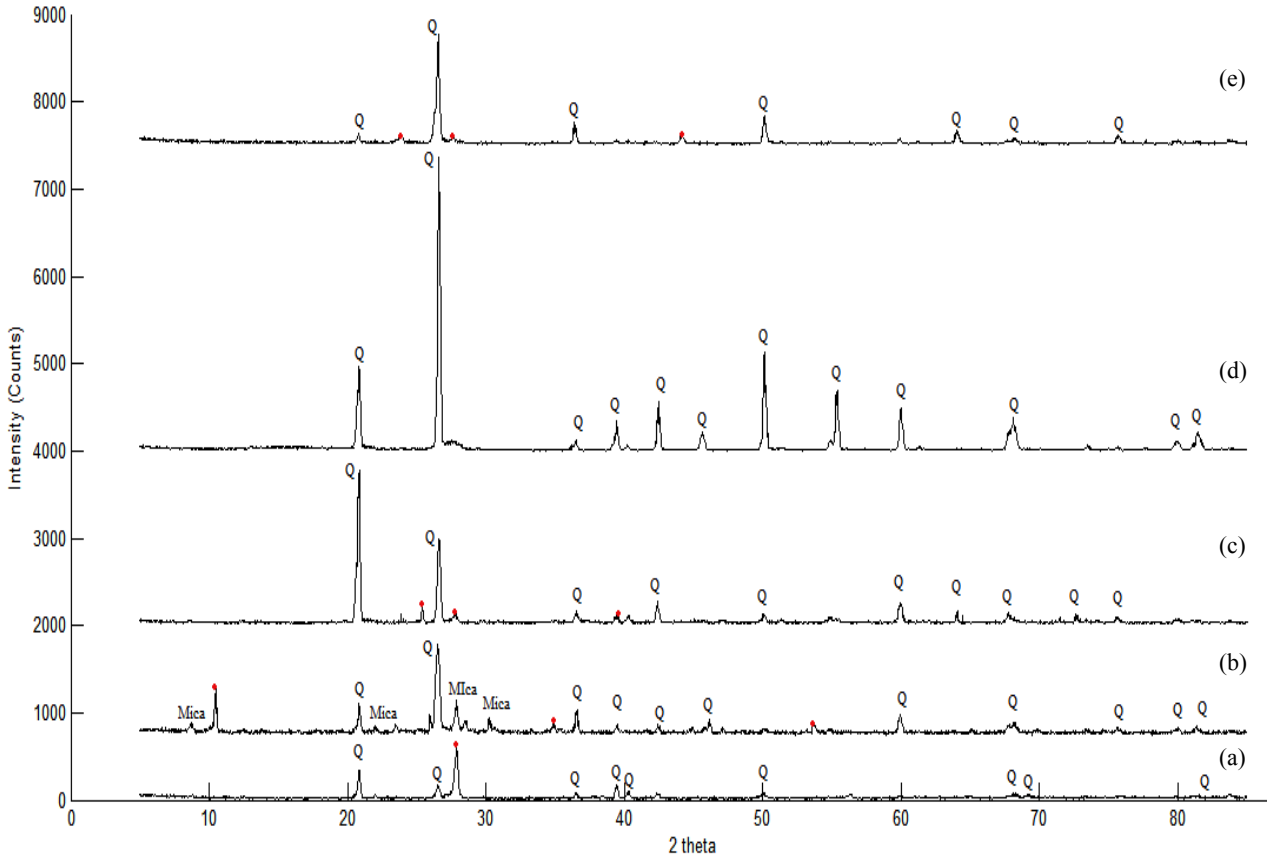

Fig 4.6: XRD result of sand samples from (a) Dalia, (b) Kuakata, (c) Patgram, (d) Bipinganj and (e) Sylhet. λ= 1.5406. In order to have better visibility instead of intensity, relative intensity is shown in y-axis. Q= Quartz, where SiO_2 is hexagonal with a= 4.91, b= 4.91, c= 5.41, α= 90, β= 90 and γ= 120. Mica in (b) is monoclinic, where a= 5.442, b= 9.435, c= 10.185, α= 90, β= 100.3 and γ= 90. The peaks coloured red dots (.) are due to trace of unknown phase.

The XRD pattern of the sand samples shows the presence of large amount of quartz (Fig 4.6). Clearly, the major portion of all five sand samples is quartz. However, the intensity of quartz is very distinctive for Bipinganj (Fig 4.6 (d)). In case of Kuakata sand sample in Fig 4.6 (b), presence of mica is visible. This mica contains Rb, Fe and hydroxyl. The intensity is quite low for both Dalia and Kuakata sand sample. Apart from Bipinganj, the other four samples show presence of peaks, which are not clear match with any particular crystal form of silica. From Table 4.14 we can see trace of α-quartz (PDF No. 87-2096), no trace of Tridymite in Bipinganj sand. Kuakata and Patgram sand sample contain quartz low mostly (PDF No. 89-1961). Kuakata sand shows the sign of presence of tridymite low ((PDF No. 88-1535). Sylhet sand shows no trace of α-quartz but with PDF 65-0466 quartz low is present. Like Bipinganj sand, Dalia sand sample also contains α-quartz. This sand sample may also contain some other form of quartz low with PDF 65-0466.

Table 4.14: Phase Identification by XRD

Sample	PDF No.	Phase/ Remarks
1. Dalia	may be 87-2096 or 85-0466	
2. Kuakata	89-1961	Quartz low (may be Tridymite low with PDF 88-1535)
3. Patgram	89-1961	Quartz low
4. Bipinganj	87-2096	Quartz low trace of α-quartz no trace of Tridymite
5. Sylhet	65-0466	Quartz low but not α-quartz

Due to these peaks in question (Table 4.14 and red dots in Fig 4.6), there was a need to conduct the XRD again varying few parameters. That is why grinding was performed in the following method to transform the sand into fine powder. Then the XRD was performed using the powdered sample with $2\theta = 0.25^{o}$.

Grinding:

Five gm of each sand sample were finely ground in an agate mortar. Earlier, in Art. 4.2.4, it was discussed that not all of five sand samples need to be grinded for further beneficiation stages (Fig 4.5) but there are lot of examples where grinding the sand sample is part of silica purification process (Art. 2.9.1.1). So, even though grinding is not performed in this work as part of purification process but it might be considered as a beneficiation step. In this work, grinding is performed only to achieve better XRD result. During, the grinding process, out of all five sand samples Sylhet sand went to power form more readily. Bipinganj sand took the highest time to go to powder form.

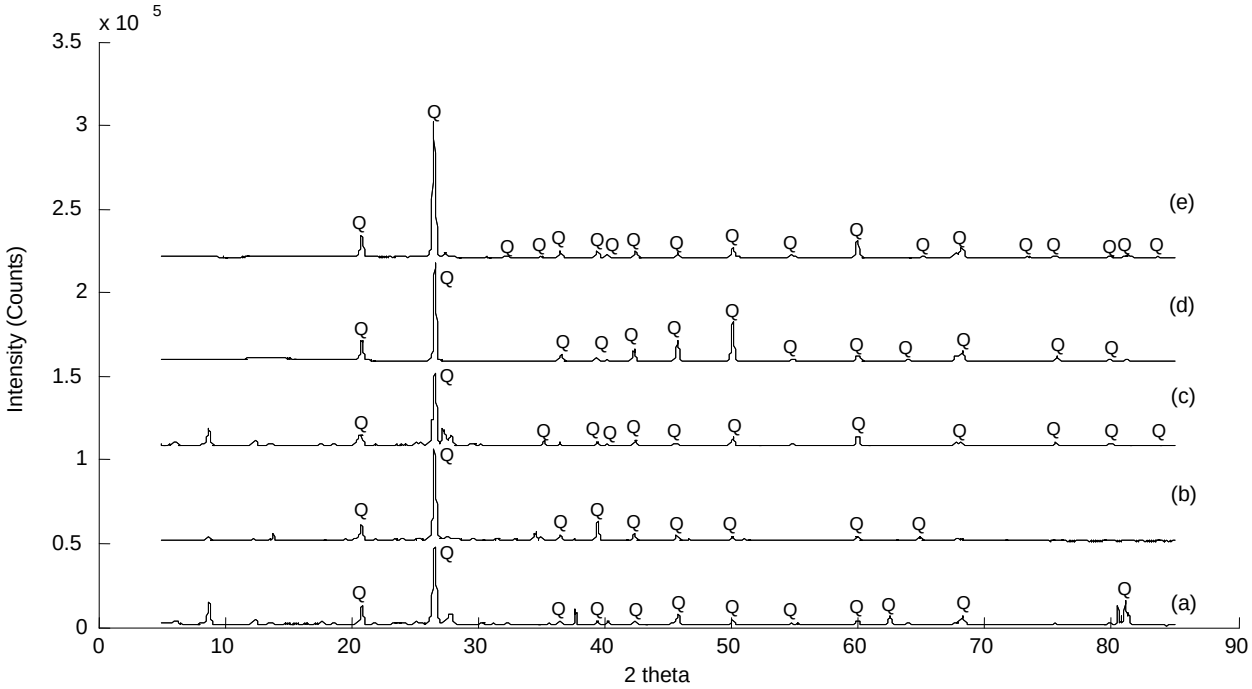

Fig 4.7: XRD result of sand samples from (a) Dalia, (b) Kuakata, (c) Patgram, (d) Bipinganj and (e) Sylhet. Q= quartz

The XRD performed on powdered samples in slower speed shows clear pattern (Fig 4.7). The pattern confirms the presence of large amount of quartz form of silica. Bipinganj and Sylhet sand shows presence of quartz and no trace of any other crystal form of silica is found in these samples. Unlike Fig 4.6, trace of unknown peaks are very low in Fig 4.7. Kuakata, Patgram and Dalia sand samples show trace of quartz along with other phases. The unidentified peaks may be of feldspars' or other silicate minerals.

To evaluate the possibility of presence of other phases than quartz Differential thermal analysis (DTA) is performed (Fig 4.8).

4.2.8 Dependence of Structure on Temperature

DTA was performed to the selected 5 samples to characterize the thermal effects- to trace the loss of combined water and/or, change of polymorphic form.

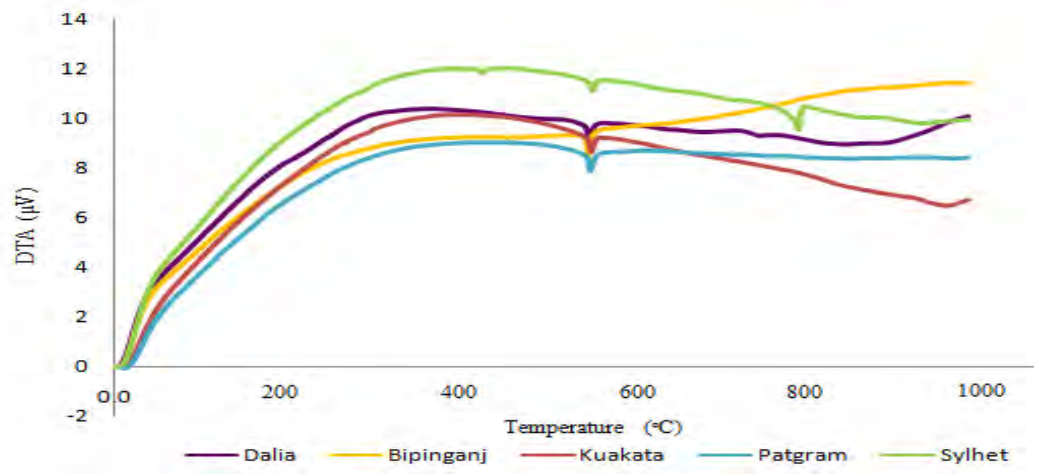

Fig 4.8: Differential thermal analysis (DTA) of samples showing peak at 573°C. Sylhet sand is showing two other additional peaks at 450°C and 810° C

From the Differential thermal analysis (DTA) a peak at ~ 573°C is found for all five of the samples (Fig 4.8). So there is a phase transformation from trigonal trapezohedral to hexagonal trapezohedral class, which means α-quartz is transforming into β-quartz at that temperature [1, 2, 25].

In case of Sylhet sand, there are another two additional peaks (at 450°C and 810° C). These peaks could be due to loss of combined water or carbon dioxide, change of polymorphic form, recombination of the elements into a different compound. To understand the reason better, the samples were exposed to the temperature of 580°C in a muffle furnace for an hour and DTA/ TGA was performed again (Fig 4.9).

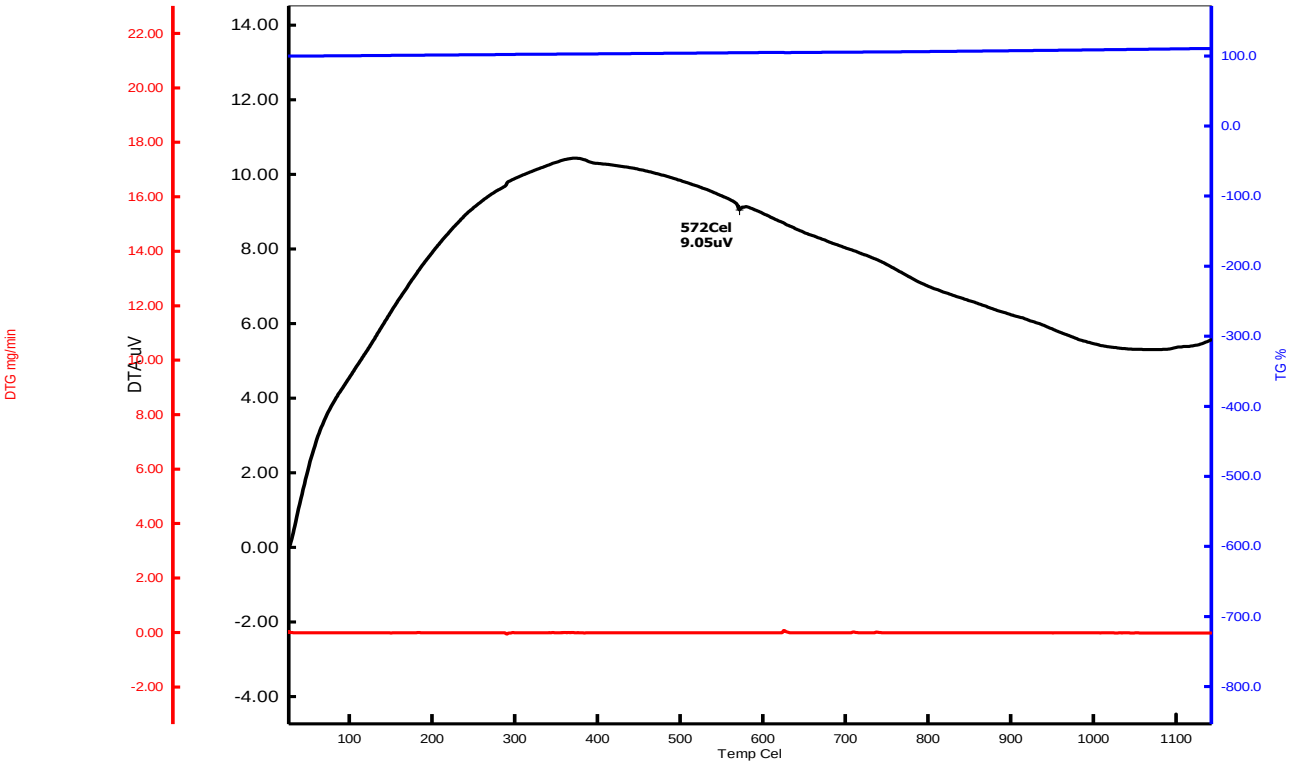
DTG mg/min
DTA uV
TG %
572Cel
9.05uV
Temp Cel

(a)

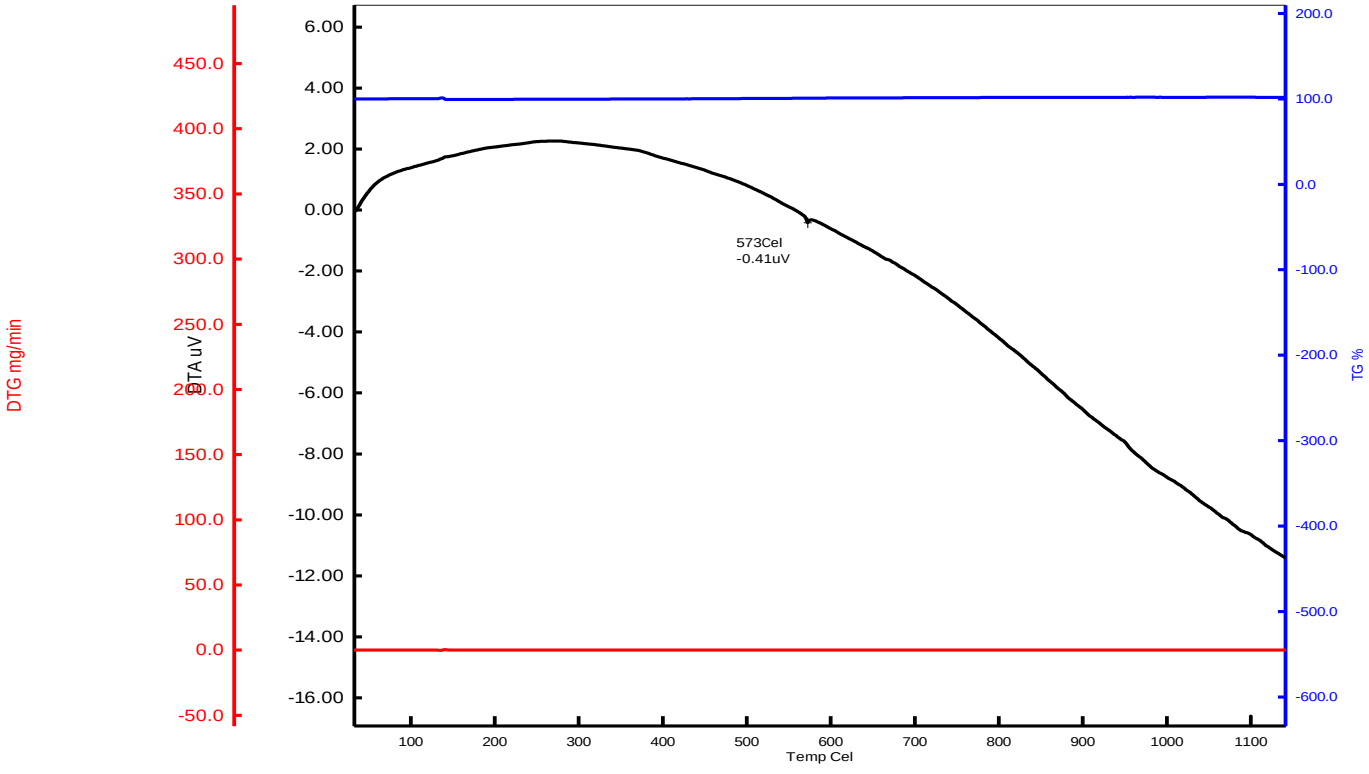
DTG mg/min
DTA uV
TG %
573Cel
-0.41uV
Temp Cel

(b)

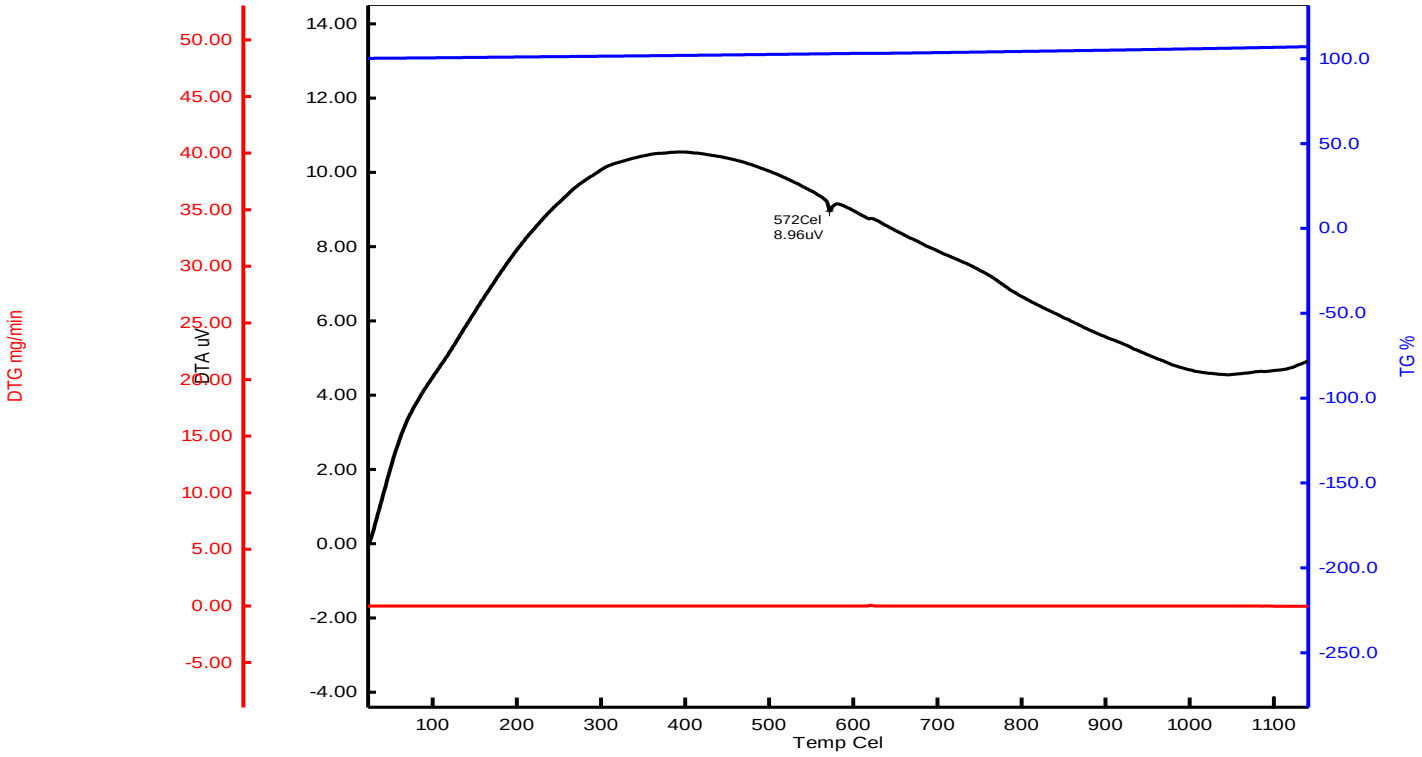
DTG mg/min
DTA uV
TG %
572Cel
8.96uV
Temp Cel

(c)

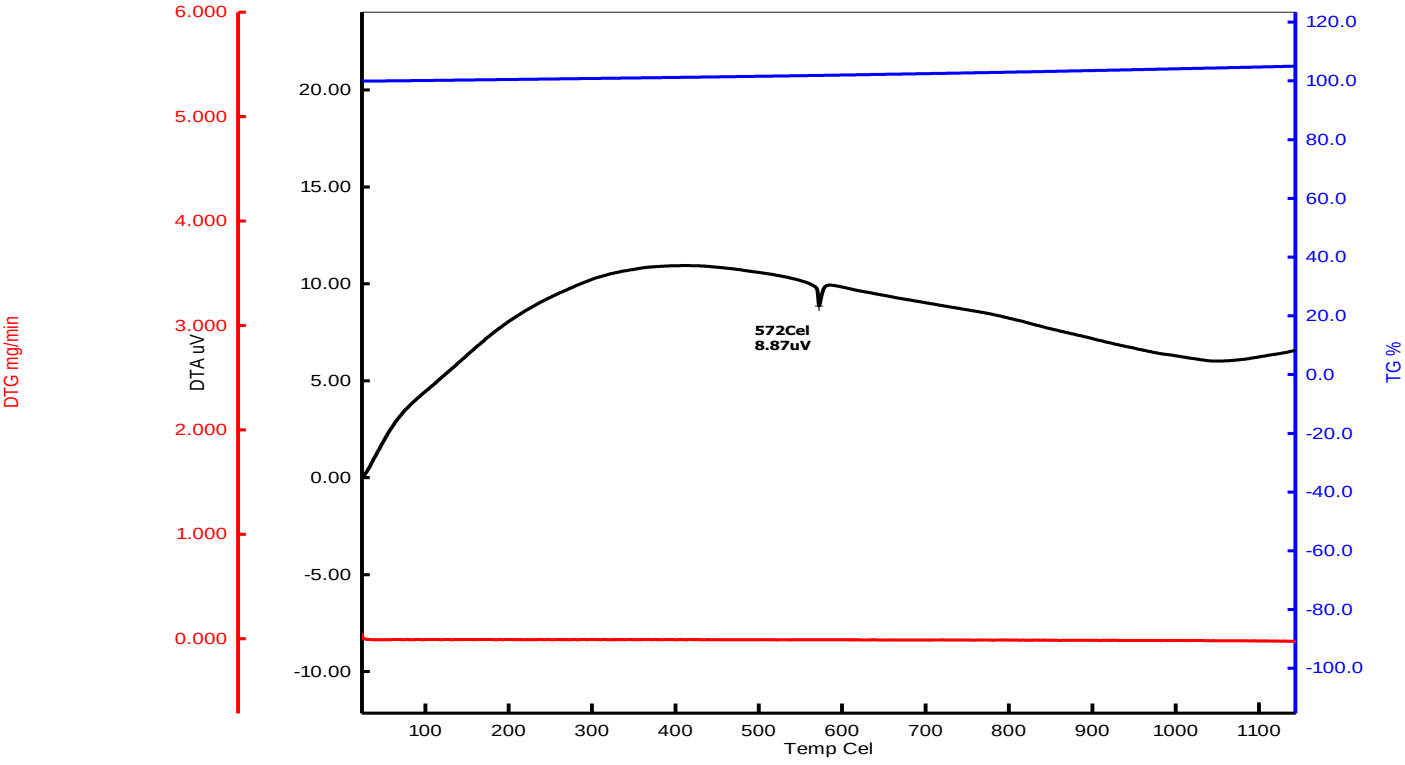
DTG mg/min
DTA uV
TG %
572Cel
8.87uV
Temp Cel

(d)

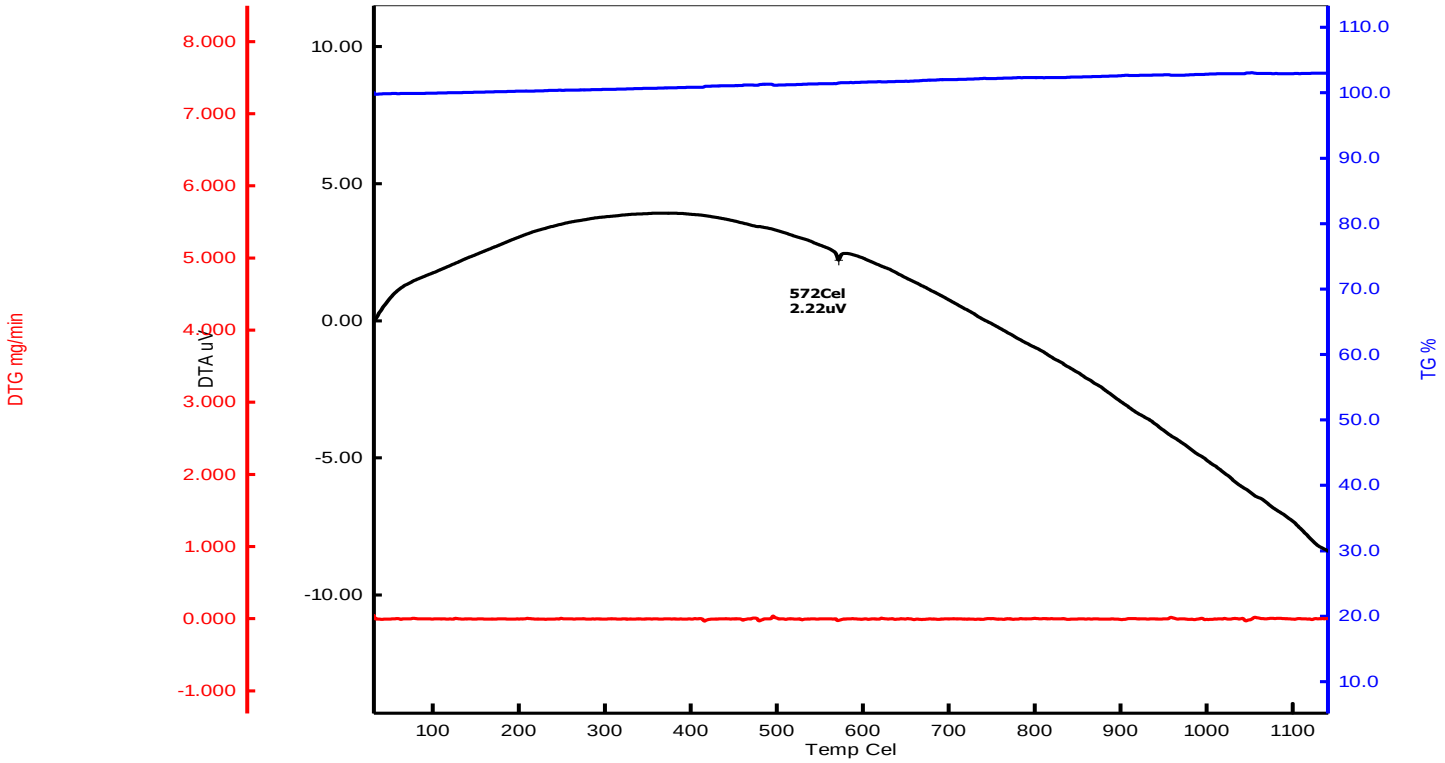

(e)

Fig 4.9: DTA/TGA of (a) Sylhet, (b) Bipinganj, (c) Dalia, (d) Patgram and (e) Kuakata sand. DTA confirms the presence of only one crystal form in the received sand i.e. trigonal trapezohedral α-quartz

Dalia, Kuakata, Patgram, Bipinganj, Sylhet- all five of the samples are showing peak at ~ 573°C (Fig 4.9), no additional peaks are found, which confirms that there is only one change in polymorphic form i.e. from α-quartz to β-quartz.

4.2.9 Organic Matter Content

Though originally the experiment was supposed to be performed in an air-tight muffle furnace, but it was executed on a regular furnace which was not air tight. More over due to transportation of the sample while measuring there could be a slight error in sample weight. The percentage of organic content is listed in Table 4.15.

Table 4.15: Organic Material Tracing

Sample	Before Heating			After Heating			
	Mp (g)	M_{PDS} (g)	M_D (g)	M_{PA} (g)	M_A (g)	M_O (g)	OM %
Dalia	35.528	85.248	50.319	85.653	50.124	0.195	0.39
Kuakata	31.762	81.817	50.054	81.498	49.736	0.316	0.63
Patgram	33.038	83.529	50.492	83.275	50.237	0.255	0.50
Bipinganj	35.339	86.339	51.000	86.303	50.964	0.036	0.07
Sylhet	32.760	82.835	50.075	82.562	49.802	0.273	0.55

The result shows presence of negligible amount of organic matter in all five samples. The highest content of only 0.07% was found in Bipinganj sand; this minor percentage may be from the dry leaves' particle mixed in the sand. These results are in good agreement with the results of thermal analysis (Fig 4.10).

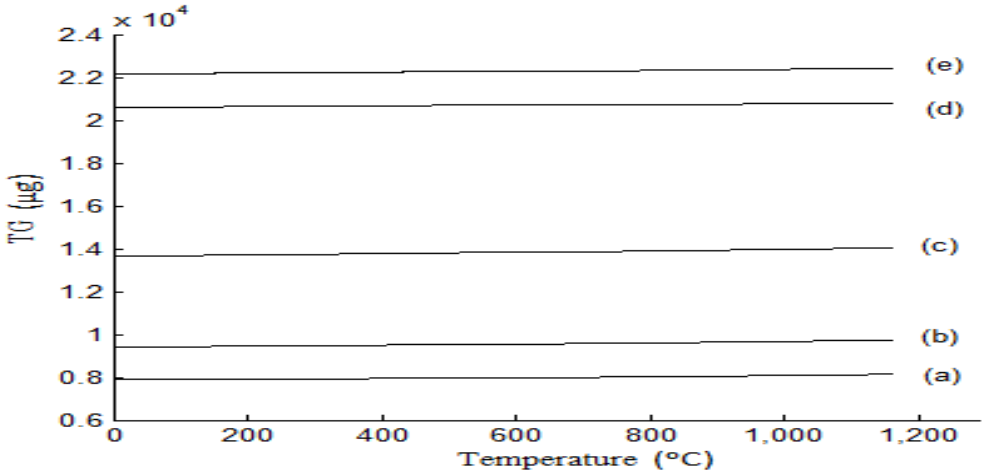

Fig 4.10: Thermo gravimetric analysis of (a) Sylhet, (b) Bipinganj, (c) Dalia, (d) Patgram and (e) Kuakata sand showing absence of organic material in the samples

From both the thermo gavitimetrical analysis almost no trace of organic matter is found (Fig 4.9 and 4.10).

4.3 Beneficiation

Benefication steps vary sample to sample according to the result of the characterization. From the characteristics mention in Art. 4.2 it can be seen that the properties are different for all five samples in terms of quality and quantity. That's why further upgradation processes implied are not alike for all the samples. Moreover, upgradation process was emphasised to the samples with high percentage of SiO_2 and the sample containing more perfect crystal of quartz.

4.3.1 Attrition

At first the samples were washed without any stirring. It started to remove the lightly adhered elements from the sand, but found to be not that effective. Next, the sample was washed with distilled water for around 20 minutes at 600 rpm and 800 rpm. And the changes were observed. Based on the result, to narrow down the parameters Sylhet sand was chosen to proceed with. The optimized speed and time for the attrition was determined by concluding the further experiment only on Sylhet sand.

From Fig 4.11, it can be seen that the extent of removal of impurities increases with an increase in the speed of agitation. The observation through optical microscope shows, sand was better cleaned at 800 and 1000 rpm. Based on the observation under stereomicroscope 800 rpm seems to be the optimum speed of agitation, due to practical reasons. At higher speeds it was difficult to keep the slurry within the reaction vessel.

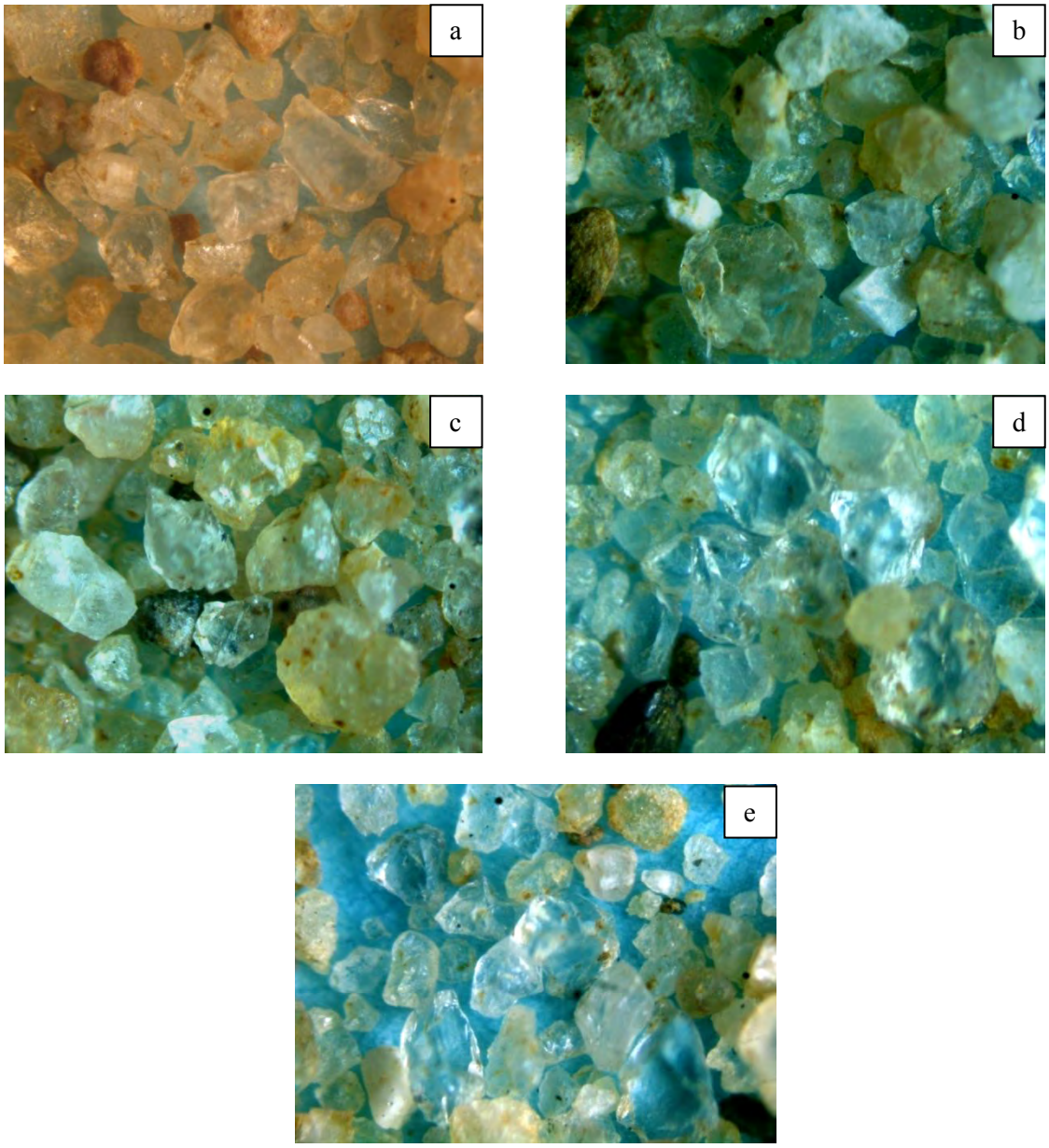

Fig 4.11: Sylhet sand (a) as received. The stereomicroscopic view (with spot magnification of 100x) of the sample washed with distilled water at (b) 400 rpm, (c) 600 rpm, (d) 800 rpm and (e) 1000 rpm. (Percentage of original width x height: 24%.) The sample was better cleaned with the increment of stirring speed.

Later XRF was performed to quantify the result. The XRF was conducted on samples washed with distilled water by 400, 800 and 1000 rpm only (Table 4.16).

Table 4.16: XRF of Sylhet sand after attrition (Variable: Speed)

Content (Weight %)	As received	400 rpm	800 rpm	1000 rpm
SiO_2	86.85	94.16	94.22	92.98
Al_2O_3	5.62	4.04	4.31	4.78
Fe_2O_3	3.17	1.27	1.25	1.50
TiO_2	0.26	0.22	--	0.27
MgO	0.31	0.22	0.21	0.28
P_2O_5	0.05	0.08	--	0.11
ZrO_2	--	0.03	0.01	0.17
Cr_2O_3	0.69	0.05	--	0.05
K_2O	2.07	--	--	--

**There is a slight calibration error in P_2O_5 and ZrO_2 percentage*.

The received sand sample contained ~86% SiO_2. After attrition the percentages increased to ~94%. The impurities like iron, aluminium were removed up to certain percentage. From Table 4.16, slight deviation can be observed for the sample with 1000 rpm from the observation made by stereo microscope (Fig 4.11). We can see that most of the impurities comes back and again adhere to the sample when the agitation is too high. Based on the XRF result, 800 rpm is the optimum stirring speed for washing the sand with distilled water.

To find out the optimized time attrition was performed again. This time the stirring speed was kept as 800 rpm and time was varied from 10 minutes to 1 hour.

The percentages of white and milky white silica was to increase up to 25-30 minutes (Fig 4.12). After that, agitation time did not indicate any visual improvement when observed under stereo-microscope. In Fig 4.12 (f), the silica is unclear comparing to (d) and (f), which indicates when the agitation is continued for long time impurities go back to silica.

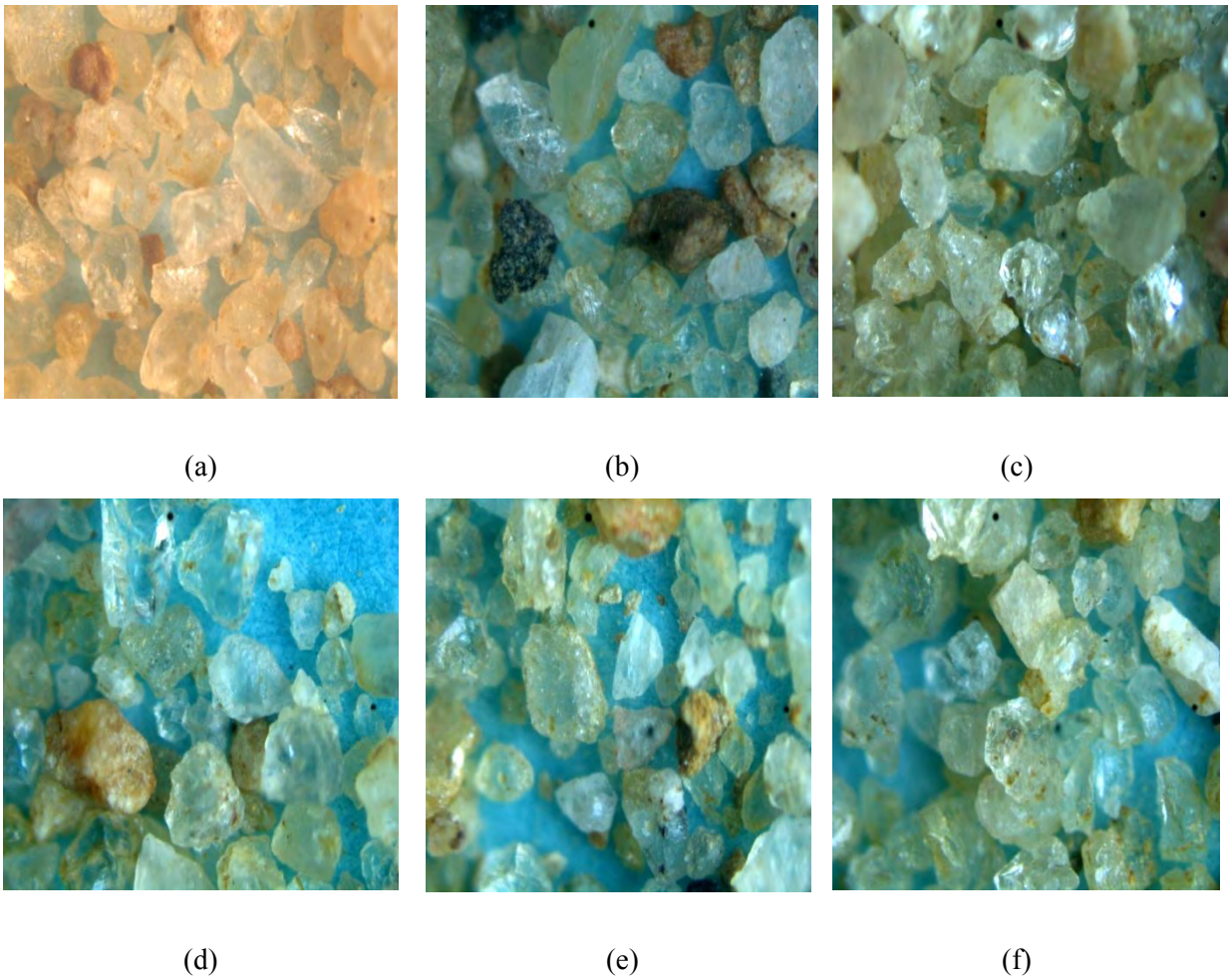

Fig 4.12: Sylhet sand (a) as received. The stereomicroscopic view (with 100x) of Sylhet sand washed with distilled water in (b) 10mins, (c) 20mins, (d) 30min (e) 40mins and (f) 1 hour. (Percentage of original height x width: 22%.) After 30 min no visible impact could be found.

Based on the stereomicroscopic observation, XRF was performed on samples stirred with distilled water for 10, 30 and 60 minutes only (Table 4.17). The XRF result shows the percentage of SiO_2 was increased upto ~94%. Just within 10 minutes, the silica percentage increased to ~92%. Potassium was completely eliminated. After 25-30minutes the SiO_2 was 94.22%. In this case, iron and aluminium content reduced to the least, comparing to other stirring time. But after 30 minutes, the result shows little non-uniformity as the improvement diminished. Thus, the optimized time is settled as 30 minutes.

Table 4.17: XRF of Sylhet sand after attrition (Variable: Time)

Content (Weight %)	As received	10mins	30mins	60mins
SiO_2	86.85	92.46	94.22	93.61
Al_2O_3	5.62	5.33	4.31	4.39
Fe_2O_3	3.17	1.52	1.25	1.31
TiO_2	0.26	0.26	--	0.38
MgO	0.31	0.30	0.21	0.23
P_2O_5	0.05	0.09	--	--
ZrO_2	--	0.02	0.01	0.30
Cr_2O_3	0.69	--	--	0.05
SrO	--	0.01	--	--
K_2O	2.07	--	--	--

**There is a slight calibration error in P_2O_5 and ZrO_2 percentage.*

After completion of experiments on attrition with time and speed variable, the optimized value settled as 800 rpm and 30 minutes.

4.3.2 Acid Washing

a) Without Mechanical Stirring

Without any mechanical stirring, 5g of each sample were taken to be acid washed.

i) Samples were washed with 1% concentration of acetic acid, hydrochloric acid, sulphuric acid, separately. The impact was very poor, that is why only few of the results are shown in the next page:

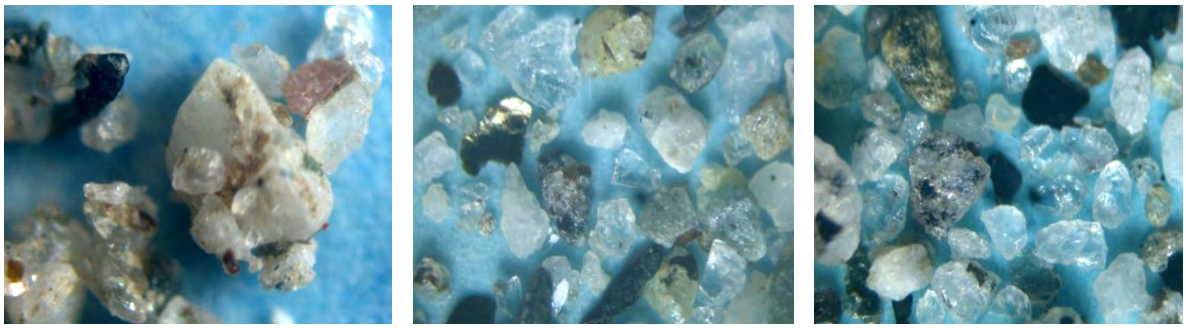

(a) (b) (c)

Fig 4.13: Stereomicroscopic image (100x) of Patgram sand (a) as received, (b) washed with 1% acetic acid and (c) 1% sulphuric acid. (Percentage of original width x height: 18 %.) The impact of the acid washing is very poor.

In Fig 4.13, it can be observed that 1% acid without any agitation has no impact on Patgram sand sample.

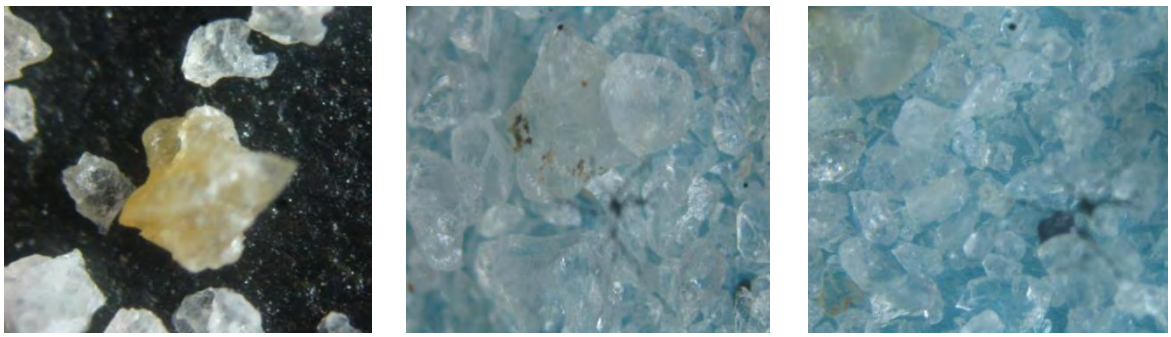

(a) (b) (c)

Fig 4.14: Stereomicroscopic image (192x) of Bipinganj sand (a) as received, (b) washed with 1% acetic acid and (c) 1% sulphuric acid. (Percentage of original width x height: 18 %.) The impact of the acid washing is very poor.

From Fig 4.14, it can be observed that 1% acid without any agitation has no impact on Bipinganj sand sample. When, this phenomenon continued, the other three samples also shown similar result (Fig 4.15). With 1:1 ratio of sample and acid, the result shows negligible beneficiation.

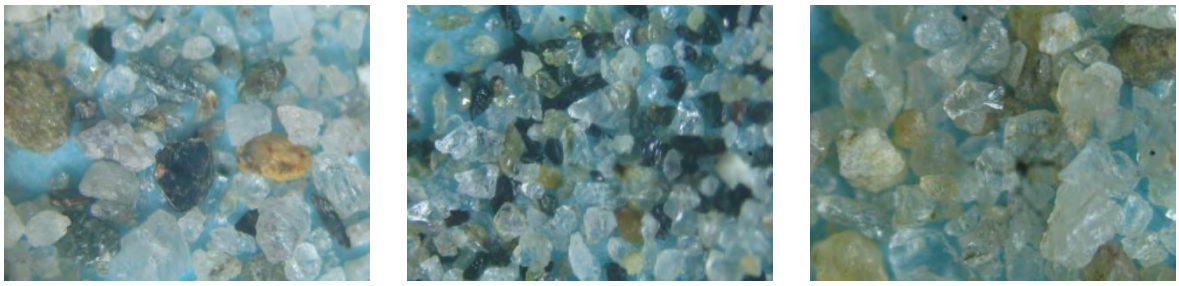

(a) (b) (c)

Fig 4.15: Stereomicroscopic image (100x) of samples washed with 1% sulphuric acid (a) Dalia, (b) Kuakata and (c) Sylhet. (Percentage of original width x height: 16 %.) The impact of the acid washing is very poor.

ii) Next, the concentration of the acid was increased for each case. At first, the ratio kept same like the previous one, i.e. 1:1.

(a) (b) (c)

Fig 4.16: Stereomicroscopic image of samples washed with 5% sulphuric acid (a) Bipinganj (100x), (b) Kuakata (192x), (c) Sylhet (192x). (Percentage of original width x height: 18 %.) The impact of the acid washing is very poor.

It can be observed from Fig 4.16 that, with 5% concentration of acids, the gain is very poor. But if the solid-liquid ratio is taken 1:2 then the scenario improves little better (Fig 4.17).

(a) (b)

Fig 4.17: Stereomicroscopic view (192x) of Patgram sand washed with 5% sulfuric acid when the sand: acid ratio is (a) 1:1, (b) 1:2. (Percentage of original width x height: 23 %.) Negligible amount of gain could be observed.

iii) As the outcome of the acid washing is visibly nil, the concentration of the acids were increased to 10%.

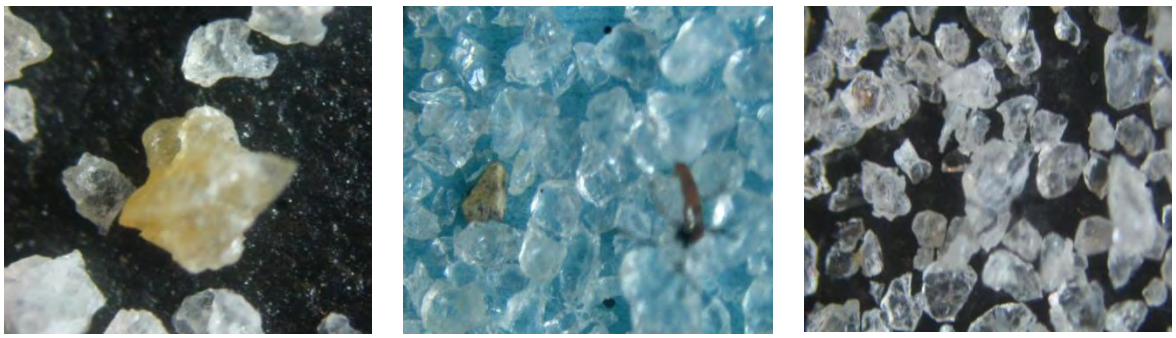

(a) (b) (c)

Fig 4.18: Stereomicroscopic view (192x) of Bipinganj sand (a) as received, (b) washed with 10% acetic acid, (c) washed with 10% sulphuric acid. (Percentage of original width x height: 18 %.) The impact is better for (c) than (b).

From Fig 4.18 it can be observed that 10% sulphuric acid has better impact on Bipinganj sand than 10% acetic acid.

(a) (b) (c)

Fig 4.19: Stereomicroscopic view (192x) of Kuakata sand (a) as received, (b) washed with 10% acetic acid, (c) washed with 10% sulphuric acid. (Percentage of original width x height: 18 %.)

Just like Bipinganj sand, Kuakata sand shows better improvement with 10% sulphuric acid, than 10% acetic acid (Fig 4.19).

As it is mentioned earlier, the solid- liquid ratio was changed for Patgram sand. With the sand to acid ratio of 1:2, Patgram sand was washed with both 10% acetic acid and 10% sulphuric acid, separately. Then, the change was observed via stereomicroscope.

(a) (b) (c)

Fig 4.20: Stereomicroscopic view (192x) of Patgram sand (a) as received, (b) washed with 10% acetic acid, (c) washed with 10% sulphuric acid. (Percentage of original width x height: 18 %.)

There is a visible improvement in the sample when it is washed with 10% sulphuric acid (Fig 4.20). Based on the previous results, the next two sand samples were washed with 10% sulphuric acid only.

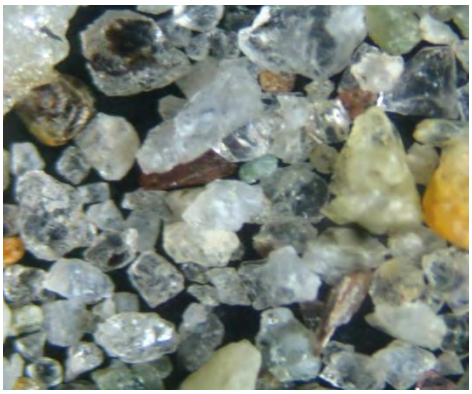

(a)

(b)

Fig 4.21: Stereomicroscopic view (192x) of samples washed with 10% sulphuric acid (a) Dalia, (b) Sylhet. (Percentage of original width x height: 22 %.)

Although it can be seen in Fig 4.18- 4.21 that there is an improvement in the samples after washing it with 10% sulphuric acid without mechanical agitation, the overall gain is still poor. That is why mechanical stirring was used in the later part of this work.

b) With Mechanical Stirring

A. Performance of Organic and Inorganic Acids

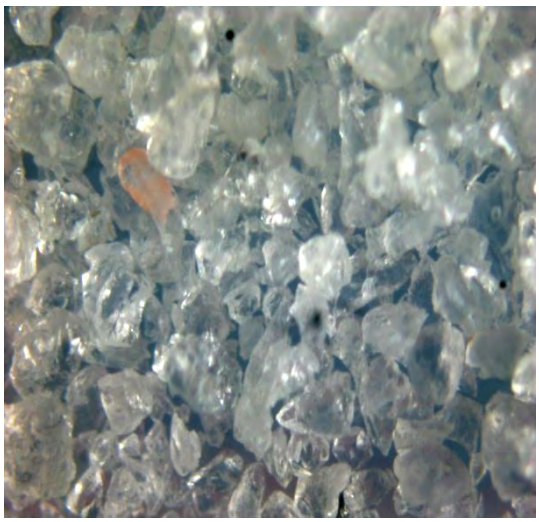

(a)

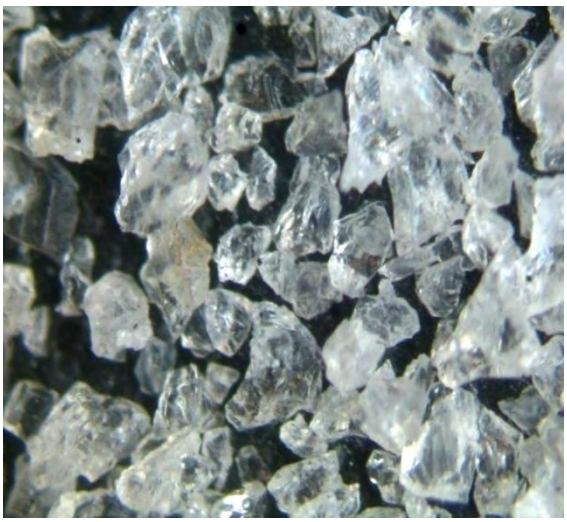

(b)

Fig 4.22: Bipinganj sand washed with (a) organic acid (10% Oxalic acid), (b) inorganic acid (10% HCl). Percentage of original height x width: 28%. The impact of organic and inorganic acid is not distinguishable by stereomicroscopic images.

In this experiment out of two organic acids, oxalic acid is found more effective than acetic acid. The inorganic acids with 10% concentration found to have more or less equal effectiveness to clean the sand particles.

There are several studies where organic acids are used to remove the impurity from the sand [50-58]. From those studies oxalic acid is found to be the most promising because of its acid strength, good complexing characteristics and high reducing power, compared to other organic acids. Based on the stereomicroscopic observations e.g. Fig 4.22, it is hard to determine the effectiveness between oxalic acid and inorganic acid like hydrochloric or sulphuric acid. The collected samples contain iron and with oxalic acid it is helpful to remove impurities like iron. Because using oxalic acid, dissolved iron can be precipitated from the leach solution as ferrous oxalate, which can be further re-processed to form pure hematite by calcinations [50]. But oxalic acid is uncomfortable to work with. Unlike other three acids being studied, room temperature is not sufficient for oxalic acid. The whole experiment needs to be performed at around 100°C. In practice and in all cases being studied, the reaction temperature was found to be critical as confirmed by many workers. Most reaction systems studied had to be conducted above 90 °C to achieve a reasonable dissolution rate. Moreover, it takes time to react.

That is why for further beneficiation steps, both acetic acid and oxalic acid were excluded.

B. Performance Variation with Acid Concentration

Taking acid concentration as a variable, the experiment was conducted with inorganic acids.

i) With HCl, varying the concentration the experiment was performed again. This time acid concentrations were 10, 15 and 20%. Sand particles of all five samples (5 gm in each case) were acid washed for 20 minutes.

Previously, the agitation speed was set at 800 rpm in case of washing the sand samples with distilled water. Unlike distilled water, acids corrode the mechanical stirrer. Moreover, it is often uncomfortable to work in an environment where acids are being stirred at such speed. That's why the agitation speed was reduced in case of acid washing and was kept near 700 rpm. It is an acceptable speed range of speed for acid wash [58, 61].

(a) (b) (c)

Fig 4.23: Acid washed sample of Dalia with 192x spot magnification (a) 10% HCl, (b) 15% HCl, (c) 20 % HCl. (Percentage of original width x height: 17 %.) Increment in acid concentration beneficiates the sample.

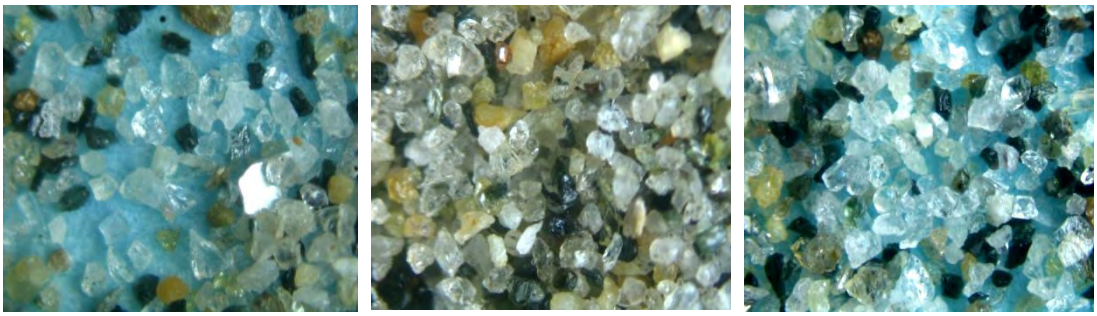

(a) (b) (c)

Fig 4.24: Acid washed sample of Kuakata with 192x spot magnification (a) 10% HCl, (b) 15% HCl, (c) 20 % HCl. (Percentage of original width x height: 17 %.) Increment in acid concentration shows slight beneficiation in the sample.

(a) (b) (c)

Fig 4.25: Acid washed sample of Patgram with 192x magnification (a) 10% HCl, (b) 15% HCl, (c) 20 % HCl. (Percentage of original width x height: 18 %.) Increment in acid concentration beneficiates the sample.

(a) (b) (c)

Fig 4.26: Acid washed sample of Bipinganj with 192x magnification (a) 10% HCl, (b) 15% HCl, (c) 20 % HCl. (Percentage of original width x height: 18 %.) Increment in acid concentration beneficiates the sample.

In case of Dalia sand sample (Fig 4.23), with the increment of acid concentration, the impurity removal was increased. In case of Kuakata sand sample (Fig 4.24) it is hard to notice significant uniform improvement. However, it seems 20% HCl has better impact on Kuakata sand.

From Fig 4.23-4.26, it can be said that the trend of removing impurities from sand particle is linearly increasing with the increment of acid concentration. However, it is very difficult to quantify the improvement by this image analysis.

ii) In similar manner, all five sand samples were washed with H_2SO_4.

(a) (b) (c)

Fig 4.27: Dalia (192x) sand sample (a) as received, washed with (b) 10% H_2SO_4, (c) 15% H_2SO_4. (Percentage of original width x height: 20 %.) Increment in acid concentration beneficiates the sample.

From Fig 4.27, it can be observed that there is a significant improvement when the sand is washed with 15% sulphuric acid.

From Fig 4.27, it can be observed that there is a significant improvement when the sand is washed with 15% sulphuric acid.

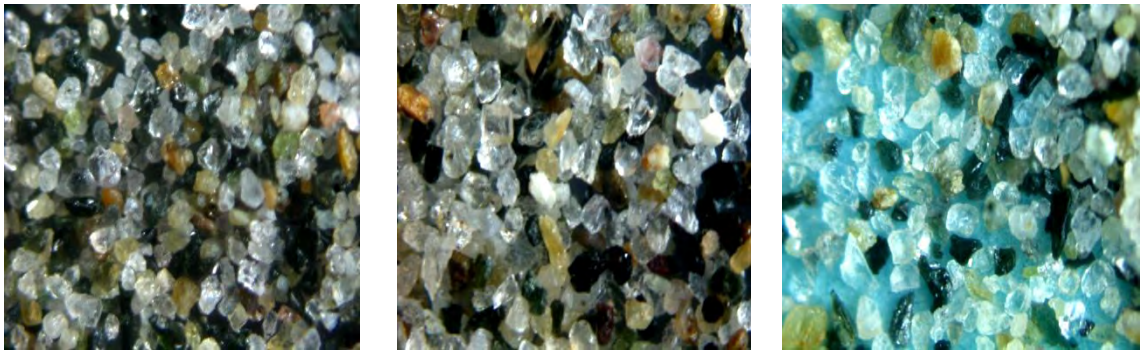

(a) (b) (c)

Fig 4.28: Kuakata (192x) sand sample (a) as received, washed with (b) 10% H_2SO_4, (c) 15% H_2SO_4. (Percentage of original width x height: 20 %.) Increment in acid concentration shows slight beneficiation in the sample.

In Fig 4.28, the images of acid washed Kuakata sand are given. In this case, after acid washing the colour of the solution was changed into light blue (Fig 4.29). With an increase in the acid concentration, the colour of the solution became brighter. No other sand sample shows such change after washing the sand with sulphuric acid. This blue colour could be due to presence of iron, aluminium and/or chromium. A qualitative analysis was performed to find out the elements performed in the reaction.

Fig 4.29: Residual solution after sulphuric acid washing of Kuakata sand

Let, X_l is the residual solution after acid washing of Kuakata Sand. X_l contains sulphuric acid. Series of reaction were performed to find out whether iron, aluminium and/or chromium are present in the solution or not.

The reaction between blue solution and ammonium hydroxide turns the solution orange/ yellow with two (three) layers. The precipitate could contain $Fe(OH)_3$, $Al(OH)_3$ and/or $Cr(OH)_3$.

Kuakata Sand + H_2SO_4 = Sand + X (Sol)

X (Sol) + NH_4OH= precipitate of 2 or 3 layers + $(NaOH + Others)_l$

This confirms that there is trace of iron as Fe_2SO_4. So NH_4OH added basicity to the iron through the OH- (hydroxide) anion. So by the reaction of Fe(II) and NH_4OH, the products are $(NH_4)_2SO_4$ and $Fe(OH)_2$. The balanced reaction is:

$FeSO_4+2NH_4OH= Fe(OH)_2+2(NH_4+)+(SO_4^{2-})$

The solution and the precipitants were filtered. While filtering the solution was turning into yellow again because of air oxidation. Now, the filtrate along with the filter paper was putted in a beaker. And caustic soda was poured into the beaker and boiled at >180ºC and filtered.

[Na reacts with glass, especially at high temperature. That's why the container (glass beaker) needs to putted down as soon as it reaches the boiling point.]

Now, at this stage there are two routes to find out the trace elements.

a) To find out is there any iron hydroxide and/or chromium hydroxide 30% hydrogen peroxide is added and boiled at 100-120 ºC. The solution turned into orange colour, which leads to the conclusion that after the reaction Cr was precipitated. Thus, Cr was present in X_l as Chromic Sulphate.

b) To find out whether the solution is of $NaAl_2$ or not few drops of Methyl orange was added. The key is to add HCl until the solution turns into orange or pink. Then NH_4OH was added. The solution turned into yellow/ orange again. But no precipitate was formed, where as white precipitate was expected. Thus, there is no trace of Al in X_l.

If (b) is true then aluminium did not participated in the reaction. For further confirmation another test was performed. For this, again X_l was taken and this time NaOH was added. The solution turned into brown. It was filtered and a clear solution and precipitate was found on the filter paper. The precipitant was eliminated. The clear solution was taken and methyl orange and HCl were added to the filtered solution. A change in colour was observed. Then ammonia was added. Again a change in colour was observed, which confirms there is no trace of aluminium. Though Kuakata sand contains around 6% Al, at room temperature Al did not take part in reaction with 15% H_2SO_4 (at 700rpm). Which means to remove Al at room temperature 15% H_2SO_4 washing with stirring

speed of at 700rpm is not enough. May be alkali washing is required to remove aluminium impurities.

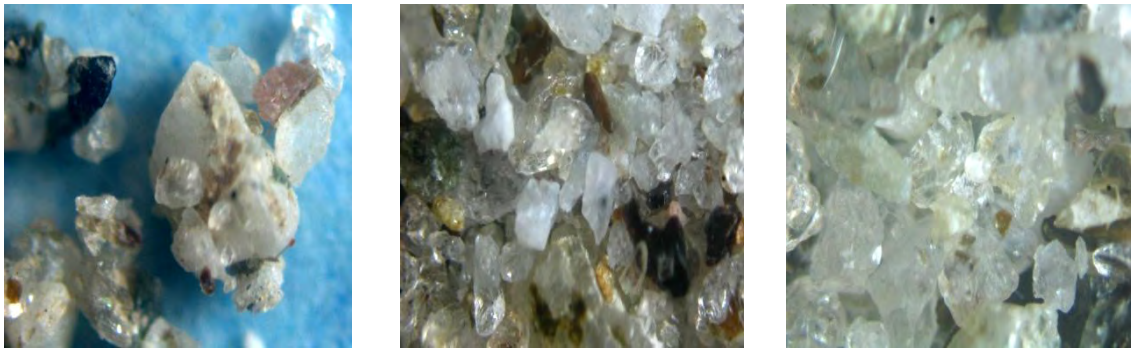

(a) (b) (c)

Fig 4.30: Patgram (192x) sand sample (a) as received, washed with (b) 10% H_2SO_4, (c) 15% H_2SO_4. (Percentage of original height x width: 18 %.) Increment in acid concentration beneficiates the sample.

Patgram sand shows significant improvement after washing the sand with 15% sulphuric acid (Fig 4.30). But, even after significant improvement the sample contained visible impurities.

(a) (b) (c)

Fig 4.31: Bipinganj (192x) sand sample (a) as received, washed with (b) 10% H_2SO_4, (c) 15% H_2SO_4. (Percentage of original height x width: 18 %.) Increment in acid concentration beneficiates the sample.

Both Bipinganj and Sylhet sand shows better improvement with the use of 15% sulphuric acid (Fig 4.31-4.32). From Fig 4.27-4.28 and Fig 4.30-4.32, it can be observed that with the increase of acid concentration the trend of removing impurities from sand particle is linearly increasing.

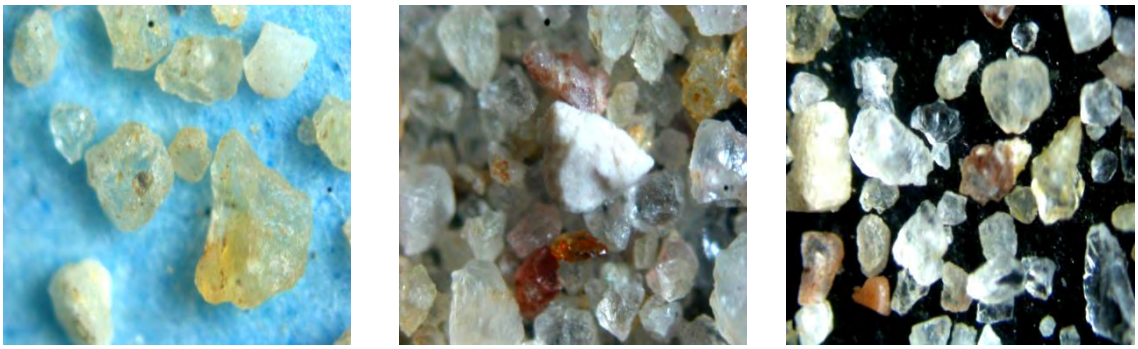

(a) (b) (c)

Fig 4.32: Sylhet (192x) sand sample (a) as received, washed with (b) 10% H_2SO_4, (c) 15% H_2SO_4. (Percentage of original height x width: 18 %.) Increment in acid concentration beneficiates the sample.

But if we try to compare improvement via HCl (Fig 4.23-4.26) and H_2SO_4 (Fig 4.27-4.28, 4.30-4.32) it can be seen that it is really hard to quantify.

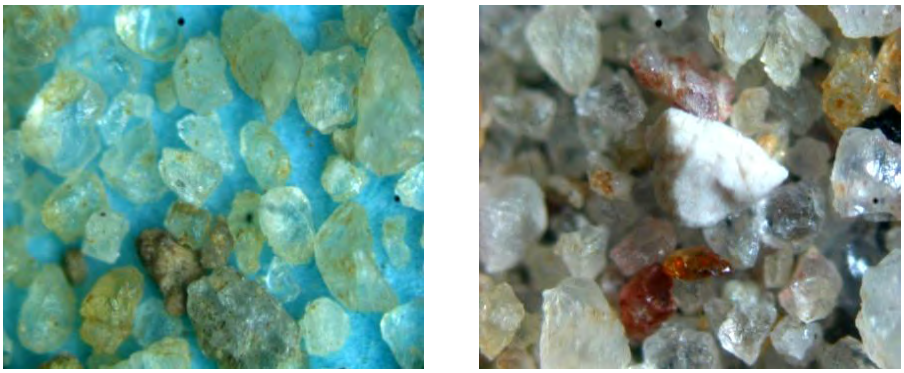

(b) (c)

Fig 4.33: Sylhet sand (a) washed with 10% HCl, (b) with 10% H_2SO_4. The impact of acids is similar.

With the stereomicroscopic observation the impact putted by the acids, separately are quite similar. A comparison is shown in Fig 4.33. That's why for further studies, only one of the inorganic acids were chosen to proceed with, i.e. 15% sulphuric acid.

iii) As it is mentioned earlier, 15% sulphuric acid was chosen for further upgratation process. Thus, an XRF was conducted on each sand sample washed with 15% sulphuric acid at 700 rpm for 20 minutes.

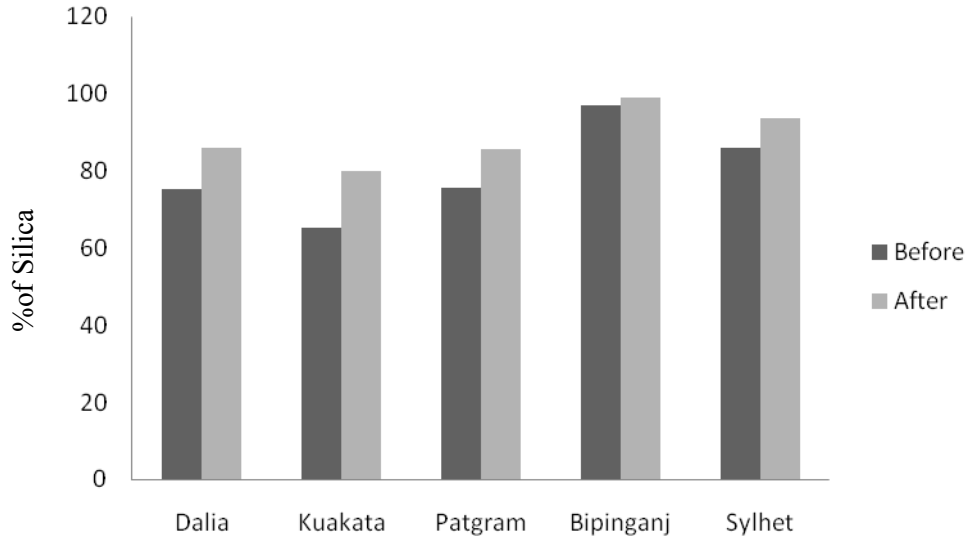

Fig 4.34: XRF analysis of sand samples (before and after acid wash)

The SiO_2% of the samples as received and after beneficiation is provided in Fig 4.34. A huge improvement can be observed for Kuakata sand. From 65.22% SiO_2 it reached to 79.91%. After washing the Bipinganj sand with 15% sulphuric acid, the silica percentage reached to 99.05%. The received sand sample from Dalia and Patgram are similar in characteristics. That is why, the change after acid washing was similar too. The silica percentage after acid washing of Dalia and Patgram were 85.97% and 85.41% respectively. In case of Sylhet sand, the increment in SiO_2% is not evident as expected. From 86.85% the silica was upgraded to 93.45%. But, in Table 4.17, it was shown that attrition at optimum condition upgraded the sand to 94.22% SiO_2. For all five samples element like Na, K was completely removed by acid washing. To analyse the XRF result further, the detail impurity level is given in Table 4.18.

In case of Dalia, Patgram and Kuakata sand there is a large residue of iron and aluminium even after acid washing (Table 4.18). Comparing Table 4.17 and 4.18, it can be seen that the iron content in Sylhet sand was better removed with sulphuric acid than by washing it with distilled water. The elements like sulphur, titanium, chromium were completely removed after washing it with water. However, in both cases, removal of aluminium was not significant indicating that an alkali wash might be necessary in order to upgrade the sample to greater than 98% SiO_2, which is the minimum limit of silica percentage to be used in the high tech applications like the production of solar grade silicon [6].

Table 4.18: XRF of impurity level of the sample (before and after acid wash)

Sample		Content (wt %)									
		P_2O_5	Al_2O_3	Fe_2O_3	ZrO_2	SO_3	TiO_2	Cr_2O_3	Rb_2O	MgO	MnO
Dalia	Before	0.08	11.94	4.62	0.01	0.01	0.29	0.58	0.01	1.16	0.08
	After	--	9.86	2.85	0.02	--	0.25	0.05	0.02	0.92	--
Kuakata	Before	0.57	11.55	8.52	0.03	0.01	1.13	0.43	0.01	2.42	0.20
	After	0.22	9.77	6.48	0.05	0.25	1.08	--	--	2.05	0.16
Patgram	Before	0.06	12.05	4.12	0.01	0.01	0.27	0.49	0.01	1.21	0.07
	After	0.10	9.81	3.32	0.02	0.20	0.31	--	0.02	0.75	0.05
Bipinganj	Before	0.01	0.90	1.12	0.02	0.01	0.19	0.43	--	0.05	0.01
	After	--	0.43	0.13	0.03	0.24	0.13	--	--	--	--
Sylhet	Before	0.05	5.62	3.17	--	0.02	0.26	0.69	0.01	0.31	0.03
	After	--	4.36	0.91	0.03	0.58	0.37	0.05	--	0.24	--

**Due to calibration, error was found (in ppm range).*

In case of Bipinganj sand, the XRF result shows few of the elements were completely removed. The iron content reduced to 0.13% and Al content reduced to 0.42%. For solar silicon application boron and phosphorus are the most critical elements [6]. There is no trace of boron in the received sand sample. The collected sample contained 100 ppm phosphorus which was removed after acid washing. Uranium and thorium are two critical elements for microelectronics applications [4]. There is no trace of any of them. The sand collected from the deposit contains high percentage of SiO_2 without any sort of refinement and after washing the sand with sulphuric acid it reaches to the desired level of silica percentage.

4.3.3 Alkali Washing

In the received sand sample, Bipinganj and Sylhet sand contains the highest percentage of SiO_2. The result obtained in previous studies (Art. 4.3.1-4.3.2) show the prospect of these two samples is higher than the other three samples. That is why only Bipinganj and Sylhet sand were taken into account for further processing. These two sand samples were washed with 20% NaOH and stirred at 700 rpm for 20 minutes. Then the change was analysed by XRF study.

Table 4.19: XRF analysis of sand samples (before and after acid wash)

Sample		Content (wt %)					
		SiO_2	Al_2O_3	Fe_2O_3	ZrO_2	Ti O_2	Cr_2O_3
Sylhet	Before	86.85	5.62	3.17	--	0.26	0.69
	After	95.31	3.60	0.78	0.03	--	0.05
Bipinganj	Before	97.05	0.90	1.12	0.02	0.19	0.43
	After	99.18	0.36	0.13	0.04	0.29	--

**Due to calibration, error was found in ppm range.*

The experiment was conducted in stainless steel container to make the procedure contamination free. The XRF result in Table 4.19 shows, increment in SiO_2% for both Bipinganj and Sylhet sand. For Sylhet sand the increment in SiO_2% is for alkali wash. To increase the silica percentage even higher, at this point temperature could be introduced as another variable to reduce the aluminium percentage in Sylhet sand.

4.4 Development of Methodology

The selected two sand samples, i.e. Bipinganj and Sylhet were gone through the optimum condition of each step, starting from attrition to alkali washing.

The methodology employed for the selected two samples as decisive one, is shown in Fig 4.35. After following the mentioned route (Fig 4.35), an XRF was performed on the upgraded sample. But before that, the stereomicroscopic view of the samples was observed.

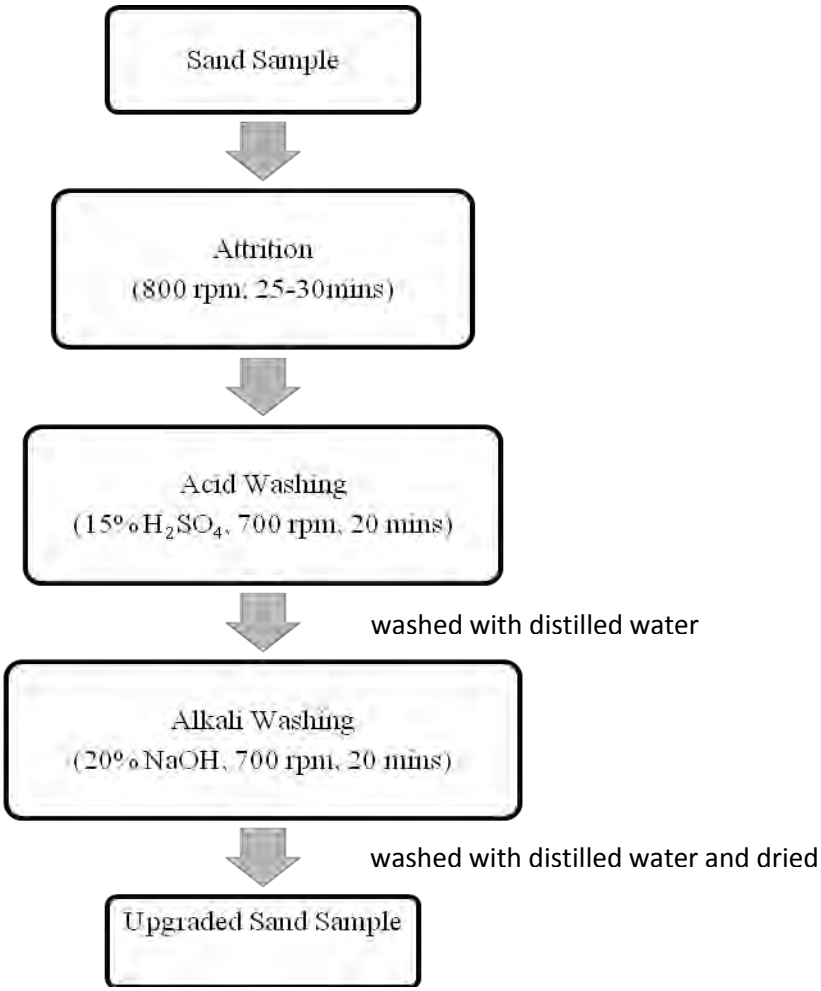

Fig 4.35: Process to upgrade the sand sample

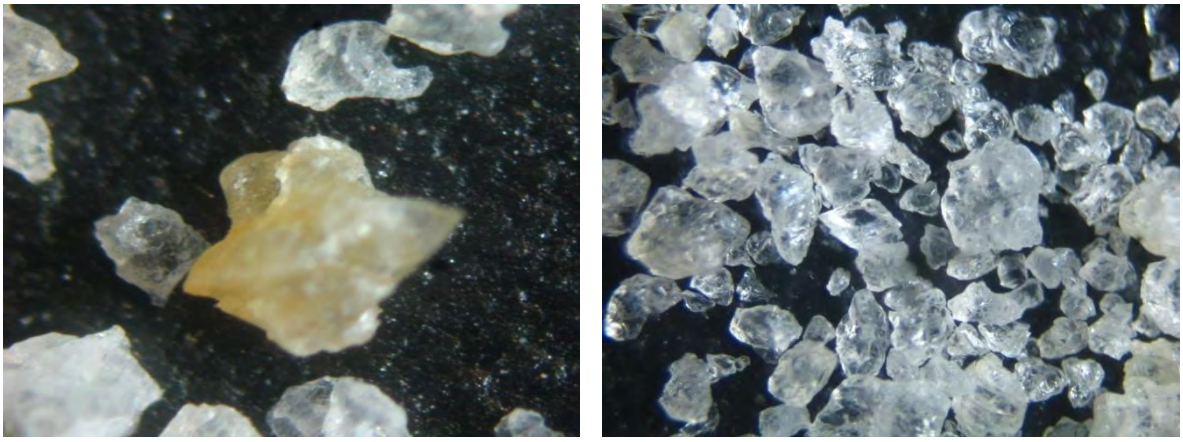

(a) (b)

Fig 4.36: Bipinganj sand (a) as received (192x), (b) at the end step of beneficiation process (100x).
(Percentage of original width x height for each image: 27 %.)

From Fig 4.36, a massive improvement can be observed. Bipinganj sand contains mostly, the clear crystals of silica.

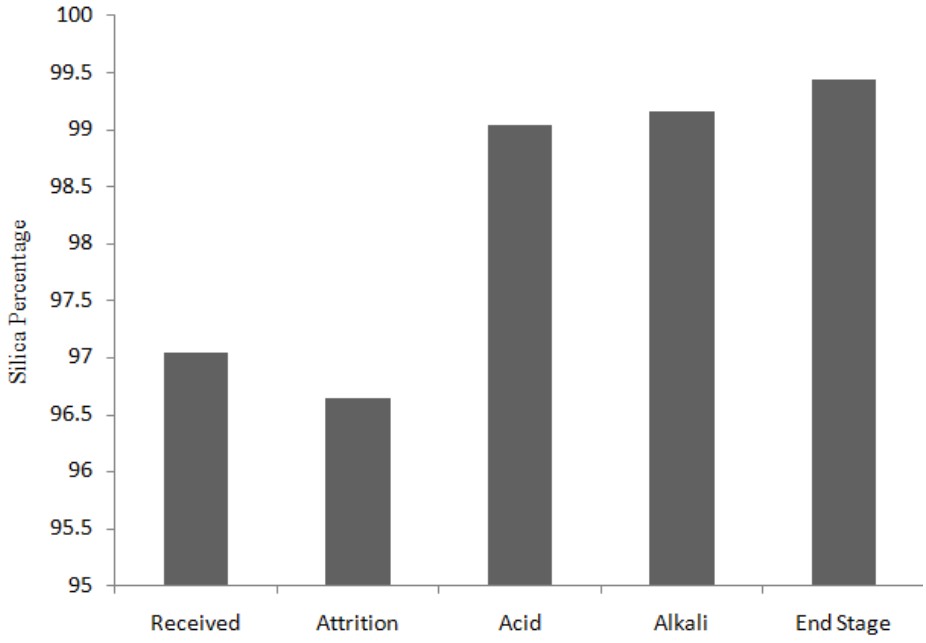

Fig 4.37: Silica content of Bipinganj sand at different conditions

In Fig 4.37, the XRF result of Bipinganj sand is provided with the percentage of silica. With a minor bump, the result shows uniformity in upgradation at each step. If the Bipinganj sand is gone through with a continuous upgradation process as mentioned in Fig 4.35, at the end stage Bipinganj sand can be upgraded as high as 99.45% SiO_2. The impurity level after final stage is given in Table 4.20.

Table 4.20: Impurity level of Bipinganj Sand (before and after enrichment)

Content (wt %)	As Received	After Enrichment
Al_2O_3	0.90	0.26
TiO_2	0.19	0.12
Fe_2O_3	1.12	0.06
CaO	0.06	0.05
K_2O	0.04	0.04
ZrO_2	0.02	0.02

**Due to calibration, error was found (in ppm range).*

Many impurities found in Table 4.2, was entirely removed after complete processing of Bipinganj sand. The developed method was able to put rest of the impurities in ppm range. From Table 4.20 it can be seen that strong impurity like iron was reduced to as low as 563ppm. In most cases, the final content in the Bipinganj sand is acceptable for using the sand as raw material in high-tech applications [6].

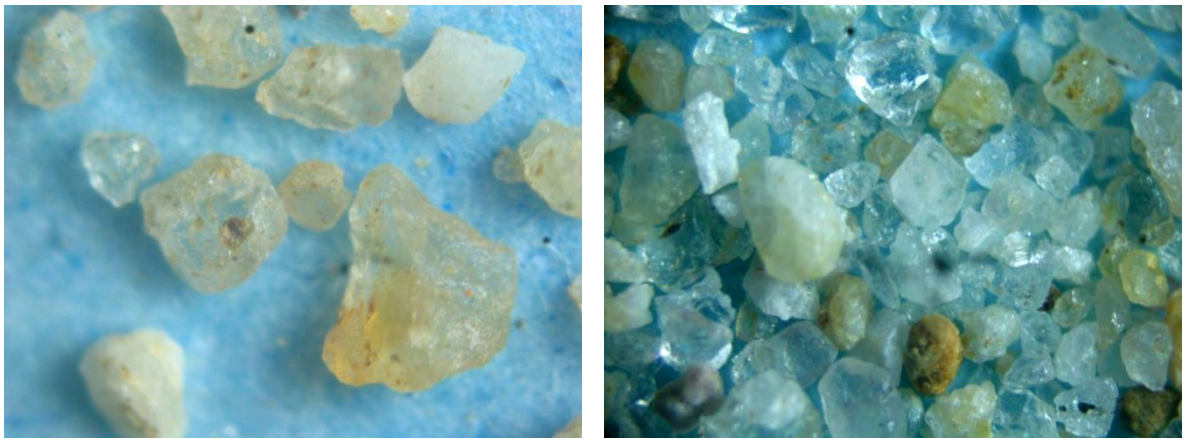

(a) (b)

Fig 4.38: Stereomicroscopic view with spot magnification of 192x of Sylhet sand (a) as received, (b) at the end step of beneficiation process. (Percentage of original width x height: 27 %.)

Like Bipinganj sand, massive improvement after end stage can be observed for Sylhet sand too. But, even after all the beneficiation steps the Sylhet sand contains visible amount of impurities (Fig 4.38).

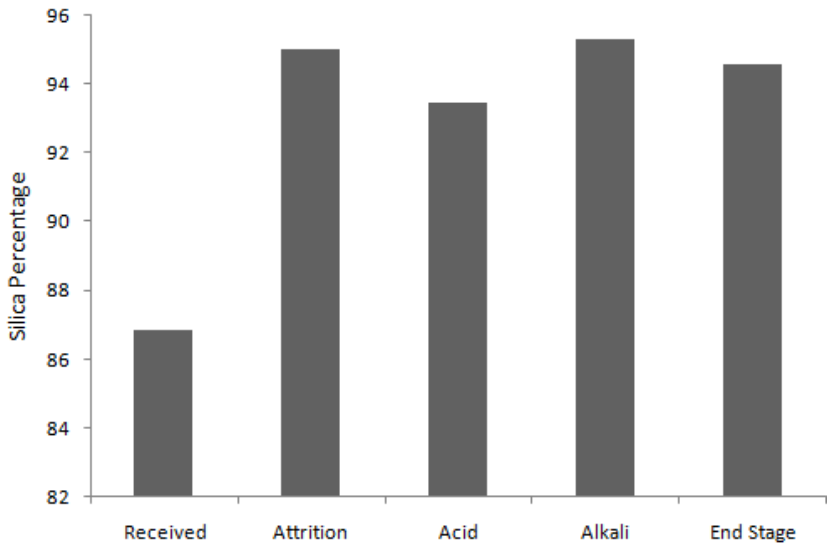

Fig 4.39: Silica content of Sylhet sand at different conditions

If Sylhet sand is gone through with the complete route, it can be upgraded from 86.85% to 94.61% SiO_2 (Fig 4.39). However, the upgradation is not in the range of acceptable level for solar silicon production. The improvement is lowest, when the sand is washed with 15% sulphuric acid at 700 rpm for 20 minutes. The upgradation level is higher that acid wash for both attrition and alkali wash. But if the proposed methodology is conducted as continuous process Sylhet sand does not content the maximum amount of silica in this established study.

The impurity level of Sylhet sand after upgrading it with the complete route is given in Table 4.21.

Table 4.21: Impurity level of Sylhet sand (before and after enrichment)

Content (wt %)	As Received	After Enrichment
Al_2O_3	5.62	2.65
TiO_2	0.26	0.43
Fe_2O_3	3.17	1.67
MgO	0.31	0.15
K_2O	2.07	0.38
ZrO_2	--	0.03
Cr_2O_3	0.69	0.08

**Due to calibration, error was found (in ppm range).*

The XRF result shows that the sample contains iron and aluminium at undesirable range. In spite of the complete route, the sample after alkali wash is more acceptable range. Even saying so, the sample is far below than the adequate range to be high purity silica. However, the result found in upgradation process (specially the attrition steps) suggests, with different route it is possible to upgrade the sand to the desired level.

Chapter Five
Conclusion

This thesis work can be divided into three steps:

- Characterization of the sand.
- Beneficiation of the sand.
- Identification of suitable deposit.

5.1 Characterization of the Sand

1) In terms of silica percentage, Bipinganj sand is naturally enriched with about >97% SiO_2, followed by Sylhet sand (86.85%), Patgram sand (75.52%), Dalia sand (75.06%) and lastly Kuakata sand 65.23%.

2) While phase identification, Bipinganj and Sylhet sand sample shows presence of only perfect α-quartz. Other three samples show trace α-quartz along with other impurities.

3) The density of pure quartz is 2.65 g/cc. The closest density was found for Bipinganj (2.6 g/cc) and Sylhet sand (2.69 g/cc) sample. The other densities found were 2.58 g/cc for Dalia, 2.57 g/cc for Patgram and the heaviest one 2.9 g/cc for Kuakata sand sample.

4) All of the samples have low moisture and negligible organic matter.

5) Kuakata and Sylhet sand particles are uniformly distributed, whereas Kuakata sand is most tightly distributed. Bipinganj, Patgram and Dalia sand particles are not uniformly distributed.

5.2 Beneficiation of the Sand

By washing the sand with distilled water at 800 rpm for 30 minutes Sylhet sand was upgraded upto 94.22% SiO_2.

By acid washing (15% H_2SO_4) Bipinganj sand sample was upgraded upto 99.05% SiO_2 and Sylhet sand was upgraded upto 93.45% SiO_2.

By alkali washing with 20% NaOH Bipinganj sand sample was upgraded upto 99.17% SiO_2 and Sylhet sand was upgraded upto 95.31% SiO_2.

Maximum upgradation point for Bipinganj sand by single beneficiation method was achieved by alkali washing, i.e. 99.17% SiO_2. By the developed method, the peak point for Sylhet sand was found to be 94.61% and for Bipinganj sand 99.45% SiO_2. Instead of the developed method the Sylhet sand sample shows best result with alkali washing (95.31% SiO_2).

5.3 Identification of suitable deposit

1) The characterization and beneficiation of the sample indicates that Bipinganj sand with high quartz percentages, low moisture content, negligible clay binder and least organic matter has the potential of being used for the production of silicon for high-tech application. For the production of Solar grade silicon (99.9999% pure Silicon), silica sand needs to be >98% pure to prepare it for the next stage. Naturally Bipinganj sand is >97% pure and in this work 99.45% purity is achieved.

2) This study shows that silica sample under investigation contains α-quartz in good percentage, has uniform particle size distribution and easy to grind. The silica content could be enhanced to 95.31% (from 86.85%) by rather simple techniques.

3) Samples from near Tista river- Dalia and Patgram, both of the samples contain similar amount of silica. Though their characteristics and response to beneficiary techniques are quite different, both of them have very good potential with certain limitations, for the possible use in high tech application.

4) Out of all five samples, Kukata sand contains the least percentage of Silica. Trace of heavy minerals and response to beneficiary techniques make it least favorable to process it for high quality silica. The characterization suggests upgradation aiming for heavy minerals where pure silica is found as by product (e.g. cox's bazaar sand, Art. 2.6.5) might be more feasible option.

5.4 Summary

In this work, sand samples from 5 deposits in Bangladesh was characterised on the basis of parameters that include composition, size, density, sphericity, moisture content, material composition and crystallinity ; few beneficiary techniques were employed and finally suitable deposits were suggested for possible using the silica sand sample as raw material in the production of silicon for high-tech applications. The study shows that Bipinganj sand has the potential to be used in the production of solar grade silicon. Another serious contender is Sylhet sand; studies should be undertaken to use Sylhet sand for high-tech applications. Patgram and

Dalia sands, with certain limitations, also have good potential. Kuakata sand sample is the least favorable to be used in such applications.

5.5 Recommendation for Further Work

The aim of the study was to identify a suitable deposit of silica within the country and to develop techniques for the purification of silica of this deposit so as to make it suitable for the production of solar grade silicon. The entire work suggests only one sand sample of such use. Based on the characterization attempts were taken to upgrade Sylhet sand. The endeavor should be continued to reach purity level of silica at least > 98%. Alkali-wash with strong base, temperature or even or physical separating process like froth flotation might be applied to achieve the desired/ required purity level. The characterization indicates the potential of Patgram and Dalia sand. Further experiments may be performed to purify them to make it high purity silica for high tech-applications. In case of Kuakata sand heavy mineral separation and/ or magnetic separation to remove heavy minerals (which are mostly paramagnetic or ferromagnetic) from silica might be applied to selectively separate minerals according to differences in their ability to be wetted, enhanced or suppressed by conditioning reagents.

Furthermore, systematic investigation might be performed within the country on the possibility of producing solar grade silicon from local silica deposits and to develop the technology of producing solar cells in Bangladesh.

References

1. Kerr, P.F. (1959) *Optical mineralogy.* McGraw-Hill Book Co., New York.
2. Berry, L. G. and Mason, B. (1959) *Mineralogy: Concepts, Descriptions, Determinations.* W.H. Freeman and Co., California.
3. NGU (2008) *High purity quartz*. Norwegian Geological Survey, Kvarts, planetenjordan FN-áret 2007-2008-2009, Trondheim.
4. Götze, J. and Möckel, R. (2012) *Quartz: Deposits, Mineralogy and Analytics*. Springer, Heidelberg.
5. Kawamoto, H. and Okuwada, K., "Development Trend for High Purity Silicon Raw Material Technologies- Expecting Innovative Silicon Manufacturing Processes for Solar Cell Applications", *Sci. & Tech. Trends*, vol. 24, pp. 38-50, 2007.
6. Kheloufi, A., Berbar, Y., Kefaifi, A., Medjahed, S. A. and Kerkar, F., "Improvement of Impurities Removal from Silica Sand by Using a Leaching Process," in *2011 International Conference on Chemical and Process Engineering*, Vol. 10, May, 2011.
7. Heaney, P. J., Prewitt, C.T. and Gibbs, G.V. (1994) *Silica - Physical behavior, geochemistry and materials applications.* Reviews in Mineralogy, Vol. 29, Mineralogical Society of America.
8. Götze, J. and Lewis, R., "Distribution of REE and trace elements in size and mineral fractions of high purity quartz sands," *Chem. Geol., vol*. 114, pp. 43–57, 1994.
9. Blankenburg, H.J., Götze, J. and Schulz, H, "Quarzrohstoffe. Deutscher Verlag für Grundstoffindustrie," Leipzig-Stuttgart, 296 S, 1994.
10. Pagel, M., Barbin, V., Blanc, Ph., Ohnenstetter, D. (2000) *Cathodoluminescence in geosciences.* Springer Verlag, Berlin Heidelberg New York Tokyo.
11. Götze, J., "Chemistry, textures and physical properties of quartz – geological interpretation and technical application," *Mineral. Mag.,* vol. 73, pp. 645-671, 2009.
12. Shaffer and Nelson, R., "The Time of Sands: Quartz-rich Sand Deposits as a Renewable Resource," *Elect. Green J.*, vol, 1(24), 2006.
13. www.anzaplan.com/strategic-minerals/high-purity-quartz/high-purity-quartz-resources Accessed: 05- Feb- 2014
14. NSW (2007) *Industrial mineral opportunities in New South Wales (Geology Bulletin 33).*NSW Government, Division of Resources and Energy, Minerals and Petroleum, Sydney.
15. Rösler, H.J. (1981) *Lehrbuch der Mineralogie*. Leipzig : VEB Deutscher Verlag für Grundstoffindustrie, 2. Aufl.
16. Jung, L. (1992) *High purity natural quartz.* Quartz Technology, Liberty Corner, New Jersey.

17. NGU (2005) *Potential resources of quartz and feldspar raw material in Sørland IV: relationships between quartz, feldspar and mica chemistry and pegmatite type 2005.075.*Norwegian Geological Survey Report, Trondheim.
18. United Nations COMTRADE database, DESA/UNSD.
    http://comtrade.un.org/db/
    Accessed: 05- Feb- 2014
19. Geological Survey, Bangladesh.
    http://www.gsb.gov.bd/english/index.php?option=com_content&view=article&id=9&Itemid=10
    Accessed: 04- Feb- 2013
20. Rahman, A. (1997) *Bangladesher khaniz shampadh o abishkarer etihash*. Geological Survey, Bangladesh, Dhaka.
21. GSB (1985) *Records of the Geological Survey of Bangladesh; Volume 3, Part 4, Glass Sand Deposits of the Balijuri Area, Sherpur District, Bangladesh.* Geological Survey, Bangladesh, Dhaka.
22. GSB (1986) *Records of the Geological Survey of Bangladesh; Volume 4, Part 5, Glass Sand Deposits of the Chauddagram Area, Comilla District, Bangladesh.* Geological Survey, Bangladesh, Dhaka.
23. Time Domain CVC Inc.
    http://timedomaincvd.com/CVD_Fundamentals/films/SiO2_properties.html
    Accessed: 05- Feb- 2014
24. Proton.
    http://www.azom.com/article.aspx?ArticleID=1114
    Accessed: 05- Feb- 2014
25. Worrall, W.E. (1975) *Clays and ceramic raw materials.* John Wiley and Sons, New York.
26. IOTA (2013) *Semiconductor Fused Quartz Grades*, *Technical Data, IOTA High Purity Quartz, IOTA-SEMI- V1F (01/13)*, Unimin Corporation, Connecticut.
27. IOTA (2013) *Monocrystalline Photovoltaic Grades*, *Technical Data, IOTA High Purity Quartz, IOTA-SOLAR- V1F (01/13)*, Unimin Corporation, Connecticut.
28. Aasly, K., *Properties and behavior of quartz for the silicon process*, Ph.D. Thesis, Department of Geology and Mineral Resources Engineering, Norwegian University of Science and Technology, 2008.
29. Sarti, D., and Einhaus, R., "Silicon Feedstock for the Multi-Crystalline Photovoltaic Industry," *J. Solar Energy Materials and Solar Cell.*, vol. 72, pp. 27-40, 2002.
30. Müller, A., Ghosha, M., Sonnenschein, R., and Woditsch, P., "Silicon for Photovoltaic

Applications," *Materials Sc. and Engr. B*, vol. 134, pp. 257-262, 2006.

31. Istratov, A.A., Buonassisi, T., Pickett, M., Heuer, A.B., and Weber, E.R., "Control of Metal Impurities in "Dirty" Multicrystalline Silicon M.D. for Solar Cells," *J. Materials Sc. and Engr. B*, vol. 134, pp. 282-286, 2006.
32. Braga, A.F., Moreira, S.P., Zampieri, P.R., Bacchin, J.M.G., and Mei P.R., "New Processes for the Production of Solar-Grade Polycrystalline Silicon," *J. Solar Energy Materials and Solar Cell*., vol. 92, pp. 418–424, 2008.
33. Deer, W. A., Howie, R.A., and Zussman, J. (1992) *An introduction to the rock forming minerals.* Longman Scientific and Technical, Essex.
34. H.A. Aulich, (1982) "Preparation of high-purity starting materials for the production of solar-grade silicon," Siemens Forschungs-und Entwicklungsberichte Bd, Vol. 11(6), pp. 327–331.
35. A. J. Caballero, and R. I. Holcombe, Process for purifying silica sand, US 4401638 A, 1983.
36. Mowla, D., Karimi, G., and Ostadnezhad, K., "Removal of hematite from silica sand ore by reverse flotation technique," *J. Separation and Purification Technol*., vol. 58, pp. 419–423, 2008.
37. Z. Zhang, J. Li, X. Li, H. Huang, L. Zhou, T. Xiong, (2012) "High efficiency iron removal from quartz sand using phosphoric acid," *Int. J. Miner. Process.*, vol. 114–117, pp. 30–34.
38. Lee, S. O., Park, Y. Y., Kim, S. J., and Kim, M. J., "Study on the kinetics of iron oxide leaching by oxalic acid," *Int. J. Miner. Process.*, vol. 80, pp. 144–152, 2006.
39. Andres, U., Jirestig, J., and Timoshkin, I., "Liberation of minerals by high voltage electrical pulses," *J. Powder Technol.*, vol. 104, pp. 37–49, 1999.
40. Martello, D. E., Bernardis, S., Larsen, R.B., Tranell, G., Sabatino, D. M., and Arnberg, L., "Electrical fragmentation as a novel refining route for hydrothermal quartz for SoG-Si production," *J. Powder Technol.* , vol. 224, pp. 209–216, 2012.
41. Martello, D. E., Tranell, G., Gaal, S., Raaness, O.S., Tang, S.K., and Arnberg, L., "Study of pellets and lumps as raw materials in silicon production from quartz and silicon carbide," *Metall. Mater. Trans. B*, vol. 42(5), pp. 939-950, 2011.
42. Nordic Mining.
    www.nordicmining.com/kvinnherad/category276.html 2011
    Accessed: 16- Feb-2011
43. Slade, W.W., Benefication of siderite contaminated sand, US Pat 3914385 A, 1975.
44. Chubb, P.A., Treatment of sand and other industrial minerals, US Pat 3297402 A, 1967.
45. Štyriaková, I., Mockovčiaková, A., Štyriak, I., Kraus, I., Uhlík, P., Madejová, J., and Orolínová, Z., "Bioleaching of clays and iron oxide coatings from quartz sands," *J. App. Clay Sci.*, vol. 61, pp. 1–7, 2012.

46. Kurtz, J.A., Band for protecting screw threads of 'piypbs, US Pat 440168, 1890.
47. William, A. F., Purification of silica sands, US Pat 2891844 A, 1959.
48. Seddon, E., Sturgeon, R., Purification of minerals, US 2592973 A, 1948.
49. Bowdish, F.W., Process for leaching sand or other particulate material, US Pat 4042671 A, 1977.
50. Taxiarchou, M., Panias, D., Douni, I. , Paspaliaris, I., and Kontopoulos, A., "Removal of Iron From Silica Sand by Leaching with Oxalic Acid," *J. Hydrometallurgy*, vol. 46, pp. 215–227, 1997.
51. Veglio, F., Passariello, B., and Abbruzzese, C., "Iron Removal Process for High-Purity Silica Sands Production by Oxalic Leaching," *Ind. Eng. Chem. Res.*, vol. 38, pp. 4443-4448, 1999.
52. Kayal, N., and Singh, N., "Stepwise Complexometric Determination of Aluminum, Titanium and Iron Concentrations in Silica Sand and Allied Materials," *Chem. Central J*., vol. 1(24), pp. 1-5, 2007.
53. Veglio, F., Passariello, B., Barbaro, M., Plescia, P., and Marabini, A.M., "Drum Leaching Tests in Iron Removal From Quartz Using Oxalic and Sulphuric Acids," *Int. J. Miner. Process*., vol. 54, pp 183–200, 1998.
54. Li, J., Li, X., Shen, Q., Zhang, Z., and Du, F., "Further Purification of Industrial Quartz by Much Milder Conditions and a Harmless Method," *Environ. Sci. Technol*., vol. 44, pp. 7673–7677, 2010.
55. Martínez, A. L., Rodríguez, M.G.D, Uribe, A.S., Carrillo, F.R.P., and Osuna, J.G.A., "Leaching Kinetics of Iron Fromlow Grade Kaolin by Oxalic Acid Solutions," *Appl. Clay Sci*., vol. 51 pp. 473–477, 2011.
56. Mandal, S.K., and Banerjee, P.C., "Iron Leaching From China Clay with Oxalic Acid: Effect of Different Physic–Chemical Parameters," *Int. J. Miner. Process.*, vol. 74, pp. 263–270, 2004.
57. Lee, S.O., Tran, T., Park, Y.Y., Kim, S.J., and Kim, M.J., "Study On The Kinetics of Iron Oxide Leaching by Oxalic Acid," *Int. J. Miner. Process.,* vol. 80, pp. 144–152, 2006.
58. Du, F., Li, J., Li, X., and Zhang, Z., "Improvement of Iron Removal From Silica Sand Using Ultrasound-Assisted Oxalic Acid," *Ultrason. Sonochem.*, vol. 18, pp. 389–393, 2011.
59. Raman, V., and Abbas, A., "Experimental Investigation on Ultrasound Mediated Particle Breakage," *Ultrason. Sonochem.*, vol. 15, pp. 55–64, 2008.
60. Mgaidi, A., Jendoubi, F., Oulahna, D., Maaoui, M.E., and Dodds, J.A., "Kinetics of the Dissolution of Sand into Alkaline Solutions: Application of a Modified Shrinking Core Model," *J. Hydrometallurgy*, vol. 71, pp. 35–446, 2004.

61. Huang, H. Li, J., Li, X., and Zhang, Z., "Iron Removal from Extremely fine Quartz and Its Kinetics," *J. Separation and Purification Technol*., vol. 108, pp. 45–50, 2013.
62. Ubaldini, S., Piga, L., Fornari, P., and Massidda, R., "Removal of Iron From Quartz Sands: A Study by Column Leaching Using a Complete Factorial Design," *J. Hydrometallurgy*, vol. 40, pp. 369-379, 1996.
63. Hugh, C.W., Method of treating quartz sands, US Pat 3282416, 1966.
64. Xakalashe, M. A., Tangstad, M., "Silicon Processing: From Quartz to Crystalline Silicon Solar Cells," in 2011 Southern African Pyrometallurgy, 2011.
65. Rajib, M., Zaman, M. M., Kabir, M.Z., Deeba, F., and Rana, S.M., "Physical Upgradation and Characterization of River Silica of Bangladesh to be Used as Glass Sand," Proceedings of Int. Conf. on Geoscience for Global Development, 2009.
66. Michel-LÈvy, A., Lacroix, A. (1888) *Les minéraux des roches.* Librairie Polytechnique, Paris.
67. Bjorn, E. S., "A Revised Michel-Le´Vy Interference Colour Chart Based on First-Principles Calculations'', *European J. of Mineralogy,* vol. 25, pp 5-10, 2013.
68. Zhang, L., and Ciftja, A., "Recycling Of Solar Cell Silicon Scrap Through Filtration, Part 1: Experimental Investigation," *J. Solar energy materials and solar cells*, vol. 92, pp. 1450-1461, 2008.
69. ASTM D 2974- Standard test methods for Moisture, Ash, and organic matter of Peat and Organic soils.
70. Solar Silicon Resources Group.
    http://www.ssrg.com.sg/quartz/qtztech
    Accessed: 05- Feb- 2014